

# TCAD Parameters for 4H-SiC: A Review

Jürgen Burin,<sup>1</sup> Philipp Gaggl,<sup>1</sup> Simon Waid,<sup>1</sup> Andreas Gsponer,<sup>1</sup> and Thomas Bergauer<sup>1</sup>

*Institute of High Energy Physics, Austrian Academy of Sciences, Nikolsdorfer Gasse 18, 1050 Wien*

(\*e-mail: [juergen.burin@oeaw.ac.at](mailto:juergen.burin@oeaw.ac.at))

(Dated: 5 November 2024)

In this paper we review the models and their parameters to describe the relative permittivity, bandgap, impact ionization, mobility, charge carrier recombination/effective masses and incomplete dopant ionization of 4H silicon carbide in computer simulations. We aim to lower the entrance barrier for newcomers and provide a critical evaluation of the status quo to identify shortcomings and guide future research. The review reveals a rich set of often diverging values in literature based on a variety of calculation and measurement methods. Although research for all the selected parameters is still active, we show that sometimes old values or those determined for other kinds of silicon carbide are commonly used.

Keywords: 4H-SiC, TCAD simulations, simulation parameters, silicon carbide

## CONTENTS

<b>I. Relative Permittivity</b>	4
A. Theory	4
B. Results	5
C. Discussion	7
<b>II. Density-of-States Effective Mass</b>	11
A. Theory	12
1. Effective Masses along Principal Directions	12
2. Density-of-States (DOS) Mass	12
3. Conductivity Effective Mass	13
4. Polaron Mass	14
B. Results	15
1. Effective Mass along Principal Directions	15
2. DOS Mass	17
3. Temperature	20
4. Effective DOS Mass for TCAD Tools	21
C. Discussion	21
<b>III. Band Gap</b>	23
A. Theory	25
1. Temperature Dependency	26
2. Doping Dependency	27
B. Results & Discussion	29
1. Temperature Dependency	31
2. Doping Dependency	34
3. TCAD Values	36
<b>IV. Impact Ionization</b>	40
A. Theory	41
B. Results	43
C. Discussion	49

<b>V. Incomplete Ionization</b>	51
A. Theory	52
B. Results	55
C. Discussion	63
<b>References</b>	65

## I. RELATIVE PERMITTIVITY

The permittivity  $\epsilon$  describes the dielectric properties that influence electromagnetic wave propagation within a material and their reflections on interfaces<sup>2</sup>. These effects are, for example, essential to describe the impact of an external electric field, which determines the capacitance values in a device. In general, the user has to provide the relative permittivity  $\epsilon_r = \epsilon/\epsilon_0$ , i.e., the ratio compared to the vacuum permittivity  $\epsilon_0 = 8.854 \times 10^{-12} \text{ F m}^{-1}$ , to the TCAD tools.

### A. Theory

In the frequency domain, the complex relative permittivity can be written as

$$\epsilon_r^*(\omega) = \epsilon'(\omega) + i\epsilon''(\omega).$$

The real part  $\epsilon'$  represents the energy stored in the material when exposed to an electric field and the imaginary part  $\epsilon''$  the losses (e.g., absorption and attenuation)<sup>2</sup>.  $\epsilon'$  and  $\epsilon''$  are tightly interconnected via the Kramers-Kronig (KK) relation<sup>3</sup>

$$\epsilon'(\omega) = 1 + \frac{2}{\pi} \int_0^\infty \frac{\omega' \epsilon''(\omega')}{\omega'^2 - \omega^2} d\omega' \quad (1a)$$

$$\epsilon''(\omega) = -\frac{2\omega}{\pi} \int_0^\infty \frac{\epsilon'(\omega')}{\omega'^2 - \omega^2} d\omega' \quad (1b)$$

In TCAD simulations of semiconductor devices  $\epsilon''$  is of diminishing importance, but  $\epsilon'$  is required to calculate capacitances or the electric field distribution. Consequently, we will focus on  $\epsilon'$  in the sequel.

In the literature the static ( $\epsilon_s$ ) and high-frequency resp. optical ( $\epsilon_\infty$ ) relative permittivity are distinguished. The former is  $\epsilon'(\omega \rightarrow 0)$  but a definition of the latter is more complicated. It denotes  $\epsilon'$  at the end of the reststrahlen range towards higher frequencies, where the real part of the refractive index is null<sup>4</sup>. In publications that focus on optical high-frequency analysis  $\epsilon_\infty$  is sometimes denoted as  $\epsilon'(0)$ <sup>5</sup>, which must not be confused with  $\epsilon_s$ . These inconsistencies were explained in the following fashion<sup>6</sup>: “We shall use  $\epsilon_\infty$  to denote the extrapolation … to zero frequency. This somewhat contradictory notation arose because  $\epsilon_\infty$  the “optical” dielectric constant, was often set … at a frequency much higher than the lattice frequency, but low compared with electronic transition frequencies. In many substances no suitable frequency exists, and it is preferable to extrapolate optical data to zero frequency …”

To clarify:  $\epsilon_\infty$  is measured at frequencies well above the long-wavelength longitudinal optical (LO) phonon frequency  $\omega_{\text{LO}}$ <sup>3</sup>.  $\omega_{\text{LO}}$  translates  $\epsilon_s$  into  $\epsilon_\infty$  and vice versa in conjunction with the transversal optical (TO) phonon frequency  $\omega_{\text{TO}}$  and the Lyddane-Sachs-Teller (LST) relationship<sup>7</sup>

$$\frac{\epsilon_s}{\epsilon_\infty} = \left( \frac{\omega_{\text{LO}}}{\omega_{\text{TO}}} \right)^2. \quad (2)$$

For  $\omega_{\text{LO}}$  we encountered the energy values 120 meV (approximately 29 THz)<sup>8–12</sup>, 104 to 121 meV<sup>13</sup> and 104.2 meV<sup>14</sup> in our search. Instead of the energy often the respective wave numbers are presented, i.e., (in  $\text{cm}^{-1}$ )  $\omega_{\text{TO}} = 793$  and  $\omega_{\text{LO}} = 974$ <sup>15</sup>,  $\omega_{\text{LO}}^{\parallel} = 964.2$ ,  $\omega_{\text{LO}}^{\perp} = 966.4$ ,  $\omega_{\text{TO}}^{\parallel} = 783$  and  $\omega_{\text{TO}}^{\perp} = 798$ <sup>16</sup>,  $\omega_{\text{TO}} = 783$  and  $\omega_{\text{LO}} = 964$ <sup>17</sup> and  $\omega_{\text{LO}} \in [967, 971]$ <sup>18</sup>.

## B. Results

Various approaches have been used to determine the relative permittivity: One possibility are calculations using the density functional theory (DFT) based local density approximation (LDA)<sup>5,8,19–24</sup> or the effective mass theory<sup>25</sup>. With these the band structure and, thus,  $\epsilon''$  is calculated and then transformed into  $\epsilon'$  using the Kramers-Kronig relations (Eq. (1)). Measurements use either some form of resonator (RES)<sup>26–28</sup>, spectroscopy (SPEC)<sup>29–31</sup>, spectroscopic ellipsometry (SE)<sup>32,33</sup> or the refractive index (RI)<sup>6,16,34</sup>. In some cases the transversal and longitudinal optical phonon frequencies are determined and used in the LST relationship (Eq. (2))<sup>32,33</sup>. Furthermore, the tight relationship between relative permittivity and complex refractive index, i.e.,  $n^*(E) = \sqrt{\epsilon(E)}$ <sup>3</sup>, with  $E = \hbar\omega$ , is utilized if  $\epsilon''$  is negligible. For fitting purposes the representation

$$n^2 = 1 + \frac{\epsilon_g}{1 - (hf/E_g)^2} \approx \epsilon_\infty + \epsilon_g \left( \frac{hf}{E_g} \right),$$

with  $hf$  the photon energy,  $E_g$  an "average band gap" and  $\epsilon_g$  proportional to the oscillator strength<sup>6</sup>, is used to extract  $\epsilon_\infty$ <sup>6,16,30,34</sup>. Finally, fitting to  $\ln(J/E)$ <sup>35</sup>, with  $J$  the current density, is also deployed.

The relative permittivity was furthermore investigated at mm-wave frequencies (MM) (10 GHz to 10 THz)<sup>27,36–39</sup> (nicely summarized by Li *et al.*<sup>28</sup>, Yanagimoto *et al.*<sup>40</sup>). Unfortunately, there are often fluctuations in the data or just single data points available, which makes an interpolation to zero frequency ( $= \epsilon_s$ ) not possible. For these reasons we had to discard most of the respective data. We also excluded publications whose values got refined in succeeding experiments<sup>41,42</sup>, that

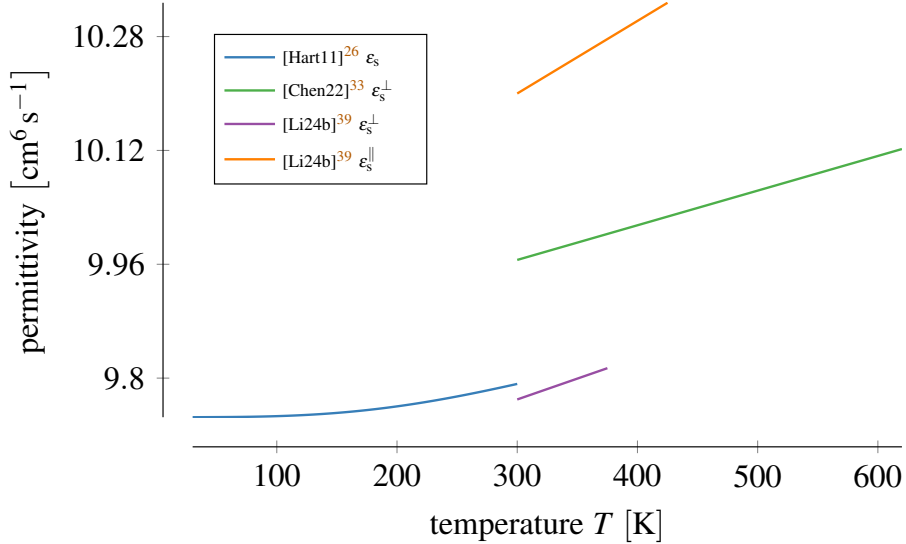


FIG. 1. Temperature dependency of the permittivity.

did not specify the investigated polytype<sup>43–46</sup> or where an extraction of the data values was not possible<sup>47</sup>.

With the listed characterization approaches values in the range of [9.6, 10.65] for the static relative permittivity and [6.25, 7.61] for the high-frequency one have been achieved (Table I). In the table we also show two references that exclusively provide 6H values because these are often referenced for 4H investigations. Wherever necessary we calculated the relative permittivity according to  $\epsilon_s = (\epsilon_s^\parallel \epsilon_s^\perp)^{\frac{1}{2}}$  resp.  $\epsilon_\infty = (\epsilon_\infty^\parallel \epsilon_\infty^\perp)^{\frac{1}{2}}$ <sup>48–52</sup>, which far more often used than  $\epsilon_s = (\epsilon_s^\parallel \epsilon_s^\perp)^{\frac{1}{2}}$  proposed by Ivanov *et al.*<sup>25</sup>.

In TCAD tools the permittivity is a constant although research showed that there is a frequency<sup>26</sup> and temperature<sup>26,33</sup> dependency. For a frequency around 40 GHz Hartnett *et al.*<sup>26</sup> provided the approximation

$$\epsilon_s(T) = 9.7445 + 3.1862 \times 10^{-5} T - 6.3026 \times 10^{-7} T^2 + 5.9848 \times 10^{-9} T^3 - 8.2821 \times 10^{-12} T^4 ,$$

with the temperature  $T$  in K. Cheng, Yang, and Zheng<sup>33</sup> approximated  $\epsilon_s^\perp = 9.82 + 4.87 \times 10^{-4} T$  and Li *et al.*<sup>39</sup>  $\epsilon_s^\perp = 9.77 * (1 + 6 \times 10^{-5}(T - 300\text{K}))$  and  $\epsilon_s^\parallel = 10.2 * (1 + 1 \times 10^{-4}(T - 300\text{K}))$ . All approximations show an increase of the permittivity with temperature (Fig. 1).

TABLE I. Published relative permittivity values.

ref.	$\epsilon_s$	$\epsilon_s^{\parallel}$	$\epsilon_s^{\perp}$	$\epsilon_{\infty}$	$\epsilon_{\infty}^{\parallel}$	$\epsilon_{\infty}^{\perp}$	method <sup>a</sup>	SiC	doping
[Patr70] <sup>b</sup>	9.78 <sup>c</sup>	10.03	9.66	6.58 <sup>c</sup>	6.7	6.52	RI	6H	-
[Ikeda80] <sup>34</sup>	9.94 <sup>c</sup>	10.32	9.76	-	-	-	RI	4H	-
[Nino94] <sup>32</sup>	9.83 <sup>c</sup>	9.98	9.76	6.62 <sup>c</sup>	6.67	6.59	SE	6H	-
[Hari95] <sup>16</sup>	-	-	-	6.63 <sup>c</sup>	6.78	6.56	RI	4H	-
[Karc96] <sup>19</sup>	10.53 <sup>c</sup>	10.9	10.352	7.02 <sup>c</sup>	7.169	6.946	DFT-LDA	4H	-
[Well96] <sup>20</sup>	-	-	-	7.02 <sup>c</sup>	7.17	6.95	DFT-LDA	4H	-
[Adol97] <sup>21</sup>	-	-	-	7.56 <sup>c</sup>	7.61	7.54	DFT-LDA	4H	-
[Ahuja02] <sup>8</sup>	-	-	-	7.11 <sup>c</sup>	7.47	6.94	DFT-LDA	4H	n-type
[Peng04] <sup>22</sup>	-	-	-	6.31 <sup>c</sup>	6.44	6.25	DFT	4H	-
[Pers05] <sup>53</sup>	9.73 <sup>c</sup>	9.94	9.63	6.47 <sup>c</sup>	6.62	6.4	DFT-LDA	4H	intrinsic
[Chin06] <sup>5</sup>	-	-	-	6.81	-	-	DFT-LDA	4H	intrinsic
[Dutt06] <sup>36</sup>	$9.97 \pm 0.02$ <sup>b</sup>	-	-	-	-	-	MM	4H	high purity
[Ivan06] <sup>25</sup>	$9.93 \pm 0.01$	-	-	-	-	-	EMT	4H	intrinsic
[Hart11] <sup>26</sup>	9.77 <sup>d</sup>	-	-	-	-	-	RES	4H	high purity
[Jone11] <sup>27</sup>	9.6	-	-	-	-	-	RES	4H	high purity
[Naft16] <sup>29</sup>	10.11 <sup>c</sup>	10.53 <sup>f</sup>	9.91 <sup>f</sup>	-	-	-	SPEC	4H	undoped
[Cout17] <sup>24</sup>	10.13 <sup>c</sup>	10.65	9.88	-	-	-	DFT-LDA	4H	-
[Tare19] <sup>30</sup>	-	-	-	$6.587 \pm 0.003$	-	-	SPEC	4H	-
[Chen22] <sup>33</sup>	9.97 <sup>g</sup>	-	-	-	-	-	SE	4H	-
[Gao22a] <sup>31</sup>	-	-	-	6.51	-	-	SPEC	4H	-
[Yang22a] <sup>35</sup>	10.21	-	-	-	-	-	$\ln(J/E)$	4H	p-type
[Li23] <sup>28</sup>	-	$10.27 \pm 0.03$	-	-	-	-	RES	4H	high purity
[Li24b] <sup>39</sup>	9.91 <sup>c</sup>	$10.20 \pm 0.05$	$9.77 \pm 0.01$	-	-	-	RES	4H	high purity

<sup>a</sup> description of the single methods in the text

<sup>b</sup> frequency range 131–145 GHz, for lower resp. higher frequencies  $\epsilon_s = 9.74$  was achieved

<sup>c</sup>  $\epsilon_s = (\epsilon_s^{\perp 2} \epsilon_s^{\parallel})^{1/3}$

<sup>d</sup> temperature and frequency dependent

<sup>e</sup> calculated from refractive index  $n$  as  $\epsilon_s = n^2$

<sup>f</sup> wavelength-dependent refractive index presented

<sup>g</sup> temperature dependent

## C. Discussion

We identified two very influential publications, largely dominating the permittivity values found in literature. Ikeda, Matsunami, and Tanaka<sup>34</sup> published, based on measurements from Shaffer<sup>54</sup>, in 1980 the first 4H-SiC permittivity data. Although these values are broadly used in liter-

ature<sup>23,55–59</sup>, we never found a citation of that particular paper. Not even cross-references among the citing publications exist.

In 1970, so ten years prior to the first 4H values, Patrick and Choyke<sup>6</sup> determined, based on measurements published in 1944<sup>60</sup>, the permittivity of the 6H polytype. Many publications on 4H-SiC used these results (see Fig. 2) despite the deviating polytype. Some authors claimed that dedicated 4H values were not available<sup>13,49,61–64</sup>, a mistake as we showed before. Nevertheless, it is still claimed up to this day<sup>33</sup>. This shows, how hard it is to get a comprehensive overview over 4H-SiC TCAD parameters. In contrast to early analysis, that clearly highlight that 6H values were used<sup>65</sup>, the majority of publications simply adopts the parameters without further remark, which leaves the false impression that proper 4H values were used.

Rounding of the original values, e.g.,  $9.66 \rightarrow 9.7 \rightarrow 10$ <sup>68,79</sup> (see Fig. 2), and mere typographical errors, e.g., turning 9.66 into 9.67<sup>88</sup> (a comprehensive analysis of all encountered inconsistencies is shown in ??), expanded the range of available values (see Figs. 3 and 4). In these figures we connected those values where at least one direct connection could be found. Due to missing references we can, however, not guarantee that all authors made their selection based on the same data. In many cases, e.g., for the prominent values  $\epsilon_s = 9.7$  or  $\epsilon_s = 10$ , it is not unreasonable to assume that simply the permittivity in one principal direction was picked.

An interesting case is  $\epsilon_s = 8.5584$ <sup>90,91</sup>, which is supposed to be based on  $\epsilon_s^\perp = 9.66$  and  $\epsilon_s^\parallel = 10.03$ <sup>89</sup>. We were not able to achieve this value analytically since the result is lower than both constituents. Only when we added the high-frequency relative permittivity to the calculations we achieved a somewhat close value of 8. Such a combination is, however, not justifiable.

Overall, the missing awareness regarding 4H related permittivity values is striking. One explanation why the same old values are reused over and over again are the often very long citation (see Fig. 2). Combined with often missing references this makes it difficult to pinpoint the origin of a value and thus assess its suitability. Another interpretation of the achieved results is that the permittivity has little impact in TCAD simulations, such that somewhat accurate 6H values are already sufficient. Nevertheless, even if this was the case, we highly encourage the scientific community to adopt the most recent measurement 4H-SiC in future publications to make these values more prominently known and, thus, lead to a wider distribution.

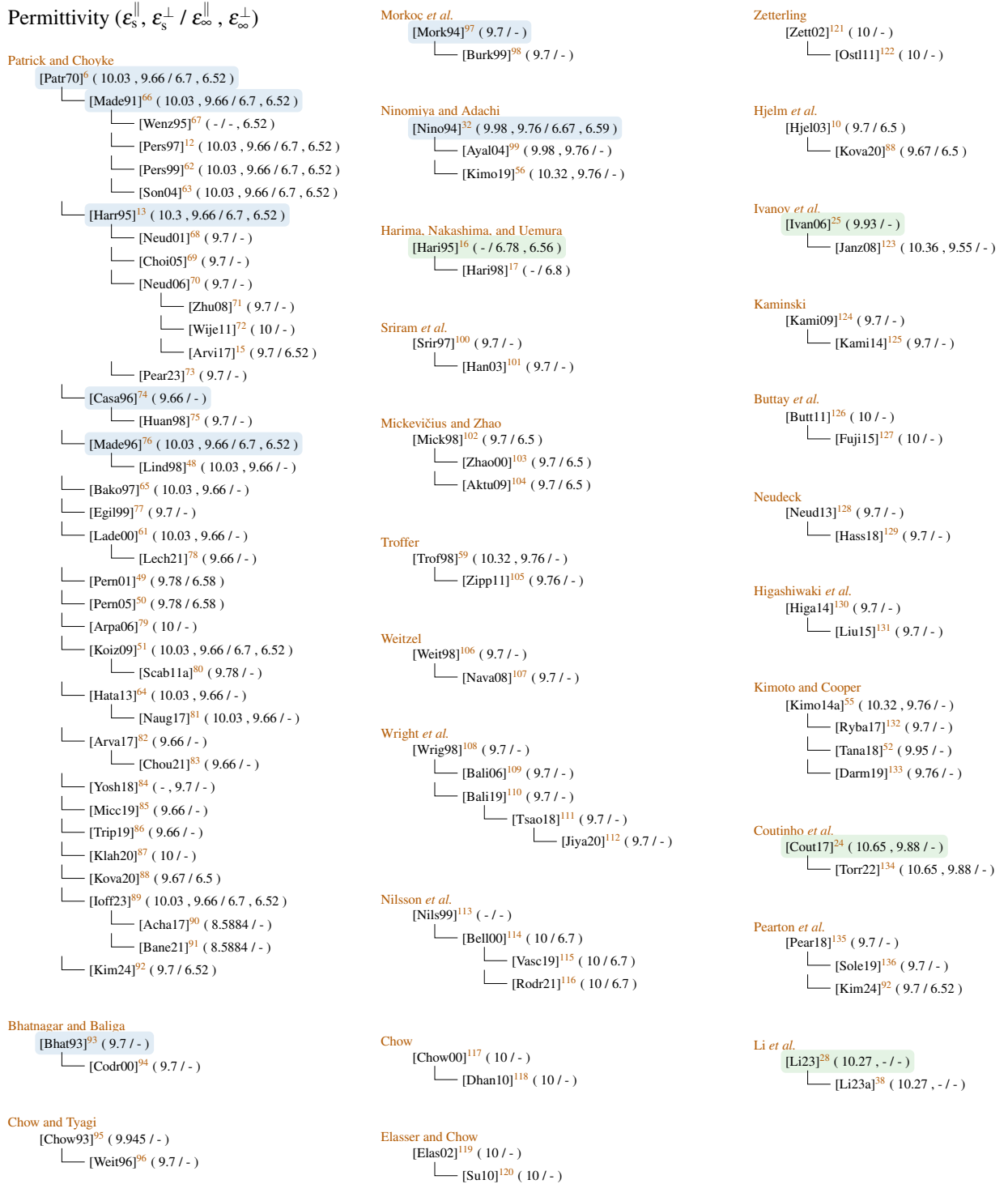


FIG. 2. Reference chains found for the relative permittivity. Publications with blue background are not focused on 4H-SiC, while those in green are novel analyses on 4H-SiC.

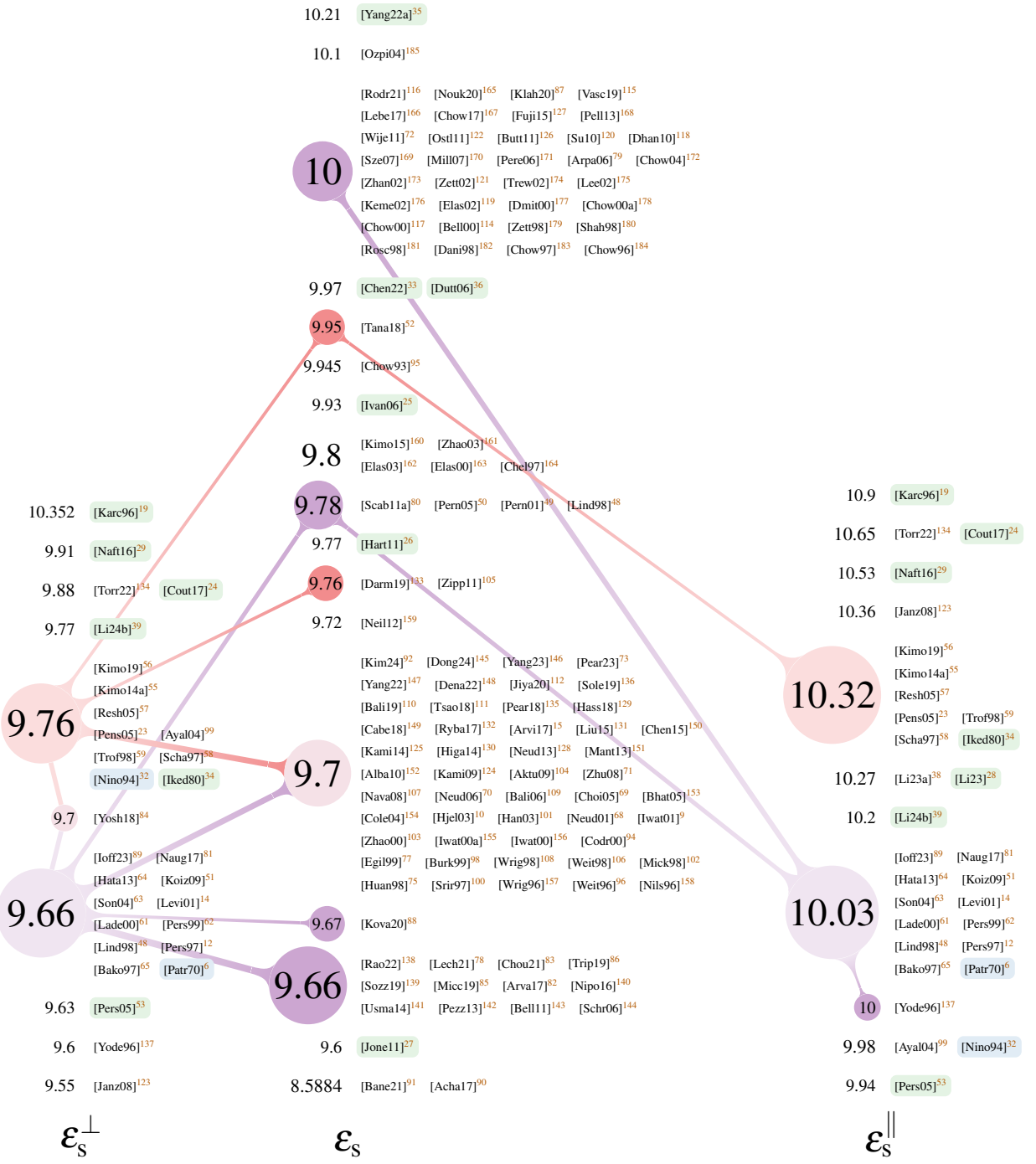


FIG. 3. Published values for the static permittivity. Connected values indicated that at least one connection has been found. References with blue background indicate investigations of non-4H silicon carbide while green background denotes basic 4H-SiC investigations.

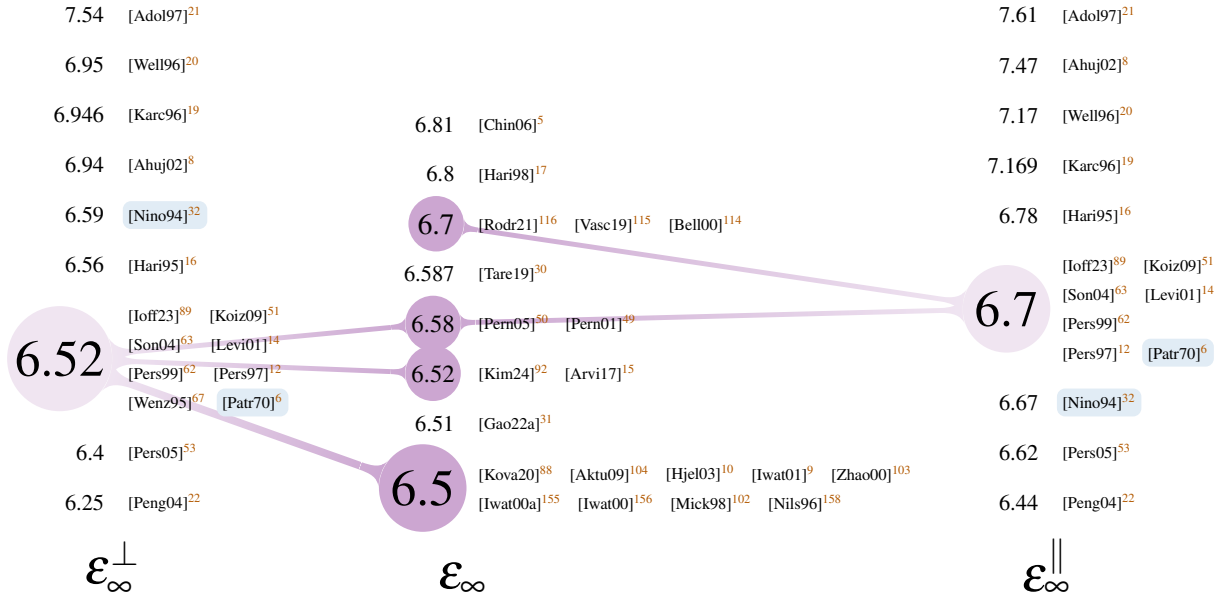


FIG. 4. Published values for the high-frequency permittivity. Connected values indicated that that at least one connection has been found. References with green background indicate investigations of non-4H silicon carbide while blue background denotes basic 4H-SiC investigations.

## II. DENSITY-OF-STATES EFFECTIVE MASS

The effective mass of charge carriers is defined as the reciprocal of the second derivative of the spherically averaged dispersion relation<sup>48</sup> and, thus, dependent on the shape of the conduction/valence band. Because the latter are not uniform in a semiconductor deviating masses for each principal direction are achieved. These direction-dependent values are then further combined to end up with more simplistic descriptions<sup>3</sup>.

In this section we investigate the effective mass of electrons and holes in each principal direction and how these get merged into the density-of-states (DOS) and conductivity mass. We extend earlier overview publications<sup>13,23,58,59,186–188</sup> and focus primarily on the DOS masses because they are used in TCAD simulations in various occasions, e.g., the calculation of the charge carrier concentration or impact and incomplete ionization. We want to highlight that in TCAD tools many additional effective masses are used, e.g., tunneling masses, quantum well masses, effective mass at the contact or in a channel or thermionic relative masses, which must not be confused.

## A. Theory

In the sequel we start with a short theoretical analysis of effective masses. For further information the interested reader is referred to the dedicated literature<sup>3,13,23,53,58,63,186,187,189</sup>. To increase the readability the effective masses are denoted relative to the free electron mass  $m_0$ , i.e.,  $m^* = m/m_0$ <sup>190</sup>.

### 1. Effective Masses along Principal Directions

For electrons the mass is specified in the directions starting in the conduction band minimum at the M point<sup>99,187,191–193</sup> (cp. ??) towards the  $\Gamma$ , K and L point, denoted in the sequel as  $m_{\text{MF}}^*$ ,  $m_{\text{MK}}^*$  and  $m_{\text{ML}}^*$ . The first two are perpendicular to the c-axis and the last one parallel<sup>165,99,194,195</sup>. In the M point two conduction bands are very close together, such that both can influence the effective mass<sup>58,193</sup>. Zhao *et al.*<sup>103</sup> even used three conduction bands. If not otherwise stated we will focus in this paper solely on the lowest one.

The valence band maximum is in the  $\Gamma$  point<sup>59,65,99</sup>. Consequently, the three relative masses are termed  $m_{\text{TM}}^*$ ,  $m_{\text{TK}}^*$  (perpendicular) and  $m_{\text{TA}}^*$  (parallel) indicating the directions towards the M, K and A point<sup>193,196</sup>. At the  $\Gamma$  point three separate bands meet<sup>63,65,191,196,197</sup>, whereat the two topmost are called heavy-hole (hh) and light-hole (lh) and the third one crystal split off (so)<sup>63,197</sup>. Although all have to be considered for an accurate estimation often only a subset is used.

### 2. Density-of-States (DOS) Mass

The effective density of states for conduction ( $N_C$ ) and valence ( $N_V$ ) band<sup>61,80,105,199,200</sup>

$$N_C = 2 M_C \left( \frac{2\pi m_{\text{de}}^* k_B T}{h^2} \right)^{3/2}$$

$$N_V = 2 \left( \frac{2\pi m_{\text{dh}}^* k_B T}{h^2} \right)^{3/2},$$

with  $M_C$  the number of conduction band minima in the first Brillouin zone<sup>200</sup>, is, for example, used to evaluate the electron and hole concentration. The utilized effective density-of-states masses  $m_{\text{de}}^*$  and  $m_{\text{dh}}^*$  are defined as<sup>23,65,77,189</sup>

$$m_{\text{de}}^* = (m_{\text{de}\perp}^* m_{\text{de}\parallel}^*)^{1/3} = (m_{\text{MF}}^* m_{\text{MK}}^* m_{\text{ML}}^*)^{1/3}$$

$$m_{\text{dh}}^* = (m_{\text{dh}\perp}^* m_{\text{dh}\parallel}^*)^{1/3} = (m_{\text{TM}}^* m_{\text{TK}}^* m_{\text{TA}}^*)^{1/3}$$

with<sup>63</sup>

$$\begin{aligned} m_{de\perp}^* &= \sqrt{m_{MF}^* m_{MK}^*}, & m_{de\parallel}^* &= m_{ML}^* \\ m_{dh\perp}^* &= \sqrt{m_{TM}^* m_{TK}^*}, & m_{dh\parallel}^* &= m_{TA}^*. \end{aligned}$$

In this case  $m_{de}^*$  is called the *single valley* DOS electron effective mass<sup>23,64,77,99</sup>, as the factor  $M_C$  is not considered. It is also very common, e.g., in some TCAD tools, to add  $M_C$  to the effective mass<sup>3,65,152,201,202</sup>, i.e.,

$$m_{de}^* = (M_C^2 m_{de\perp}^* {}^2 m_{de\parallel}^*)^{1/3}.$$

In this review we will only present the single valley values and highlight all publications where we found expressions including  $M_C$ .

For an effective mass of the holes it is also necessary to combine the masses of heavy ( $m_{hh}^*$ ) and light ( $m_{lh}^*$ ) holes, which can be achieved by<sup>48,50,169</sup>

$$m_{dh}^* = \left( m_{hh}^* {}^{3/2} + m_{lh}^* {}^{3/2} \right)^{2/3}. \quad (3)$$

This expression is already a simplification, because for accurate results the energy difference between the bands has to be considered<sup>65</sup>. This leads to

$$m_h^*(T) = \left[ m_{h1}^{3/2} + m_{h2}^{3/2} \exp\left(-\frac{\Delta E_2}{k_B T}\right) + m_{h3}^{3/2} \exp\left(-\frac{\Delta E_3}{k_B T}\right) \right]^{2/3} \quad (4)$$

where  $\Delta E_2$  and  $\Delta E_3$  denote the energy separation between the bands.

*a. Temperature Dependency* The changing amount of charge carriers with temperature can be compactly modeled by using a *thermal DOS effective mass*<sup>189,203</sup>. There is no explicit form available but it was calculated by Wellenhofer and Rössler<sup>189</sup> (electrons and holes separately) and Tanaka *et al.*<sup>52</sup> (average effective mass). Later Schadt<sup>58</sup>, Hatakeyama, Fukuda, and Okumura<sup>64</sup> fitted the results from Wellenhofer and Rössler<sup>189</sup> with an equation of the form

$$m^*(T) = \left( \frac{z_0 + z_1 T + z_2 T^2 + z_3 T^3 + z_4 T^4}{1 + n_1 T + n_2 T^2 + n_3 T^3 + n_4 T^4} \right)^\eta \quad (5)$$

for both electrons and holes. Such a change in the effective DOS mass is not yet covered in TCAD simulations suites.

### 3. Conductivity Effective Mass

For investigations of the mobility in 4H-SiC<sup>9,52,58,75,155,156,204–208</sup> the mobility mass is a crucial simplification, e.g., in<sup>187</sup>

$$\mu = \frac{e\tau}{m_c^*},$$

with  $\mu$  the mobility,  $e$  the elementary charge and  $\tau$  the lifetime (see ??). The conductivity mass must not be confused with the DOS mass since its definition<sup>3,209</sup>

$$m_{ce}^* = \frac{3m_{ce\perp}^* m_{ce\parallel}^*}{m_{ce\perp}^* + 2m_{ce\parallel}^*}$$

$$m_{ch}^* = \frac{3m_{ch\perp}^* m_{ch\parallel}^*}{m_{ch\perp}^* + 2m_{ch\parallel}^*}$$

with<sup>204,205</sup>

$$\frac{2}{m_{ce\perp}^*} = \frac{1}{m_{MK}^*} + \frac{1}{m_{M\Gamma}^*}, \quad m_{ce\parallel}^* = m_{ML}^*$$

$$\frac{2}{m_{ch\perp}^*} = \frac{1}{m_{\Gamma M}^*} + \frac{1}{m_{\Gamma K}^*}, \quad m_{ch\parallel}^* = m_{\Gamma A}^*$$

which results in<sup>75</sup>

$$\frac{3}{m_{ce}^*} = \frac{1}{m_{M\Gamma}^*} + \frac{1}{m_{MK}^*} + \frac{1}{m_{ML}^*}$$

$$\frac{3}{m_{ch}^*} = \frac{1}{m_{\Gamma M}^*} + \frac{1}{m_{\Gamma K}^*} + \frac{1}{m_{\Gamma A}^*}.$$

is fundamentally different. In the sequel we will solely concentrate on the DOS mass.

#### 4. Polaron Mass

In the Si-C bond of silicon carbide, carbon atoms are more electronegative than silicon ones. This results in a partly ionic crystal<sup>63</sup>. Within this surrounding a charge carrier, together with its self-induced polarization, forms a quasiparticle, which is called a polaron<sup>210</sup>. This can also be described by longitudinal optical vibrations that generate an electric field along the direction of the vibration which interacts with the charge carriers<sup>63,190</sup>. Effectively, the carrier is “dressed” by a charge leading to a deviating effective mass<sup>12</sup>. The adapted mass  $m_p$ , called *polaron mass*, is slightly higher than the bare mass  $m$  and can be calculated as<sup>12,53,63</sup>

$$m_p = m \frac{1 - 8 \times 10^{-4} \alpha^2}{1 - \alpha/6 + 3.4 \times 10^{-3} \alpha^2} \approx m \left(1 - \frac{\alpha}{6}\right)^{-1}$$

with the Fröhlich constant  $\alpha$  defined as

$$\alpha = \frac{1}{2} \left( \frac{1}{\epsilon_\infty} - \frac{1}{\epsilon_s} \right) \frac{e^2}{\hbar \omega_{LO}} \left( \frac{2m\omega_{LO}}{\hbar} \right)^{1/2} \frac{1}{4\pi\epsilon_s}.$$

In the latter  $e$  denotes the elementary charge,  $\epsilon_s/\epsilon_\infty$  the static/high-frequency dielectric constant and  $\omega_{\text{LO}}$  the longitudinal optical phonon frequency (see Section I). We want to highlight that in some definitions in literature<sup>210–212</sup> the last term  $1/4\pi\epsilon_s$  is missing due to a differing unit system.

Note that in (optically detected) cyclotron resonance measurements always the polaron mass is extracted. For a better comparability it is thus necessary to adapt non-polaron masses, e.g., those achieved by calculations<sup>193</sup>.

## B. Results

In the following we show the results of our investigations. Note that we discarded conductivity masses, e.g., by Mikami, Kaneko, and Kimoto<sup>214</sup>, and solely concentrate on the DOS mass here. We also did not include the results by Son *et al.*<sup>215</sup> since Son *et al.*<sup>63</sup> later stated that the smaller values are due to “errors caused by a broad and asymmetric ODCR line shape with the peak position slightly shifted to lower magnetic fields”.

### 1. Effective Mass along Principal Directions

To determine the effective masses mainly band structure calculations are used. The most common ones are based on the density functional theory (DFT) local density approximation (LDA)<sup>67,104,158,189,192–194,216</sup>. Differing methods, e.g., projector augmented wave (PAW)<sup>196,217</sup>, (full-potential) linearized augmented plane wave ((FP)LAPW)<sup>12,53,63,191,218</sup>, (orthogonalized) linear combination of atomic orbital ((O)LCAO)<sup>5,219</sup>, full-potential linear muffin-tin orbital method (FPLMTO)<sup>220</sup> and hybrid pseudo-potential and tight-binding (HPT)<sup>221</sup>, were utilized in this context. Other calculations include empirical pseudo potentials (EPM)<sup>114,222</sup> and RSP Hamiltonians (RSPH)<sup>197</sup>.

Results achieved by these calculations are sometimes combined using Monte Carlo (MC)<sup>104,158</sup> simulations or genetic algorithm fitting (GAF)<sup>225,226</sup>. In some cases the literature values were used as starting point for further analyses. Based on the data from Son *et al.*<sup>215</sup> such a refinement was executed by Nilsson, Sannemo, and Petersson<sup>158</sup>, whose results then served as starting point for a fitting by Mickevičius and Zhao<sup>102</sup>. Similarly, Mikami, Kaneko, and Kimoto<sup>214</sup> calculated the hole mass as the second derivative of the E-k dispersion by Persson and Lindefelt<sup>191</sup>.

The calculations are complemented by measurements, for example by optically detected cy-

TABLE II. Effective masses in principal directions. Multiple values for the same band are calculated by differing algorithms.

ref.	electron				band	hole				method <sup>a</sup>	polaron
	$m_{\text{MF}}^*$ [ $m_0$ ]	$m_{\text{MK}}^*$ [ $m_0$ ]	$m_{\text{ML}}^*$ [ $m_0$ ]			$m_{\Gamma\text{M}}^*$ [ $m_0$ ]	$m_{\Gamma\text{K}}^*$ [ $m_0$ ]	$m_{\Gamma\text{A}}^*$ [ $m_0$ ]			
[Kack94] <sup>216</sup>	0.62	0.13	0.39	-	-	4.23	2.41	1.73	hh	DFT-LDA	-
	-	-	-	-		0.45	0.77	1.73	lh	DFT-LDA	-
	-	-	-	-		0.74	0.51	0.21	so	DFT-LDA	-
[Karc95] <sup>192</sup>	0.66	0.31	0.3	-	-	-	-	-	-	DFT-LDA	-
[Lamb95] <sup>220</sup>	0.58	0.28	0.31	-	-	-	-	-	-	DFT-LDA	-
[Wenz95] <sup>67</sup>	0.6	0.28	0.19	-	-	-	-	-	-	DFT-LDA	-
[Nils96] <sup>158</sup>	0.43	0.43	0.28	1	-	-	-	-	-	DFT-LDA	-
	0.52	0.21	0.45	2	-	-	-	-	-	DFT-LDA	-
[Pers96] <sup>191</sup>	0.57	0.28	0.31	-	-	-	-	-	-	DFT-LDA	-
[Volm96] <sup>223</sup>	$0.58 \pm 0.01$	$0.31 \pm 0.01$	$0.33 \pm 0.01$	-	-	-	-	-	-	ODCR	y
[Chen97] <sup>221</sup>	1.2	0.19	0.33	-	-	-	-	-	-	DFT-LDA	-
[Pers97] <sup>12</sup>	0.57	0.28	0.31	1	-	-	-	-	-	DFT-LDA	-
	0.59	0.31	0.34	1	-	-	-	-	-	DFT-LDA	-
	0.61	0.29	0.33	1	-	-	-	-	-	DFT-LDA	y
	0.78	0.16	0.71	2	-	-	-	-	-	DFT-LDA	-
	0.8	0.18	0.75	2	-	-	-	-	-	DFT-LDA	-
	0.85	0.17	0.77	2	-	-	-	-	-	DFT-LDA	y
[Pers98a] <sup>224</sup>	-	-	-	-	0.7	3.04	1.64	1	fit	-	-
	-	-	-	-	0.6	0.34	1.64	2	fit	-	-
[Bell00] <sup>114</sup>	0.57	0.23	0.27	-	-	-	-	-	-	EPM	-
[Zhao00a] <sup>219</sup>	$0.62 \pm 0.03$	$0.27 \pm 0.02$	$0.31 \pm 0.02$	-	-	-	-	-	-	DFT-LDA	-
[Penn01] <sup>222</sup>	$0.60 \pm 0.05$	$0.20 \pm 0.02$	$0.36 \pm 0.02$	-	-	-	-	-	-	EPM	-
[Iwat03] <sup>194</sup>	0.59	0.29	-	-	-	-	-	-	-	DFT-LDA	-
[Iwat03a] <sup>206</sup>	0.58	0.3	-	-	-	-	-	-	-	Hall	-
[Dong04] <sup>193</sup>	0.53	0.27	0.3	-	0.86	0.95	1.58	1	DFT-LDA	-	-
	-	-	-	-	0.55	0.52	1.32	2	DFT-LDA	-	-
	-	-	-	-	1.13	1.30	0.21	3	DFT-LDA	-	-
[Chin06] <sup>5</sup>	0.47	-	0.38	-	-	-	-	-	-	DFT-LDA	-
[Ng10] <sup>225</sup>	0.66	0.31	0.34	-	-	-	-	-	-	GAF	-
[Kuro19] <sup>196</sup>	0.54	0.28	0.31	-	0.54	0.54	1.48	-	DFT-LDA	-	-
[Lu21] <sup>217</sup>	0.54	0.3	-	-	2.77	1.82	1.52	-	DFT-LDA	-	-

<sup>a</sup> for explanation see text

clotron resonance (ODCR)<sup>190,208,215,223,227</sup>, photoluminescence<sup>77</sup>, infrared absorption (IR)<sup>200</sup>, Raman scattering<sup>16</sup> and Hall effect measurements<sup>51,206,228,229</sup>. However, for the relative masses in the principal directions (see Table II) calculations clearly dominate. Only two measurements<sup>206,223</sup> could be found for the electron masses whereat not a single experimental evaluation for hole masses was achieved.

In literature the hole bands are either denoted as heavy-hole (hh), light-hole (lh) and crystal split-off (so) or simply as 1, 2, 3. According to the found values we are confident to say that  $1 \equiv \text{hh}$ ,  $2 \equiv \text{lh}$  and  $3 \equiv \text{so}$ .

## 2. DOS Mass

For a comprehensive overview on DOS masses we combine calculations based on the effective masses in the principal directions and values presented in literature (see Table III and Table IV). Again, calculations clearly dominate, however, an increased amount of measurements<sup>51,190,206,215,223,228,229</sup>, including some for the hole mass, could be acquired.

The values show significant deviation. In addition Schadt<sup>58</sup> stated that they are only valid close to the band minimum/maximum as they are calculated there or at very low temperature. Furthermore, Son *et al.*<sup>63</sup> claimed that if the polaron effect is added to the results from Persson and Lindefelt<sup>191,218</sup> the values  $m_{\text{dh}\perp}^* = 0.66$  and  $m_{\text{dh}\parallel}^* = 1.76$  are achieved, which fit the results from ODCR measurements well. In the opinion of these authors it is also important to consider spin-orbit couplings for holes. Zhao *et al.*<sup>103</sup> is the only publication that also provided parameters for a third conduction band, which is, however, 2 eV above the lowest one in the M-point.

According was achieved over the last decades regarding the value of  $M_C$ . Although in early publications rather high values of  $M_C = 12^{230,231}$  or  $M_C = 6^{188,232,233}$  were encountered, almost all more recent publications agree upon  $M_C = 3^{9,14,23,48,58,61,64,65,80,89,105,140,201,203,224,234-236}$ .

We found some deviations among the utilized formalisms. Pennington and Goldsman<sup>237</sup> used  $\sqrt{m_{\text{ML}}^* m_{\text{MK}}^*}$  as the DOS effective mass of electrons, i.e.,  $m_{\text{de}}^* = m_{\text{de}\perp}^*$ . Tilak, Matocha, and Dunne<sup>238</sup> reused the value of  $m_{\text{de}}^*$  but calculated the perpendicular one themselves, which lead to almost identical values. Persson and Lindefelt<sup>224</sup> used for the calculation of the effective mass, i.e.,  $m_{\text{de}}^* = (m_{\text{de}\perp 1}^* m_{\text{de}\parallel}^*)^{1/3}$  only one of the perpendicular masses, which was in the sequel reused<sup>50</sup>. In contrary, Gao *et al.*<sup>31</sup> used  $m_{\text{de}}^* = m_{\text{de}\parallel}^*$ . Ivanov, Magnusson, and Janzén<sup>42</sup> used  $m_{\text{de}\perp}^* = \sqrt{m_{\text{ML}}^* m_{\text{MK}}^*} = 0.32$  resp  $m_{\text{de}\parallel}^* = m_{\text{ML}}^* + 0.58$  by citing Faulkner<sup>239</sup>. We were unable

TABLE III. First half of DOS masses. Multiple values for the same band are calculated by differing algorithms.

ref.	electron				hole				method <sup>h</sup>	polaron
	$m_{de}^*$ [ $m_0$ ]	$m_{de\perp}^*$ [ $m_0$ ]	$m_{de\parallel}^*$ [ $m_0$ ]	band	$m_{dh}^*$ [ $m_0$ ]	$m_{dh\perp}^*$ [ $m_0$ ]	$m_{dh\parallel}^*$ [ $m_0$ ]	band		
[Loma73] <sup>228</sup>	0.20 <sup>a</sup>	0.21	0.19	-	-	-	-	-	Hall	-
[Loma74] <sup>229</sup>	0.20 <sup>a</sup>	0.21	0.19	-	-	-	-	-	Hall	-
[Gotz93] <sup>200</sup>	0.19	0.176	0.224	-	-	-	-	-	IR	-
[Kack94] <sup>216</sup>	0.31 <sup>a</sup>	0.28 <sup>b</sup>	0.39 <sup>c</sup>	-	2.60 <sup>a</sup>	3.19 <sup>b</sup>	1.73 <sup>c</sup>	hh	DFT-LDA	-
	-	-	-	-	0.84 <sup>a</sup>	0.59 <sup>b</sup>	1.73 <sup>c</sup>	lh	DFT-LDA	-
	-	-	-	-	0.43 <sup>a</sup>	0.61 <sup>b</sup>	0.21 <sup>c</sup>	so	DFT-LDA	-
[Hari95] <sup>16</sup>	0.35 <sup>a</sup>	$0.30 \pm 0.07$	$0.48 \pm 0.12$	-	-	-	-	-	Raman	-
[Karc95] <sup>192</sup>	0.39 <sup>a</sup>	0.45 <sup>b</sup>	0.30 <sup>c</sup>	-	-	-	-	-	DFT-LDA	-
[Kord95] <sup>208</sup>	-	0.42	-	-	-	-	-	-	ODCR	y
[Lamb95] <sup>220</sup>	0.35 <sup>a</sup>	0.4	0.27	-	-	-	-	-	DFT-LDA	-
[Son95] <sup>215</sup>	0.37 <sup>a</sup>	0.42	$0.29 \pm 0.03$	-	-	-	-	-	ODCR	y
[Wenz95] <sup>67</sup>	0.32 <sup>a</sup>	0.41 <sup>b</sup>	0.19 <sup>c</sup>	-	-	-	-	-	DFT-LDA	-
[Nils96] <sup>158</sup>	0.37 <sup>a</sup>	0.43 <sup>b</sup>	0.28 <sup>c</sup>	1	-	-	-	-	DFT-LDA	-
	0.37 <sup>a</sup>	0.33 <sup>b</sup>	0.45 <sup>c</sup>	2	-	-	-	-	DFT-LDA	-
[Pers96] <sup>191</sup>	0.37 <sup>a</sup>	0.40 <sup>b</sup>	0.31 <sup>c</sup>	-	-	-	-	-	DFT-LDA	-
[Volm96] <sup>223</sup>	0.39 <sup>a</sup>	0.42 <sup>b</sup>	0.33 <sup>c</sup>	-	-	-	-	-	ODCR	y
[Bako97] <sup>65</sup>	-	-	-	-	0.84	-	-	1	-	-
	-	-	-	-	0.79	-	-	2	-	-
	-	-	-	-	0.78	-	-	3	-	-
[Chen97] <sup>221</sup>	0.42 <sup>a</sup>	0.48 <sup>b</sup>	0.33 <sup>c</sup>	-	-	-	-	-	DFT-LDA	-
[Hemm97] <sup>201</sup>	-	-	-	-	1	-	-	-	-	-
[Lamb97] <sup>197</sup>	-	-	-	-	0.85 <sup>a</sup>	0.62	1.6	hh	RSPH	-
	-	-	-	-	0.84 <sup>a</sup>	0.62	1.55	lh	RSPH	-
	-	-	-	-	0.81 <sup>a</sup>	1.58	0.21	so	RSPH	-
[Pers97] <sup>12</sup>	0.37 <sup>a</sup>	0.40 <sup>b</sup>	0.31 <sup>c</sup>	1	0.82 <sup>a</sup>	0.59	1.56	1	DFT-LDA	-
	0.40 <sup>a</sup>	0.43 <sup>b</sup>	0.34 <sup>c</sup>	1	0.82 <sup>a</sup>	0.59	1.6	1	DFT-LDA	-
	0.39 <sup>a</sup>	0.42 <sup>b</sup>	0.33 <sup>c</sup>	1	0.82 <sup>a</sup>	0.59	1.56	2	DFT-LDA	y
	0.44 <sup>a</sup>	0.35 <sup>b</sup>	0.71 <sup>c</sup>	2	0.82 <sup>a</sup>	0.59	1.6	2	DFT-LDA	-
	0.48 <sup>a</sup>	0.38 <sup>b</sup>	0.75 <sup>c</sup>	2	0.78 <sup>a</sup>	1.49	0.21	3	DFT-LDA	-
	0.48 <sup>a</sup>	0.38 <sup>b</sup>	0.77 <sup>c</sup>	2	0.79 <sup>a</sup>	1.49	0.22	3	DFT-LDA	y

$$^a m_{de}^* = (m_{de\perp}^* m_{de\parallel}^*)^{1/3}$$

$$^b m_{de\perp}^* = \sqrt{m_{MI}^* m_{MK}^*}$$

$$^c m_{de\parallel}^* = m_{ML}^*$$

$$^d m_{dh}^* = (m_{dh\perp}^* m_{dh\parallel}^*)^{1/3}$$

$$^e m_{dh\perp}^* = \sqrt{m_{TM}^* m_{TK}^*}$$

$$^f m_{dh\parallel}^* = m_{TA}^*$$

<sup>h</sup> explanation see text

TABLE IV. Second half of DOS masses. Multiple values for the same band are calculated by differing algorithms.

ref.	electron				hole				method <sup>h</sup>	polaron
	$m_{de}^*$ [ $m_0$ ]	$m_{de\perp}^*$ [ $m_0$ ]	$m_{de\parallel}^*$ [ $m_0$ ]	band	$m_{dh}^*$ [ $m_0$ ]	$m_{dh\perp}^*$ [ $m_0$ ]	$m_{dh\parallel}^*$ [ $m_0$ ]	band		
[Well97] <sup>189</sup>	0.394	-	-	-	-	-	-	-	DFT-LDA	-
[Lind98] <sup>48</sup>	-	-	-	-	1.7	-	-	hh	DFT-LDA	-
-	-	-	-	-	0.48	-	-	lh	DFT-LDA	-
[Pers98a] <sup>224</sup>	-	-	-	-	0.94	1.46 <sup>b</sup>	1.64 <sup>c</sup>	1	fit	-
-	-	-	-	-	0.84	0.45 <sup>b</sup>	1.64 <sup>c</sup>	2	fit	-
-	-	-	-	-	0.88	-	-	3	fit	-
[Egil99] <sup>77</sup>	0.37	-	-	-	-	-	-	-	PL	-
[Pers99b] <sup>218</sup>	-	-	-	-	0.85 <sup>a</sup>	0.62	1.61	1	DFT-LDA	-
-	-	-	-	-	0.84 <sup>a</sup>	0.61	1.62	1	DFT-LDA	-
-	-	-	-	-	0.78 <sup>a</sup>	0.56	1.52	2	DFT-LDA	-
-	-	-	-	-	0.78 <sup>a</sup>	0.58	1.42	2	DFT-LDA	-
-	-	-	-	-	0.78 <sup>a</sup>	1.5	0.21	3	DFT-LDA	-
-	-	-	-	-	0.76 <sup>a</sup>	1.46	0.21	3	DFT-LDA	-
[Bell00] <sup>114</sup>	0.33 <sup>a</sup>	0.36 <sup>b</sup>	0.27 <sup>c</sup>	-	-	-	-	-	EPM	-
[Son00] <sup>190</sup>	0.39 <sup>a</sup>	$0.45 \pm 0.02$	$0.30 \pm 0.02$	-	0.91 <sup>a</sup>	$0.66 \pm 0.02$	$1.75 \pm 0.02$	-	ODCR	y
[Zhao00] <sup>103</sup>	0.37 <sup>a</sup>	0.42	0.28	1	-	-	-	-	-	-
-	0.44 <sup>a</sup>	0.35	0.71	2	-	-	-	-	-	-
-	0.40 <sup>a</sup>	0.66	0.15	3	-	-	-	-	-	-
[Zhao00a] <sup>219</sup>	0.37 <sup>a</sup>	$0.41 \pm 0.02$	0.31 <sup>c</sup>	-	-	-	-	-	DFT-LDA	-
[Penn01] <sup>222</sup>	0.34 <sup>a</sup>	$0.35 \pm 0.02$	$0.31 \pm 0.05$	-	-	-	-	-	EPM	-
[Iwat03] <sup>194</sup>	-	0.41 <sup>b</sup>	-	-	-	-	-	-	DFT-LDA	-
[Iwat03a] <sup>206</sup>	-	0.42 <sup>b</sup>	-	-	-	-	-	-	Hall	-
[Dong04] <sup>193</sup>	0.35 <sup>a</sup>	0.38 <sup>b</sup>	0.30 <sup>c</sup>	-	1.09 <sup>a</sup>	0.90 <sup>b</sup>	1.58 <sup>c</sup>	1	DFT-LDA	-
-	-	-	-	-	0.72 <sup>a</sup>	0.53 <sup>b</sup>	1.32 <sup>c</sup>	2	DFT-LDA	-
-	-	-	-	-	0.67 <sup>a</sup>	1.21 <sup>b</sup>	0.21 <sup>c</sup>	3	DFT-LDA	-
[Chin06] <sup>5</sup>	-	-	0.38 <sup>c</sup>	-	-	-	-	-	DFT-LDA	-
[Aktu09] <sup>104</sup>	0.40	-	-	-	-	-	-	-	DFT-LDA	-
[Koiz09] <sup>51</sup>	-	-	-	-	0.5	-	-	-	Hall	-
[Ng10] <sup>225</sup>	0.41 <sup>a</sup>	0.45 <sup>b</sup>	0.34 <sup>c</sup>	-	-	-	-	-	GAF	-
[Kuro19] <sup>196</sup>	0.36 <sup>a</sup>	0.39 <sup>b</sup>	0.31 <sup>c</sup>	-	0.76 <sup>a</sup>	0.54 <sup>b</sup>	1.48 <sup>c</sup>	-	DFT-LDA	-
[Lu21] <sup>217</sup>	-	0.40 <sup>b</sup>	-	-	1.97 <sup>a</sup>	2.25 <sup>b</sup>	1.52 <sup>c</sup>	-	DFT-LDA	-

$$^a m_{de}^* = (m_{de\perp}^*{}^2 m_{de\parallel}^*)^{1/3}$$

$$^b m_{de\perp}^* = \sqrt{m_{\Gamma M}^* m_{MK}^*}$$

$$^c m_{de\parallel}^* = m_{ML}^*$$

$$^d m_{dh}^* = (m_{dh\perp}^*{}^2 m_{dh\parallel}^*)^{1/3}$$

$$^e m_{dh\perp}^* = \sqrt{m_{\Gamma M}^* m_{\Gamma K}^*}$$

$$^f m_{dh\parallel}^* = m_{\Gamma A}^*$$

<sup>h</sup> explanation see text

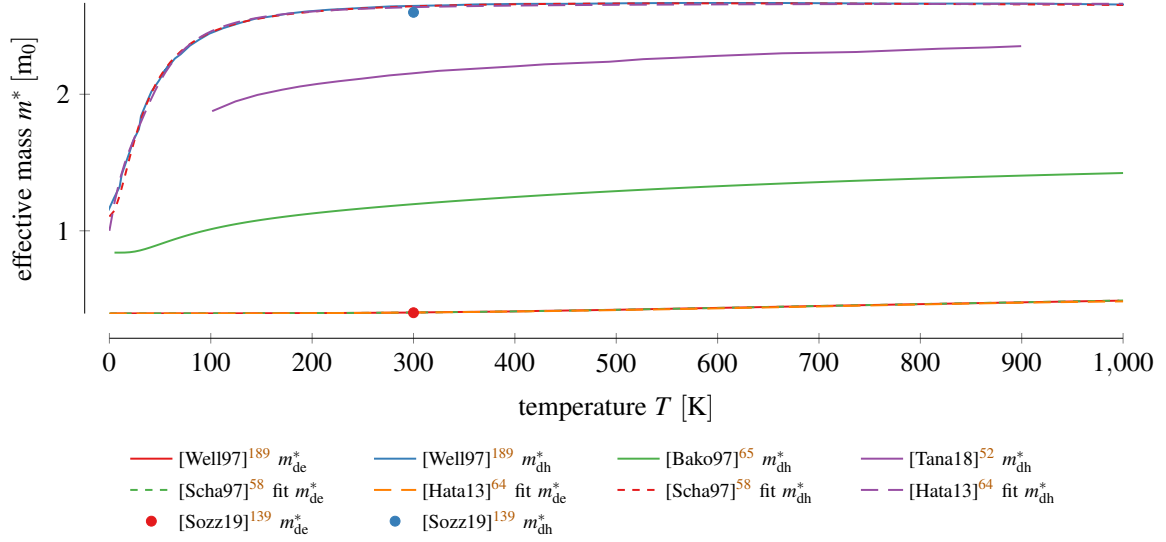


FIG. 5. Temperature dependency of the DOS mass.

TABLE V. Fitting parameters in Eq. (5) to calculations by Wellenhofer and Rössler<sup>189</sup>.

ref.	mass	$z_0$	$z_1$	$z_2$	$z_3$	$z_4$	$n_1$	$n_2$	$n_3$	$n_4$	$\eta$
[Scha97] <sup>58</sup>	$m_{de}^*$	0.3944	$-6.822 \times 10^{-4}$	$1.335 \times 10^{-6}$	$3.597 \times 10^{-10}$	0	$-1.776 \times 10^{-3}$	$3.65 \times 10^{-6}$	0	0	1
[Scha97] <sup>58</sup>	$m_{dh}^*$	1.104	$1.578 \times 10^{-2}$	$3.087 \times 10^{-3}$	$-7.635 \times 10^{-8}$	0	$1.387 \times 10^{-2}$	$1.126 \times 10^{-3}$	0	0	1
[Hata13] <sup>64</sup>	$m_{de}^*$	0.394	0	$3.09 \times 10^{-8}$	$2.23 \times 10^{-10}$	$-1.65 \times 10^{-13}$	0	0	0	0	1
[Hata13] <sup>64</sup>	$m_{dh}^*$	1	$6.92 \times 10^{-2}$	0	0	$1.88 \times 10^{-6}$	0	$6.58 \times 10^{-4}$	0	$4.32 \times 10^{-7}$	2/3

to retrace these equations. Transformed to the set of equations used in this paper we, thus, get  $m_{de\perp}^* = 0.42$  and  $m_{de\parallel}^* = 0.33$ . A more comprehensive listing of all inconsistencies is presented in ??.

### 3. Temperature

The temperature dependency of the DOS masses was calculated by Tanaka *et al.*<sup>52</sup> and Wellenhofer and Rössler<sup>189</sup> (see Fig. 5). Since these calculations can not be described implicitly there exist two fittings for the latter<sup>58,64</sup> using Eq. (5). The respective parameters are shown in Table V.

The temperature scaling of the hole mass considering the separation between the three valence bands in the  $\Gamma$  point<sup>65</sup> (see Eq. (4), also shown in the figure) is described by the coefficients  $m_{h1} = 0.84$ ,  $m_{h2} = 0.79$ ,  $m_{h3} = 0.78$ ,  $\Delta E_2 = 9$  meV and  $\Delta E_3 = 73$  meV. Bakowski, Gustafsson, and Lindefelt<sup>65</sup> stated that these are only valid for low temperatures, which might explain the big

deviations compared to the calculations by Wellenhofer and Rössler<sup>189</sup>. Also shown in the figure are the parameters extracted by Sozzi *et al.*<sup>139</sup> from Wellenhofer and Rössler<sup>189</sup> at 300 K, i.e.,  $m_{de}^* = 0.4$  and  $m_{dh}^* = 2.6$ .

#### 4. Effective DOS Mass for TCAD Tools

For TCAD simulations solely the effective electron and hole masses are interesting. We, therefore, collected all values found for  $m_{de}^*$  and  $m_{dh}^*$  (see Fig. 6). We also added values that we calculated from fundamental masses according to the formalism presented earlier. We just used the first conduction band for  $m_{de}^*$  and Eq. (3) to calculate  $m_{dh}^*$  considering the first two valence bands only.

For electrons the masses are dominantly using values of  $0.37 \pm 0.05$ . For holes the spread is more significant. Although the majority used  $1 \pm 3$  there are also values  $> 2.6$  available. This can be retraced to the significant temperature dependency. Ambivalent in this context is  $m_{dh}^* = 1.2$ . While Bakowski, Gustafsson, and Lindefelt<sup>65</sup> calculated this value for the mass at 300 K others<sup>152,240</sup> seemingly calculated  $m_{dh}^* = \sqrt{m_{dh\perp}^* m_{dh\parallel}^*}$ , i.e., twice the parallel instead of the perpendicular component, resulting in  $m_{dh}^* = 1.26^{57}$  based on the masses by Son *et al.*<sup>190</sup>. Crude rounding then leads to the desired value.

### C. Discussion

The majority of the investigations on the density-of-states masses in 4H-SiC have been conducted in a time frame of one decade between 1994 and 2004. Although the earliest studies in the 70s were measurements, nowadays dominantly calculations are utilized. For the hole mass, actually, up to this day only two measurements could be identified.

Our investigations showed that the value for  $m_{dh}^*$  has to be carefully picked, as a significant change with temperature was observed. Many of the available values, especially those based on calculations, are only valid close to 0 K. For more realistic results a much higher mass has to be used. Nevertheless, almost all temperature dependency fittings are based on the same calculation by Wellenhofer and Rössler<sup>189</sup>. Despite these large variations, temperature is rarely considered<sup>59,105</sup>. Rakheja *et al.*<sup>244</sup> explicitly claims the presented values to correspond to 300 K, although the reference investigation<sup>190</sup> was carried out at 4.4 K.

From the references (see Fig. 8 and Fig. 7) we are able to identify the publications by Persson

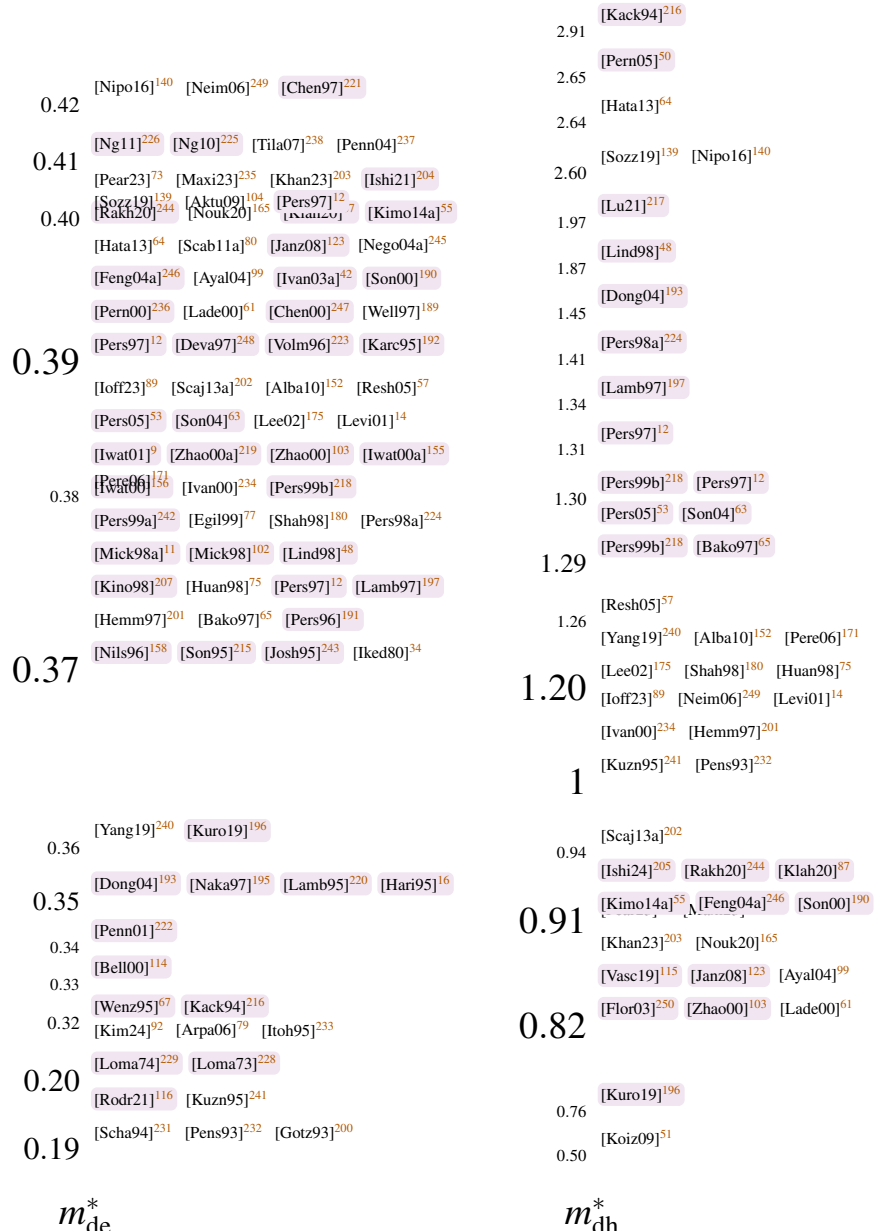


FIG. 6. Effective DOS masses for TCAD tools. A purple background denotes values that we calculated from more fundamental masses using the equations presented in this paper.

*et al.*<sup>12,191,218,224</sup> but also by Volm *et al.*<sup>223</sup>,<sup>189</sup> and<sup>190</sup> as very influential.

At last we shortly want to notice that there have been hints that the DOS mass is also doping dependent<sup>3</sup>. This was shown for 6H-SiC<sup>242</sup> but not yet for 4H.

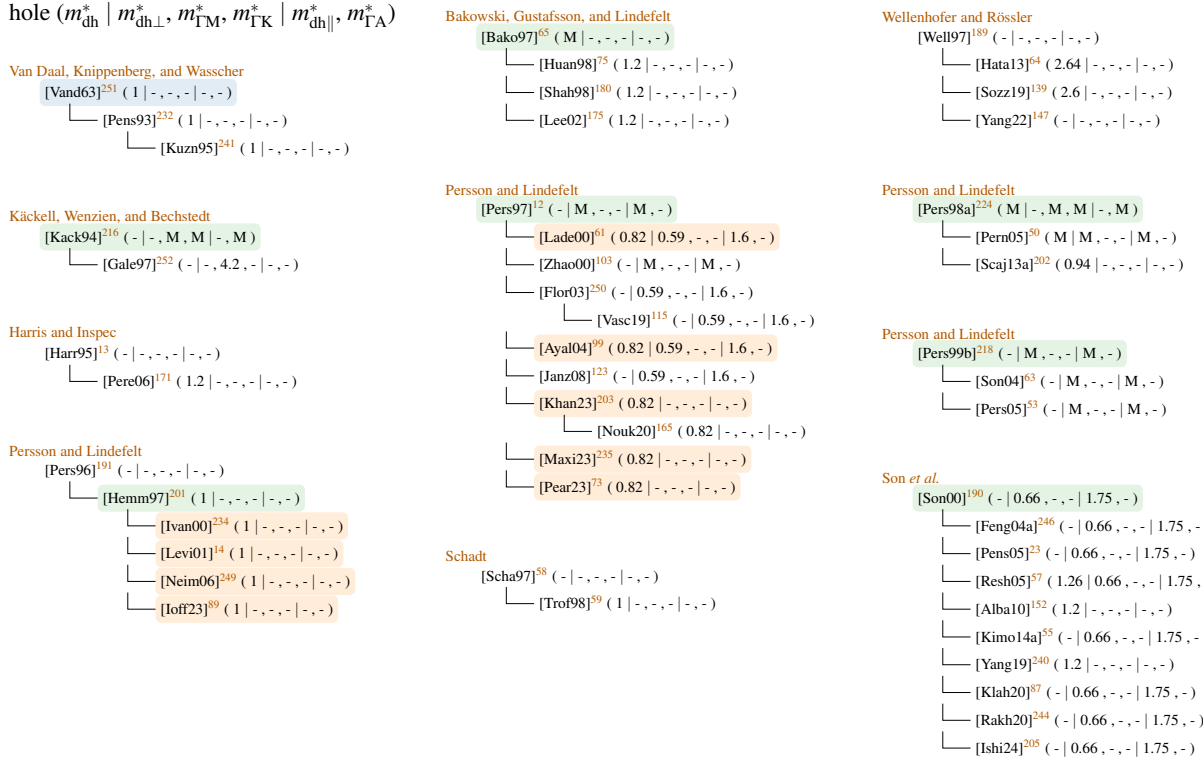


FIG. 7. DOS reference chain for holes. 'M' denotes that multiple values are found in the publication. Entries with green background show fundamental investigations, orange references we inferred based on the used data.

### III. BAND GAP

The band diagram of a material specifies the energy of a charge carrier for a given direction-dependent momentum. The electrons are described by the *conduction band* and the holes by the *valence band*. If both touch the material is called a conductor while a large gap, called the *band gap*, characterizes an insulator. Materials having a band gap in between these two extremes are called semiconductors. This shows that an exact knowledge of the band gap is instrumental to describe the electronic properties of 4H-SiC.

In TCAD simulations the band gap  $E_g$  is essential for the carrier concentration, in the drift diffusion equation and also for the barrier heights in Schottky contacts. Because  $E_g$  is often stated in the exponent, where small changes can have a huge impact, a high accuracy is desired. In this section we are, thus, going to investigate band gap energies published in literature by extending existing overviews<sup>128,254</sup>. Overall, we conclude that the majority of the currently used values are, with high confidence, based on measurement from the year 1964. Despite various variations and

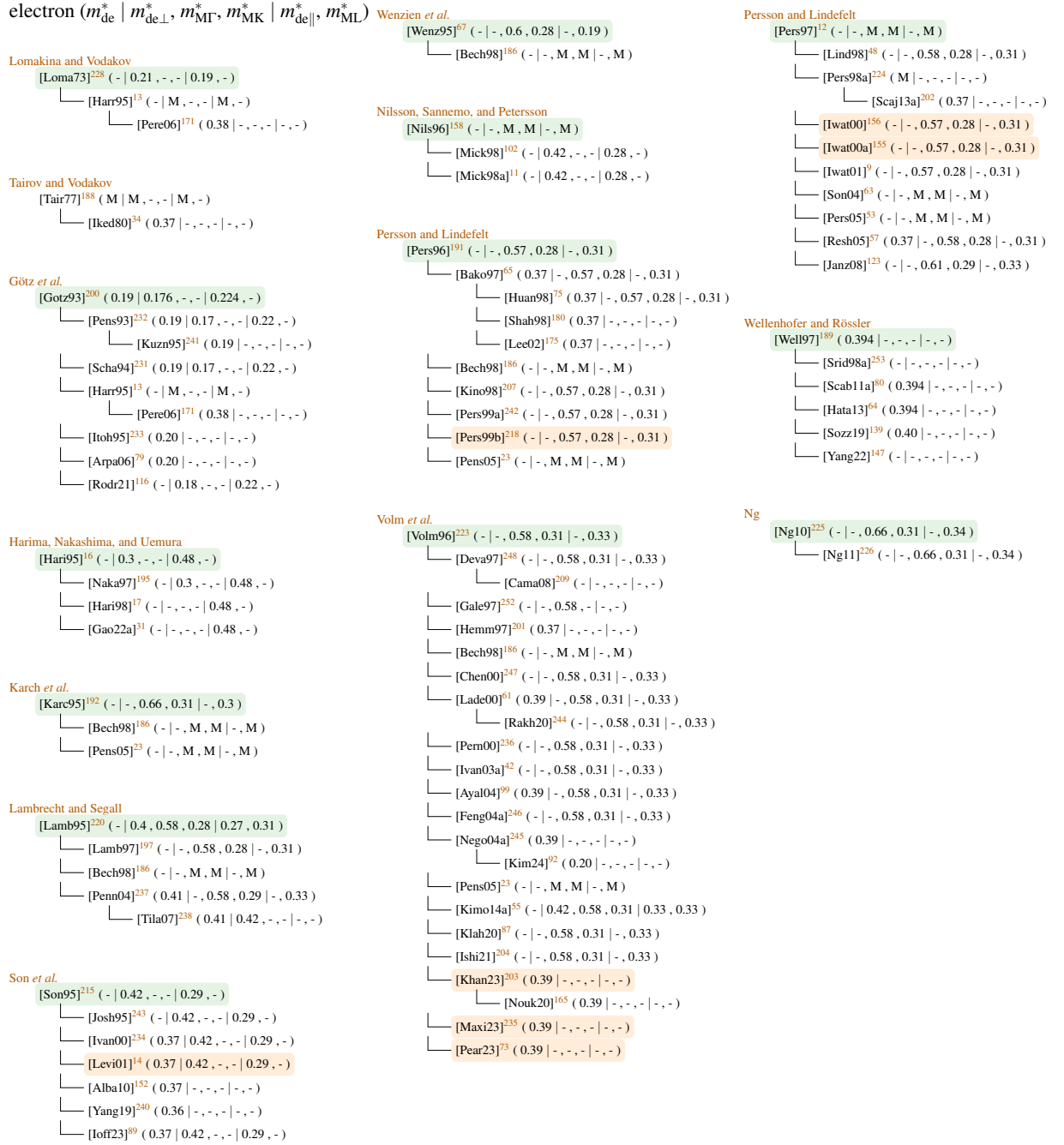


FIG. 8. DOS reference chain for electrons. 'M' denotes that multiple values are found in the publication. Entries with green background show fundamental investigations, orange references we inferred based on the used data and blue investigation based not on 4H.

changes the most commonly used value coincidentally fits latest measurements, however further investigations are required for proper confirmation.

## A. Theory

The band gap is measured between the highest energy value of the valence band in the  $\Gamma$  point (see ??) and the lowest one of the conduction band in the M-point<sup>5,63,89</sup>. Because these are not at the same location 4H-SiC is a so-called indirect semiconductor, which means that some transfer of moment, e.g., by a phonon, is required for the minimum energy difference. Electrons can also be lifted from the valence to the conduction band in the  $\Gamma$  point and then gradually relax towards the minimum, however, in that case more than the band gap energy is required to create an electron-hole pair. An overview of ionization energies for these cases is provided by Gsponer *et al.*<sup>255</sup>, who extracted a value of  $(7.83 \pm 0.02)$  eV from their own measurements.

Our statement that electrons are lifted from the valence to the conduction is not completely correct. Actually, the electron first forms an exciton by Coulomb interactions with the hole it left behind<sup>256–259</sup>. This setup can be compared to the hydrogen atom but with much larger radii due to the much lower effective masses. Additional energy has to be provided before the electron can move freely within the conduction band. Consequently, the band gap energy  $E_g$  is the sum of the energy required to generate the exciton, i.e., the exciton band gap energy  $E_{gx}$ , and the energy to free the electron from the exciton, i.e., the *free exciton binding energy*  $E_x$  (see Eq. (6)<sup>152</sup>).

$$E_g = E_{gx} + E_x \quad (6)$$

The free exciton binding energy  $E_x$  must not be confused with the *bound* exciton binding energy<sup>34,87,200,208,230,256,260–265</sup>. An exciton, which is neutral and thus can relatively easily travel through the lattice, can achieve an energetically better configuration when attaching itself to an impurity<sup>256</sup>. The energy reduction relative to  $E_{gx}$  is represented by the bound exciton binding energy, which depends on the impurity atom, the lattice site and the charge state<sup>266</sup>. Typical values reported in literature are comparable to the free exciton binding energy (in the range of a few meV). Because the same symbol  $E_x$  is used it is challenging to distinguish bound and free exciton binding energy.

The band gap energy is not a constant. First and foremost it varies among the polytypes of silicon carbide. It was empirically shown that the band gap scales linearly with the degree of

hexagonality, i.e., the ratio of hexagonal to cubic lattice sites<sup>55,267–269</sup>. Because 4H-SiC has a hexagonality of 50 %<sup>270</sup> (cp. Section V) its band gap energy is located halfway between the extreme values. In addition the band gap changes with pressure<sup>3</sup>, under strain<sup>196</sup> and for varying temperature and doping concentrations. These have a significant effect on the device behaviour as the shift in the band edges create, for example, potential barriers which influence the carrier transport across junctions<sup>271</sup>.

In the sequel we are going to investigate band gap narrowing described by Eq. (7), whereat  $E_g(T)$  denotes the temperature induced variation and  $\Delta E_g(N_D^+, N_A^-)$  the doping-induced one.

$$E_g(T, N_D^+, N_A^-) = E_g(T) - \Delta E_g(N_D^+, N_A^-) \quad (7)$$

## 1. Temperature Dependency

Lattice vibrations cause a shift of the band energies and changes in the electron-lattice interaction energy<sup>272</sup>. Because these changes differ among energy levels the effective band gap changes<sup>273</sup>. The temperature dependent band gap (see Eq. (8))<sup>3</sup> contains effects from thermal expansion ( $\Delta E_{\text{th}}(T)$ ) and electron-phonon interaction ( $\Delta E_{\text{ph}}(T)$ ).

$$E_g(T) = E_g(0) - \Delta E_{\text{th}}(T) - \Delta E_{\text{ph}}(T) \quad (8)$$

These effects are hard to separate in experiments<sup>3</sup>, which was, so far, only achieved by Cheng, Yang, and Zheng<sup>33</sup>. Because  $\Delta E_{\text{th}}(T)$  has a much weaker impact<sup>274</sup> and the scaling of both contributions is comparable<sup>275</sup> the models for  $\Delta E_{\text{ph}}(T)$  are, in general, used to describe both with reasonable accuracy. Arvanitopoulos *et al.*<sup>82</sup> extended Eq. (8) by adding an additive term  $\Delta_g^{\text{Fermi}}$  to account for carrier statistics. This is, however, only necessary for devices whose size is close to the de-Broglie wavelength.

For high temperatures the band gap decreases linearly<sup>61,276,277</sup> while for low temperatures non-linear behavior, i.e., quadratic<sup>277</sup> or plateau-like behavior<sup>278</sup> is observed. Quadratic behavior is described by the empirical Varshni relation in Eq. (9)<sup>279</sup> with  $T_g$  some arbitrary characterization temperature.

$$E_g(T) = E_g(T_g) + \alpha \left( \frac{T_g^2}{T_g + \beta} - \frac{T^2}{T + \beta} \right) \quad (9)$$

Multiple authors<sup>274,275,278</sup> criticize that it is not possible to retrace the parameters of this model to physical mechanism-specific quantities (e.g.,  $\beta$  was said to be approximately the Debye temperature which turned out to be not the case, since it sometimes even got negative<sup>141,280,281</sup>) and

the model is unable to provide adequate interpretation of available data sets at low and high temperature<sup>282,283</sup>. For example, Pässler<sup>283</sup> tried to match the values from Choyke, Hamilton, and Patrick<sup>267</sup> but achieved only unrealistic results.

A physically based approach describing a plateau-like behavior at cryogenic temperature is a model of Bose-Einstein type in Eq. (10)<sup>278,284</sup> with  $\Theta_B$  the mean frequency of the involved phonons and  $\alpha_B$  the strength of the electron-phonon interaction<sup>3</sup>.

$$E_g(T) = E_B - \alpha_B \left( 1 + \frac{2}{e^{\Theta_B/T} - 1} \right) \quad (10)$$

The rate of change of the band gap at low temperatures is strongly material specific and depends on the phonon dispersion  $\Delta$ <sup>283</sup>. Eq. (9) is most accurate for  $\Delta \gg 1$ <sup>277,285</sup>, while Eq. (10) represents the lower limit ( $\Delta \rightarrow 0$ ) and is most suitable for  $\Delta < \frac{1}{3}$ <sup>283</sup>. Because most semiconductors show a dispersion in the range of 0.3–0.6<sup>283</sup> Pässler<sup>274,283</sup> proposed the model shown in Eq. (11) with  $\varepsilon$  the entropy and  $\Theta_p$  the average phonon temperature.

$$E_g(T) = E_g(0) - \frac{\varepsilon \Theta_p}{2} \left[ \sqrt[p]{1 + \left( \frac{2T}{\Theta_p} \right)^p} - 1 \right] \quad (11)$$

$$p \approx \sqrt{\frac{1}{\Delta^2} + 1}$$

This model was subsequently extended by Pässler<sup>277</sup> to cover a wider range of the phonon dispersion  $\Delta$  and, thus, promises to bridge the gap between Eq. (9) and Eq. (10).

## 2. Doping Dependency

The band gap also changes due to many-body effects of free carriers, i.e., their interactions among each other and with dopants, which become dominant for small carrier-to-carrier distances (high doping concentrations)<sup>286</sup>. Examples are interactions within a band, across bands and with ionized dopants<sup>48,286,287</sup>. The single effects were investigated extensively on their own<sup>286</sup> and got eventually merged, based on a similar analysis for silicon<sup>287</sup>, for 4H-SiC by Lindefelt<sup>48</sup> to the

model shown in Eq. (12).

$$\begin{aligned}
\Delta E_g(N_D^+, N_A^-) &= -\Delta E_{(n/p)c}(N_D^+) + \Delta E_{(n/p)v}(N_A^-) \\
\Delta E_{nc}(N_D^+) &= A_{nc} \left( \frac{N_D^+}{10^{18}} \right)^{1/3} + B_{nc} \left( \frac{N_D^+}{10^{18}} \right)^{1/2} < 0 \\
\Delta E_{nv}(N_D^+) &= A_{nv} \left( \frac{N_D^+}{10^{18}} \right)^{1/4} + B_{nv} \left( \frac{N_D^+}{10^{18}} \right)^{1/2} > 0 \\
\Delta E_{pc}(N_D^+) &= A_{pc} \left( \frac{N_A^-}{10^{18}} \right)^{1/4} + B_{pc} \left( \frac{N_A^-}{10^{18}} \right)^{1/2} < 0 \\
\Delta E_{pv}(N_D^+) &= A_{pv} \left( \frac{N_A^-}{10^{18}} \right)^{1/3} + B_{pv} \left( \frac{N_A^-}{10^{18}} \right)^{1/2} + C_{pv} \left( \frac{N_A^-}{N_{A0}} \right)^{1/4} > 0
\end{aligned} \tag{12}$$

$\Delta E_{nc}$  and  $\Delta E_{pc}$  denote the change of the conduction band due to *n* and *p* type doping. Because the conduction band energy level drops these factors are negative and thus have to be subtracted from the increase of the valence band denoted by  $\Delta E_{nv}$  and  $\Delta E_{pv}$ .

The term featuring  $C_{pv}$  was added in an extension proposed by Persson, Lindefelt, and Sernelius<sup>62</sup>. The authors define the validity of this model for ionized charge carrier concentrations (see Section V) above a few  $10^{18} \text{ cm}^{-3}$  and claim that a larger displacement is observable in 4H compared to other polytypes. More specifically, the valence band displacement is larger than the conduction band one. Other publications distribute the band gap narrowing equally across valence and conduction band<sup>82</sup> or chose a contribution of  $\Delta E_c/E_g = 0.7$ <sup>288</sup>.

Some TCAD tools merge the prefactor and the denominator  $10^{18}$  often called Jain-Roulston model<sup>287</sup>, as shown in Eq. (13). We get  $A_{xc}^j/A_{xc} = 10^{-6}$  and  $B_{xy}^j/B_{xy} = 10^{-9}$  with  $x \in \{n, p\}, y \in \{c, v\}$ . For the remaining parameters the correlation is not so simply, i.e., we get  $A_{xc}^j/A_{xc} = \approx 3.162 \times 10^{-5}$ . For better comparison we transferred all parameters of Eq. (13) back to their respective counterparts in Eq. (12), except the sum of  $B_{xy}$ , which could obviously not be separated.

$$\begin{aligned}
\Delta E_{gn} &= -A_{nc}^j (N_D^+)^{1/3} + (B_{nv}^j - B_{nc}^j) (N_D^+)^{1/2} + A_{nv}^j (N_D^+)^{1/4} \\
-\Delta E_{gp} &= A_{pc}^j (N_A^-)^{1/3} + (B_{pv}^j - B_{pc}^j) (N_A^-)^{1/2} + A_{pv}^j (N_A^-)^{1/4}
\end{aligned} \tag{13}$$

An alternative approach to describe the doping dependency is to use the Slotboom model (see Eq. (14)), which was originally developed for Si. Ruff, Mitlehner, and Helbig<sup>289</sup> first did it for 6H and Lades<sup>61</sup> later followed for 4H-SiC by fitting to the results in Eq. (12) with  $N$  the and  $N_{n,p}$ .

$$\Delta E_g = C_{n,p} \left( \ln \left( \frac{N}{N_{n,p}} \right) + \sqrt{\left( \ln \left( \frac{N}{N_{n,p}} \right) \right)^2 + G} \right) \tag{14}$$

A more physically based approach is to interpret the band gap reduction as renormalization due to electron-electron interactions alone. To describe this effect Schubert<sup>286</sup> proposed the band gap narrowing described by Eq. (15).

$$\Delta E_g = \frac{e^2}{4\pi\epsilon r_s} \quad (15)$$

The screening radius  $r_s$  is given by the Debye and Thomas-Fermi radii leading to the descriptions for the non-degenerate (see Eq. (16)) and degenerate (see Eq. (17)) case with  $n$  the charge carrier concentration.

$$\Delta E_g = \frac{e^3 \sqrt{n}}{4\pi\epsilon^{3/2} \sqrt{k_B T}} \quad (\text{Debye, non-degenerate}) \quad (16)$$

$$\Delta E_g = \frac{e^3 \sqrt{m_{de}^*(3n)^{1/3}}}{4\pi^{5/3} \epsilon^{3/2} \hbar} \quad (\text{Thomas-Fermi, degenerate}) \quad (17)$$

We want to highlight that in state-of-the-art TCAD tools only Eq. (9) and Eq. (14) are supported out of the box, although some feature the possibility to write custom code for band gap narrowing.

## B. Results & Discussion

Multiple methods to determine the band gap, which were partially discussed by Nava *et al.*<sup>107</sup>, De Napoli<sup>148</sup>, were used in literature. Most of them focus on measurements, e.g., transmission spectroscopy (TS)<sup>8,33</sup>, spectroscopic ellipsometry<sup>290</sup>, photo absorption (PA)<sup>266,267,282,291</sup>, optical admittance (OA)<sup>292</sup>, exciton electroabsorption (EE)<sup>265</sup>, free carrier absorption (FCA)<sup>276</sup>, free exciton luminescence (FEL)<sup>264</sup>, photoluminescence (PL)<sup>208,263,293</sup>, photoconductivity (PC)<sup>294</sup> and wavelength-modulated absorption (WMA)<sup>87,295</sup>. Sometimes the results of multiple measurements are combined to improve the accuracy<sup>260</sup>. Stefanakis and Zekentes<sup>296</sup> states that the free carrier absorption method overestimates the band gap while optical absorption studies deliver more accurate results.

An alternative are calculations, which include empirical pseudopotentials (EP)<sup>114,297–299</sup>, density functional theory local density approximation (DFT-LDA)<sup>5,12,63,134,193,196,217,219,221,300</sup>, rectangular barrier of finite height (RB)<sup>301</sup>, fitting (FT)<sup>14,55,61,64</sup> and genetic algorithm fitting (GAF)<sup>225</sup>.

With these methods mainly results for low temperatures were achieved (see Table VI). Predominantly the exciton band gap energy was measured, whereat the achieved values seem to agree on  $E_{gx} = (3.265 \pm 0.002)$  eV. For the band gap energy only two investigations could be found which deliver  $E_g = 3.285$  eV respectively  $E_g = 3.28$  eV. The calculations show a much larger spread,

however, the latest investigations all propose significantly lower values of  $E_g = (3.15 \pm 0.03)$  eV. For room temperature only few dedicated measurements are available<sup>8,276,282,290,302</sup>, whereas the ones by Ahuja *et al.*<sup>8</sup> have a quite big uncertainty of 98 meV. We only found one publication that investigated the anisotropy<sup>282</sup> achieving the same exciton (band gap) energy for fields parallel resp. perpendicular to the c-axis. The doping induced band gap narrowing is in general not known for these measurements.

TABLE VI: Band gap energies and their temperature dependency fittings. If no temperature dependency parameters (for Eq. (9)) are shown  $T_g$  represents the measurement temperature for the shown energies. Highlighted lines represent no 4H results and calculations.

ref.	band gap			temperature dep.			interval [K]	method <sup>303</sup>
	$E_g$ [eV]	$E_{gx}$ [eV]	$E_x$ [meV]	$T_g$ [K]	$\alpha$ [eV K <sup>-1</sup> ]	$\beta$ [K]		
[Choy57] <sup>291 304</sup>	-	-	-	-	$3.3 \times 10^{-4}$	-	-	PA
[Choy64] <sup>267</sup>	-	$3.263 \pm 0.003$	-	4	-	-	-	PA
[Choy64a] <sup>266 305</sup>	-	3.265	-	4.7	-	-	-	PA
[Jung70] <sup>298</sup>	2.8	-	-	0	-	-	-	EP
[Dubr75] <sup>265</sup>	-	-	$20 \pm 15$	2	-	-	-	EE
[Dubr77] <sup>301</sup>	3.2	-	-	0	-	-	-	RB
[Ikeda80b] <sup>264</sup>	-	3.2639	10	77	-	-	-	FEL
[Gavr90] <sup>306</sup>	2.89	-	-	0	-	-	-	DFT-LDA
[Back94] <sup>297</sup>	3.28	-	-	0	-	-	-	EP
[Park94] <sup>307</sup>	2.14	-	-	0	-	-	-	EP
[Kord95] <sup>208</sup>	-	3.265	-	4.2	-	-	-	PL
[Wenz95] <sup>67</sup>	3.56	-	-	0	-	-	-	DFT-LDA
[Evwa96] <sup>292</sup>	$3.41 \pm 0.03$	-	-	40	-	-	-	OA
[Itoh96] <sup>263 305</sup>	-	3.265	-	4.25	-	-	-	PL
[Kaec96] <sup>308</sup>	2.18	-	-	0	-	-	-	DFT-LDA
[Bako97] <sup>65</sup>	3.19	-	-	300	$3.3 \times 10^{-4}$	0	300–700	FT
[Chen97] <sup>221</sup>	3.27	-	-	0	-	-	-	DFT-LDA
[Pers97] <sup>12</sup>	2.9	-	-	0	-	-	-	DFT-LDA
[Vanh97] <sup>299</sup>	3.28	-	-	0	-	-	-	EP
[Ivan98] <sup>293</sup>	-	3.266	-	2	-	-	-	PL
[Bell00] <sup>114</sup>	3.05	-	-	0	-	-	-	EP
[Lade00] <sup>61 309</sup>	-	3.265	40	0	$3.3 \times 10^{-4}$	$1.05 \times 10^3$	4–200	FT
	-	3.265	40	0	$3.3 \times 10^{-2}$	$1 \times 10^5$	4–600	FT
	-	3.342	40	0	$3.3 \times 10^{-4}$	0	300–700	FT
[Srid00] <sup>295</sup>	-	3.267	-	2	-	-	-	WMA
[Zhao00a] <sup>219</sup>	3.11	-	-	0	-	-	-	DFT-LDA
[Levi01] <sup>14 310</sup>	3.23	-	-	300	$6.5 \times 10^{-4}$	1300	-	FT
[Ahuja02] <sup>8</sup>	$3.260 \pm 0.098$	-	-	300	-	-	-	TS
[Gale02] <sup>276</sup>	3.285	-	-	0	$3.5 \times 10^{-4}$	1100	0–650	FCA
	3.2625	-	-	300	$2.4 \times 10^{-4}$	0	300–650	FCA
[Ivan02] <sup>294</sup>	3.285	-	$20.5 \pm 1.0$	2	-	-	-	PC

[Shal02] <sup>302</sup>	3.18	-	-	300	-	-	-	PL
[Dong04] <sup>193</sup>	2.194	-	-	0	-	-	-	DFT-LDA
[Son04] <sup>63</sup>	3.35	-	-	0	-	-	-	DFT-LDA
[Bala05] <sup>280 311</sup>	3.26	-	-	300	$4.15 \times 10^{-4}$	-131	-	-
[Chin06] <sup>5</sup>	2.433	-	-	0	-	-	-	DFT-LDA
[Griv07] <sup>282</sup>	-	3.267	$30 \pm 10$	0	-	-	0–500	PA
[Tama08a] <sup>312 311</sup>	3.23	-	-	300	$7.036 \times 10^{-4}$	1509	-	-
[Ng10] <sup>225</sup>	3.28	-	-	0	-	-	-	GAF
[Hata13] <sup>64 310</sup>	3.285	3.265	20	0	$9.06 \times 10^{-4}$	2030	0–800	FT
[Kimo14a] <sup>55 310</sup>	-	3.265	20	2	$8.2 \times 10^{-4}$	1800	-	FT
[Yama18] <sup>300</sup>	3.12	-	-	0	-	-	-	DFT-LDA
[Kuro19] <sup>196</sup>	3.15	-	-	0	-	-	-	DFT-LDA
[Klah20] <sup>87</sup>	-	3.2659	40	1.4	-	-	-	WMA
[Lech21] <sup>78 311</sup>	3.265	-	-	0	$10.988 \times 10^{-3}$	32744.3	-	FT
[Lu21] <sup>217</sup>	3.17	-	-	0	-	-	-	DFT-LDA
[Chen22] <sup>33</sup>	3.44	-	-	0	$5.27 \times 10^{-4}$	0	300–620	TS
[Huan22b] <sup>313</sup>	3.18	-	-	0	-	-	-	DFT-LDA
[Torr22] <sup>134</sup>	3.17	-	-	0	-	-	-	DFT-LDA
[Khan23] <sup>203 311</sup>	3.285	-	-	0	$3.3 \times 10^{-4}$	240	-	-
[Main24] <sup>290</sup>	$3.30 \pm 0.02$	-	-	300	-	-	-	SE

The free exciton binding energy  $E_x$  was first estimated by Hagen, Van Kemenade, and Van Der Does De Bye<sup>314</sup> to be around 20 meV, with the side note that further investigations are needed. Later, five measurements were published<sup>87,264,265,282,294</sup>. The achieved values range from 10–40 meV. The value of 10 meV<sup>264</sup> was determined for the activation energy for thermal quenching of free excitons, however, Devaty and Choyke<sup>248</sup> argue that these values are too low to be free exciton binding energies.

## 1. Temperature Dependency

Very few measurements on the temperature dependency are available<sup>33,266,276,282</sup>. The remaining models<sup>14,55,61,64</sup> fit the data published by Choyke<sup>260</sup>, Choyke, Patrick, and Hamilton<sup>266</sup>, Choyke, Hamilton, and Patrick<sup>267</sup> from the 1960s. Surprisingly, the model development only started at the beginning of the 2000s. In 1997 Bakowski, Gustafsson, and Lindefelt<sup>65</sup> were still forced to use the 6H values. In 2004 Ayalew<sup>99</sup> stated that not reliable data are available.

The origin of some of the proposed model parameters<sup>78,203,280</sup> could not be traced back to any scientific publication. Occasionally, we were able to them back to prominent TCAD simulation suites, where these were used as default values. Although Tamaki *et al.*<sup>312</sup> provides a reference

for the used model<sup>74</sup>, we were unable to verify the parameters. By comparison we found that the results are very close to those predicted by Kimoto and Cooper<sup>55</sup> (see Fig. 9).

To describe the temperature dependency the majority resorts to the Varshni model (see Eq. (9)). We would like to highlight that the value  $\alpha = 3.3 \times 10^{-4} \text{ eV K}^{-1}$  was determined by Choyke and Patrick<sup>291</sup> for an undefined polytype of SiC. According to the utilized band gap we suspect it to be 21R-SiC device although Bakowski, Gustafsson, and Lindefelt<sup>65</sup> argued that it was 6H. Nevertheless, a wide range of fittings utilizes this value, i.e., that 4H and 6H share the same temperature dependency<sup>161</sup>. Nallet *et al.*<sup>315</sup> even references 6H values directly<sup>289</sup>, which, however, go back to the same data by Choyke and Patrick<sup>291</sup>.

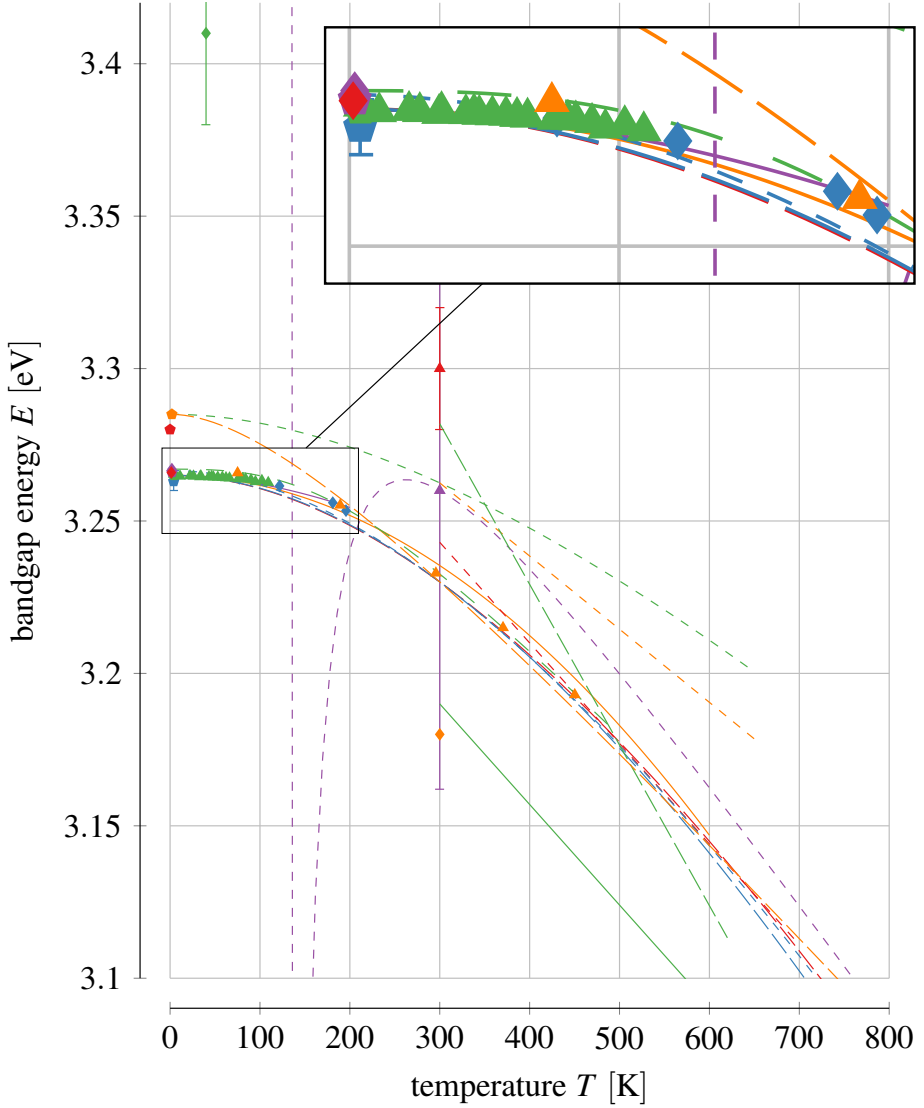
The model presented in Eq. (11) is solely used by Grivickas *et al.*<sup>282</sup> with the parameters shown in Eq. (18).

$$\Theta_p = 450 \text{ K}, \quad \varepsilon = 3 \times 10^{-4} \text{ eV K}^{-1}, \quad p = 2.9. \quad (18)$$

From a graphical representation of the band gap energy versus temperature (see Fig. 9) the deviations of the models becomes evident. We do not show the fitting by Hatakeyama, Fukuda, and Okumura<sup>64</sup> which is identical to the one by Kimoto and Cooper<sup>55</sup>. Similarly, the parameters provided by Lechner<sup>78</sup> reproduce the fitting from Lades<sup>61</sup> (4–600 K).

First of all it has to be noted that the measurements nicely distinguish  $E_g$  and  $E_{gx}$ . The same can not be said for the fittings. For example, Levinstejn, Rumyantsev, and Shur<sup>14</sup> denoted to describe  $E_g$  but the values agree more to  $E_{gx}$ . Also the fitting by Bakowski, Gustafsson, and Lindefelt<sup>65</sup>, who simply took the band gap at 0 K and applied the scaling factor  $\alpha$ , turns out to underestimate the band gap. Newer models, e.g., the one by Cheng, Yang, and Zheng<sup>33</sup>, suggest a much different slope with temperature, actually crossing the traces of  $E_{gx}$  with  $E_g$ . The model by Khanna<sup>203</sup> matches  $E_g$  at low temperatures but at around 200 K it is equal to  $E_{gx}$  and follows that value from there onward. The fitting by Balachandran, Chow, and Agarwal<sup>280</sup> is only feasible for  $T \geq 300 \text{ K}$  as it has a singularity at 131 K.

The plateau achieved by the Pässler model in Eq. (11) is barely visible, showing that the deviations are only subtle. Lades<sup>61</sup> approximated the shape with the Varshni model by just fitting it in a very narrow temperature range. The phonon dispersion of 4H-SiC  $\Delta = 0.29^{282}$  is rather low, which would actually indicates that Eq. (10) is the most suitable, however, Eq. (11) seems to be accurate as well. Even more, Stefanakis and Zekentes<sup>296</sup> compared the single models and identifies Eq. (9) as the most suitable one. In fact, we did not find a single instance where Eq. (10) was used to describe 4H-SiC.



- |   |  |  |
|---|--|--|
| • [Choy64] <sup>267</sup> $E_{\text{gx}}$         | • [Choy64a] <sup>266</sup> $E_{\text{gx}}$   | • [Ikeda80b] <sup>264</sup> $E_{\text{gx}}$  |
| • [Kord95] <sup>208</sup> $E_{\text{gx}}$         | • [Evwa96] <sup>292</sup> $E_g$              | • [Itoh96] <sup>263</sup> $E_{\text{gx}}$    |
| • [Ivan98] <sup>293</sup> $E_{\text{gx}}$         | • [Srid00] <sup>295</sup> $E_{\text{gx}}$    | • [Ahuja02] <sup>8</sup> $E_g$               |
| • [Ivan02] <sup>294</sup> $E_g$                   | • [Shal02] <sup>302</sup> $E_g$              | • [Griv07] <sup>282</sup> $E_{\text{gx}}$    |
| • [Ng10] <sup>225</sup> $E_g$                     | • [Klah20] <sup>87</sup> $E_{\text{gx}}$     | • [Main24] <sup>290</sup> $E_g$              |
| — [Bako97] <sup>65</sup> $E_g$ (V)                | — [Lade00] <sup>61</sup> $E_{\text{gx}}$ (V) | — [Lade00] <sup>61</sup> $E_{\text{gx}}$ (V) |
| - - - [Lade00] <sup>61</sup> $E_{\text{gx}}$ (V)  | - - - [Levi01] <sup>14</sup> $E_g$ (V)       | - - - [Gale02] <sup>276</sup> $E_g$ (V)      |
| - - - [Gale02] <sup>276</sup> $E_g$ (V)           | - - - [Bala05] <sup>280</sup> $E_g$ (V)      | - - - [Tama08a] <sup>312</sup> $E_g$ (V)     |
| - - - [Hata13] <sup>64</sup> $E_{\text{gx}}$ (V)  | - - - [Chen22] <sup>33</sup> $E_g$ (V)       | - - - [Khan23] <sup>203</sup> $E_g$ (V)      |
| - - - [Griv07] <sup>282</sup> $E_{\text{gx}}$ (P) |  |  |

FIG. 9. Band gap measurements and models. The latter are, if available, only shown in the specified confidence interval. (V) denotes a fitting using the Varshni model and (P) fitting with the Pässler model.

TABLE VII. Parameters for ionized dopants induced band gap narrowing.

ref.	method	n-type				p-type				
		$A_{nc}$	$B_{nc}$	$A_{nv}$	$B_{nv}$	$A_{pc}$	$B_{pc}$	$A_{pv}$	$B_{pv}$	$C_{pv}$
		[meV]								
[Lind98] <sup>48</sup>	calculation	-15	-2.93	19	8.74	-15.70	-0.39	13	1.15	-
[Pers99] <sup>62</sup>	calculation	-17.91	-2.20	28.23	6.24	-16.15	-1.07	-35.07	6.74	56.96

TABLE VIII. Parameters for ionized dopants induced band gap narrowing Slotboom model.

ref.	type	$C$	$N$	$G$
		[eV]	[cm <sup>-3</sup> ]	[1]
[Lade00] <sup>61</sup>	n	$2 \times 10^{-2}$	$10^{17}$	0.5
	p	$9 \times 10^{-3}$	$10^{17}$	0.5

## 2. Doping Dependency

Two fittings for the doping dependent narrowing model in Eq. (12) could be found (see Table VII). We want to highlight that these are solely based on calculations. Measurement results are available<sup>282,316</sup>, but due to their sparsity (see Fig. 11) they are not suitable to verify the calculations.

The main issue we identified regarding the parameters is an incorrect sign, as often all parameters become negative (see Fig. 10). The fact that in some cases, e.g., by Lophitis *et al.*<sup>317</sup>, the Jain-Roulston form is used (see Eq. (13)) makes a direct comparison of the parameters challenging. Furthermore, the parameter for the term with exponent 1/2 are sometimes combined<sup>142,143,152</sup>, which makes it potentially impossible to apply them accurately in certain TCAD tools. A detailed analysis of all the inconsistencies we found in literature is provided in ??.

For the Slotboom model, that is used by various publications<sup>61,78,99</sup>, one set of parameters is available<sup>61</sup> (see Table VIII). In contrast to the other models the band gap narrowing is linear in the semi-logarithmic plot (see Fig. 11). In a reasonable doping concentration range the deviation for p-type material is quite low but for n-type material considerable. The models of<sup>48</sup> and<sup>62</sup> only differ by a small amount.

Lindfelft ( $A_{\text{nc}}, A_{\text{nv}}$ ) ( $B_{\text{nc}}, B_{\text{nv}}$ ) ( $A_{\text{pc}}, A_{\text{pv}}$ ) ( $B_{\text{pc}}, B_{\text{pv}}$ ) ( $C_{\text{pv}}$ )

**Lindfelft**

- [Lind98]<sup>48</sup> ( $-1.5 \times 10^{-2}, 1.9 \times 10^{-2}$ ) ( $-2.93 \times 10^{-3}, 8.74 \times 10^{-3}$ ) ( $-1.57 \times 10^{-2}, 1.3 \times 10^{-2}$ ) ( $-3.87 \times 10^{-4}, 1.15 \times 10^{-3}$ ) (-)
  - └─ [Levi01]<sup>14</sup> ( $-1.5 \times 10^{-2}, 1.9 \times 10^{-2}$ ) ( $-2.93 \times 10^{-3}, 8.74 \times 10^{-3}$ ) ( $-1.57 \times 10^{-2}, 1.3 \times 10^{-2}$ ) ( $-3.87 \times 10^{-4}, 1.15 \times 10^{-3}$ ) (-)
  - └─ [Well01]<sup>318</sup> (-, -) (-, -) (-, -) (-)
  - └─ [Cha08]<sup>319</sup> ( $-1.5 \times 10^{-2}, 1.9 \times 10^{-2}$ ) ( $-2.93 \times 10^{-3}, 8.74 \times 10^{-3}$ ) (-, -) (-, -) (-)
    - └─ [Chen12]<sup>320</sup> ( $-1.5 \times 10^{-2}, 1.9 \times 10^{-2}$ ) ( $-2.93 \times 10^{-3}, 8.74 \times 10^{-3}$ ) (-, -) (-, -) (-)
  - └─ [Alba10]<sup>152</sup> ( $-1.5 \times 10^{-2}, 1.9 \times 10^{-2}$ ) ( $1.7 \times 10^{-2}$ ) ( $1.57 \times 10^{-2}, 1.3 \times 10^{-2}$ ) ( $1.54 \times 10^{-2}$ ) (-)
  - └─ [Zhan10]<sup>321</sup> ( $-1.5 \times 10^{-2}, 1.9 \times 10^{-2}$ ) ( $-2.93 \times 10^{-3}, 8.74 \times 10^{-3}$ ) (-, -) (-, -) (-)
  - └─ [Bell11]<sup>143</sup> ( $-1.5 \times 10^{-2}, 1.9 \times 10^{-2}$ ) ( $1.17 \times 10^{-2}$ ) ( $1.57 \times 10^{-2}, 1.3 \times 10^{-2}$ ) ( $1.54 \times 10^{-3}$ ) (-)
  - └─ [Habi11]<sup>271</sup> ( $-1.5 \times 10^{-2}, 1.9 \times 10^{-2}$ ) ( $-2.93 \times 10^{-3}, 8.74 \times 10^{-3}$ ) ( $-1.57 \times 10^{-2}, 1.3 \times 10^{-2}$ ) ( $-3.87 \times 10^{-4}, 1.15 \times 10^{-3}$ ) (-)
  - └─ [Buon12]<sup>322</sup> ( $-1.5 \times 10^{-2}, -1.9 \times 10^{-2}$ ) ( $-2.93 \times 10^{-3}, -8.74 \times 10^{-3}$ ) (-, -) (-, -) (-)
  - └─ [Pezz13]<sup>142</sup> ( $1.5 \times 10^{-2}, 1.9 \times 10^{-2}$ ) ( $1.17 \times 10^{-2}$ ) ( $1.57 \times 10^{-2}, 1.3 \times 10^{-2}$ ) ( $1.54 \times 10^{-3}$ ) (-)
  - └─ [Stef14]<sup>296</sup> ( $-1.5 \times 10^{-2}, 1.9 \times 10^{-2}$ ) ( $-2.93 \times 10^{-3}, 8.74 \times 10^{-3}$ ) ( $-1.57 \times 10^{-2}, 1.3 \times 10^{-2}$ ) ( $-3.87 \times 10^{-4}, 1.15 \times 10^{-3}$ ) (-)
  - └─ [Zegh19]<sup>323</sup> ( $-1.5 \times 10^{-2}, 1.9 \times 10^{-2}$ ) ( $1.17 \times 10^{-2}$ ) ( $-1.37 \times 10^{-2}, 1.3 \times 10^{-2}$ ) ( $1.54 \times 10^{-3}$ ) (-)
  - └─ [Zegh20]<sup>324</sup> ( $-1.5 \times 10^{-2}, 1.9 \times 10^{-2}$ ) ( $1.17 \times 10^{-2}$ ) ( $-1.37 \times 10^{-2}, 1.3 \times 10^{-2}$ ) ( $1.54 \times 10^{-3}$ ) (-)
  - └─ [Ioff23]<sup>89</sup> ( $-1.5 \times 10^{-2}, -1.9 \times 10^{-2}$ ) ( $-2.93 \times 10^{-3}, -8.74 \times 10^{-3}$ ) ( $-1.57 \times 10^{-2}, -1.3 \times 10^{-2}$ ) ( $-3.87 \times 10^{-4}, -1.15 \times 10^{-3}$ ) (-)
  - └─ [Maxi23]<sup>235</sup> ( $-1.5 \times 10^{-2}, -1.9 \times 10^{-2}$ ) ( $-2.93 \times 10^{-3}, -8.74 \times 10^{-3}$ ) ( $-1.57 \times 10^{-2}, -1.3 \times 10^{-2}$ ) ( $-3.87 \times 10^{-4}, -1.15 \times 10^{-3}$ ) (-)

**Persson, Lindfelft, and Sernelius**

- [Pers99]<sup>62</sup> ( $-1.791 \times 10^{-2}, 2.823 \times 10^{-2}$ ) ( $-2.2 \times 10^{-3}, 6.24 \times 10^{-3}$ ) ( $-1.615 \times 10^{-2}, -3.507 \times 10^{-2}$ ) ( $-1.07 \times 10^{-3}, 6.74 \times 10^{-3}$ ) ( $5.696 \times 10^{-2}$ )
  - └─ [Nipo16]<sup>140</sup> (-, -) (-, -) (-, -) (-, -) (-)
  - └─ [Loph18]<sup>317</sup> ( $-1.791 \times 10^{-2}, 2.823 \times 10^{-2}$ ) ( $-2.2 \times 10^{-3}, 6.24 \times 10^{-3}$ ) ( $-7.311 \times 10^{-2}, 3.507 \times 10^{-2}$ ) ( $-1.07 \times 10^{-3}, 6.74 \times 10^{-3}$ ) (-)

Slotboom ( $C_{\text{n}}, N_{\text{n}} \mid C_{\text{p}}, N_{\text{p}} \mid G$ )

**Lades**

- [Lade00]<sup>61</sup> ( $2 \times 10^{-2}, 1 \times 10^{17} \mid 9 \times 10^{-3}, 1 \times 10^{17} \mid 5 \times 10^{-1}$ )
  - └─ [Ayal04]<sup>99</sup> ( $2 \times 10^{-2}, 1 \times 10^{17} \mid 9 \times 10^{-3}, 1 \times 10^{17} \mid 5 \times 10^{-1}$ )
  - └─ [Lech21]<sup>78</sup> ( $2 \times 10^{-2}, 1 \times 10^{17} \mid -, - \mid 5 \times 10^{-1}$ )

FIG. 10. Citations and extracted parameters for the doping dependency of the band gap. If solely a single value is shown for parameter  $B$  then the publication only provides  $B_{\text{c}} + B_{\text{v}}$ .   are fundamental investigations and   connections predicted from the used values.

The band gap narrowing according to Eq. (17) is also shown, because it also occasionally used<sup>288,296</sup>, whereat Stefanakis and Zekentes<sup>296</sup> used a slightly different form of the Thomas-Fermi radius shown in Eq. (19) with  $n_0$  the equilibrium carrier density.

$$\Delta E_{\text{g}} = \frac{e^2}{4\pi\epsilon_0\epsilon_s} \left( \frac{3n_0 e^2}{2\epsilon_0 E_F} \right)^{1/2} \quad (19)$$

Unfortunately our calculations did not succeed to reproduce the results achieved in these publications so we extracted the curve from Donnarumma, Palankovski, and Selberherr<sup>288</sup>. Surprising for us is also the shape of the narrowing, which becomes almost linear in the semi-logarithmic plot for high doping concentrations. With the simple assumption  $n = N_{\text{D}}^+$  resp.  $n = N_{\text{A}}^-$  this does not

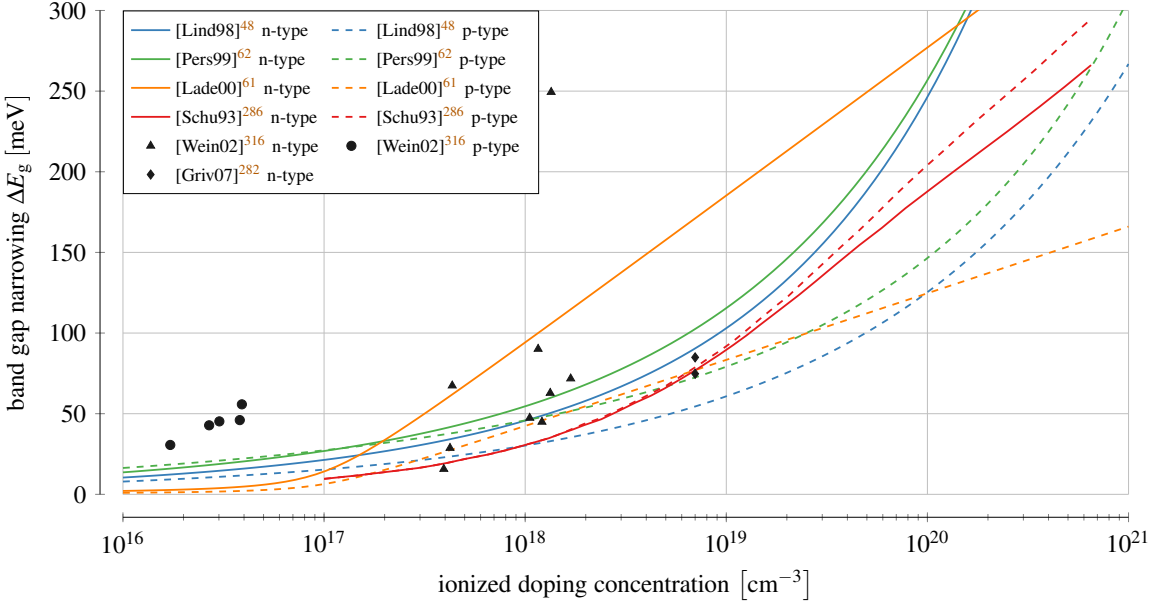


FIG. 11. Doping induced band gap narrowing. The different models complemented by measurement results for p- and n-type material are shown.

seem to be possible. Last Johannesson and Nawaz<sup>325</sup> used the Debye radius from Eq. (16), based on the calculations by Lanyon and Tuft<sup>326</sup>.

### 3. TCAD Values

An overwhelming amount of band gap values can be found in literature (see Fig. 12). Measurements mainly focused on the exciton band gap energy  $E_{gx}$  at low temperatures, resulting in values of  $(3.265 \pm 0.002)$  eV. Using the broadly accepted value of  $E_x = 20$  meV (see also Fig. 15) a band gap energy of  $E_g = 3.285$  eV is achieved, which has also been confirmed by dedicated measurements. The additional higher and lower values mainly stem from temperature dependency models, which were designed for higher temperatures and, thus, lack accuracy at low one. In general, only a few values for the parameters  $\alpha$  and  $\beta$  are used (see Fig. 13), however, the energy value ( $E_g(T_g)$ ) in Eq. (8)) is varied resulting in this wide range of values. Also calculations often deviate significantly. At room temperature few measurements are available such that values are dominated by model fitting.

The question that remains to be answered is on which values the various models for the band gap  $E_g$  are based upon, since there are very few measurements available. Our analysis revealed

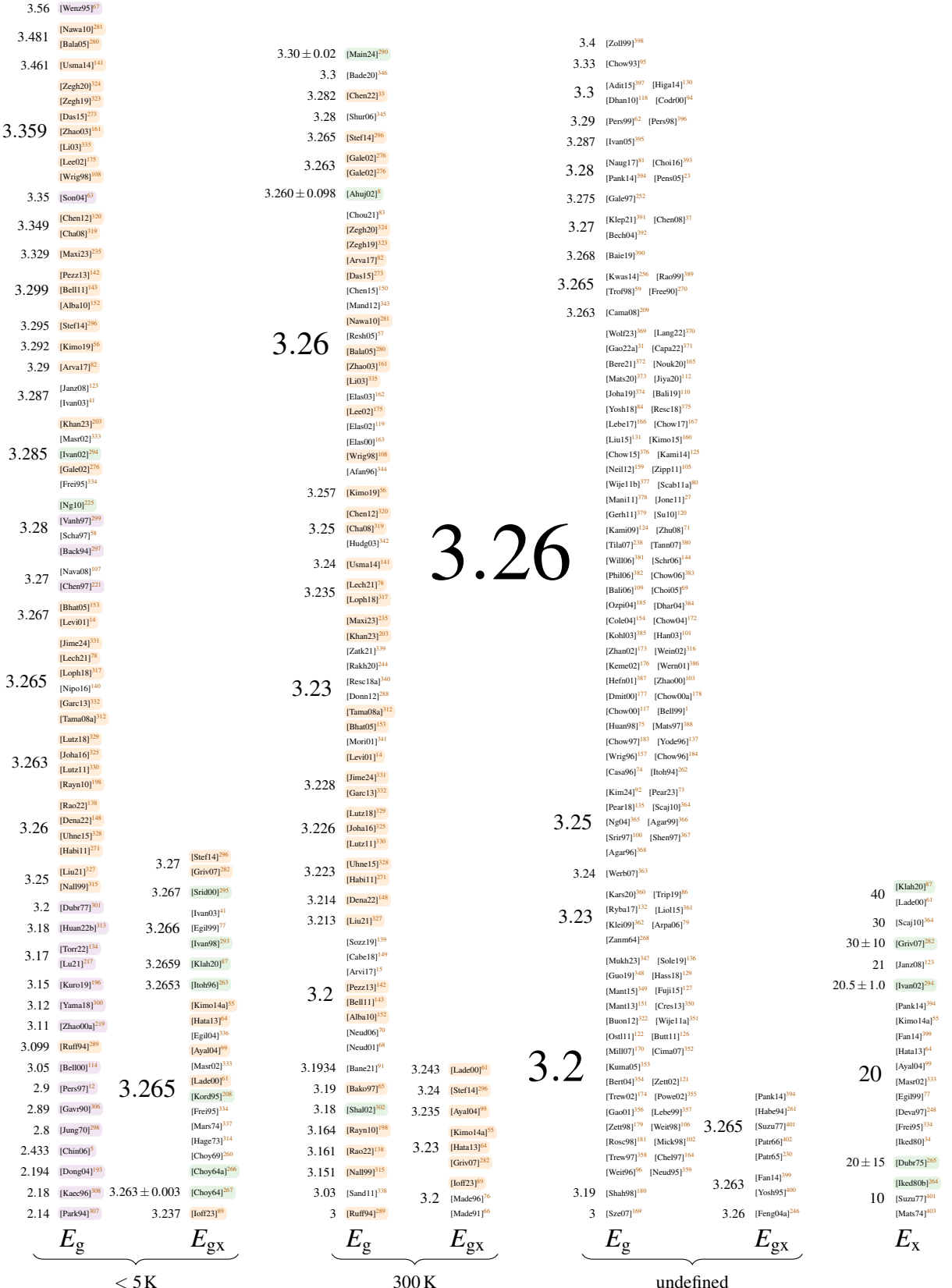


FIG. 12. Values for band gaps at varying temperatures. values correspond to calculations, ones to measurements and ones are values calculated from models.

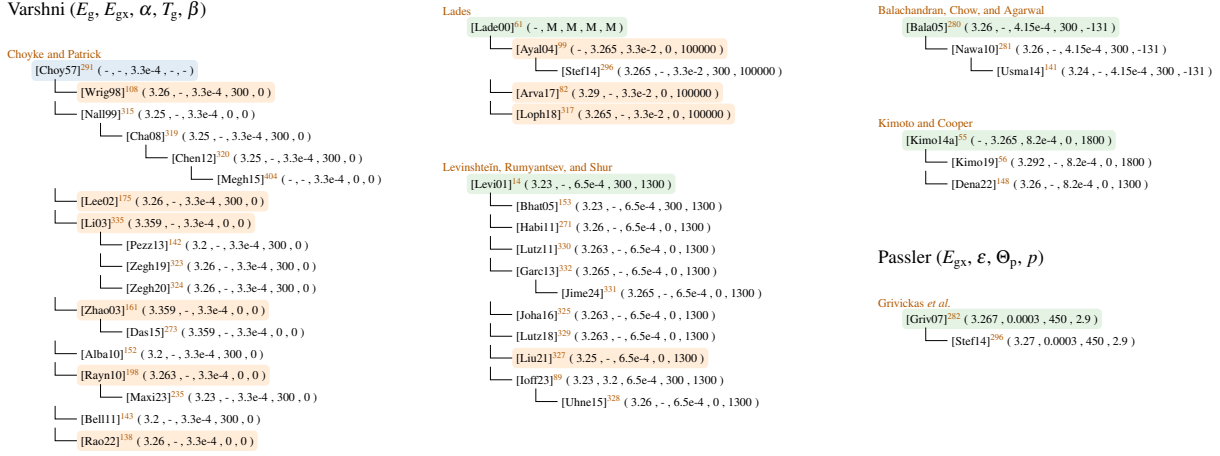


FIG. 13. Citations and the respective values for the temperature dependency.  entries indicate values that have not been determined for 4H-SiC,  are fundamental investigations and  connections predicted from the used values.

that it sounds to assume, that all the values currently in use go back to the investigations of  $E_{\text{gx}}$  by Choyke, Patrick, and Hamilton<sup>266</sup>, Choyke, Hamilton, and Patrick<sup>267</sup> in 1964. Already in 1970 Junginger and Van Haeringen<sup>298</sup> rounded the achieved values of  $E_{\text{gx}} = 3.263 \text{ eV}$  to  $E_g = 3.26 \text{ eV}$ . The same things were observed for the results from Choyke, Patrick, and Hamilton<sup>266</sup>, i.e.,  $E_{\text{gx}} = 3.263 \text{ eV}$ . Stunningly, not only the value was changed but the exciton band gap energy was turned into the band gap energy, completely neglecting the free exciton binding energy. In fact, the excitonic values are nowadays only encountered in sophisticated publications.

Zanmarchi<sup>268</sup> introduced in 1964 for the first time the value  $E_g = 3.23 \text{ eV}$ , which is also commonly used today. Due to missing data at that time it is reasonable to assume that it was derived based on low temperature measurements of the exciton band gap. Also  $E_g = 3.2 \text{ eV}$  seems to result from rounding  $E_g = 3.265 \text{ eV}$ . This was values was also achieved by Dubrovskii and Lepneva<sup>301</sup> who added the excitation band gap  $E_{\text{gx}} = 3.265 \text{ eV}$ <sup>260</sup> and  $E_x = 20 \text{ meV}$  to achieve  $E_g = 3.2 \text{ eV}$ . Solely for  $E_g = 3.25 \text{ eV}$  we have no clear explanation, but maybe it is simply the result of a typographical error when transferring  $E_g = 3.265 \text{ eV}$ .

The outcome of our analysis is thus, that it is possible that the room temperature band gap energies commonly used in literature go back to low temperature exciton band gap energy measurements six decades ago. The fact that Ahuja *et al.*<sup>8</sup> achieved the same value of  $E_g = 3.23 \text{ eV}$  as Zanmarchi<sup>268</sup> 60 years ago shows, that multiple avenues to a specific values are possible and thus such statements not easy to prove. Nevertheless, since we did not find any other derivations,

## Band Gap ( $E_g$ , $E_{\text{gx}}$ , $T$ )

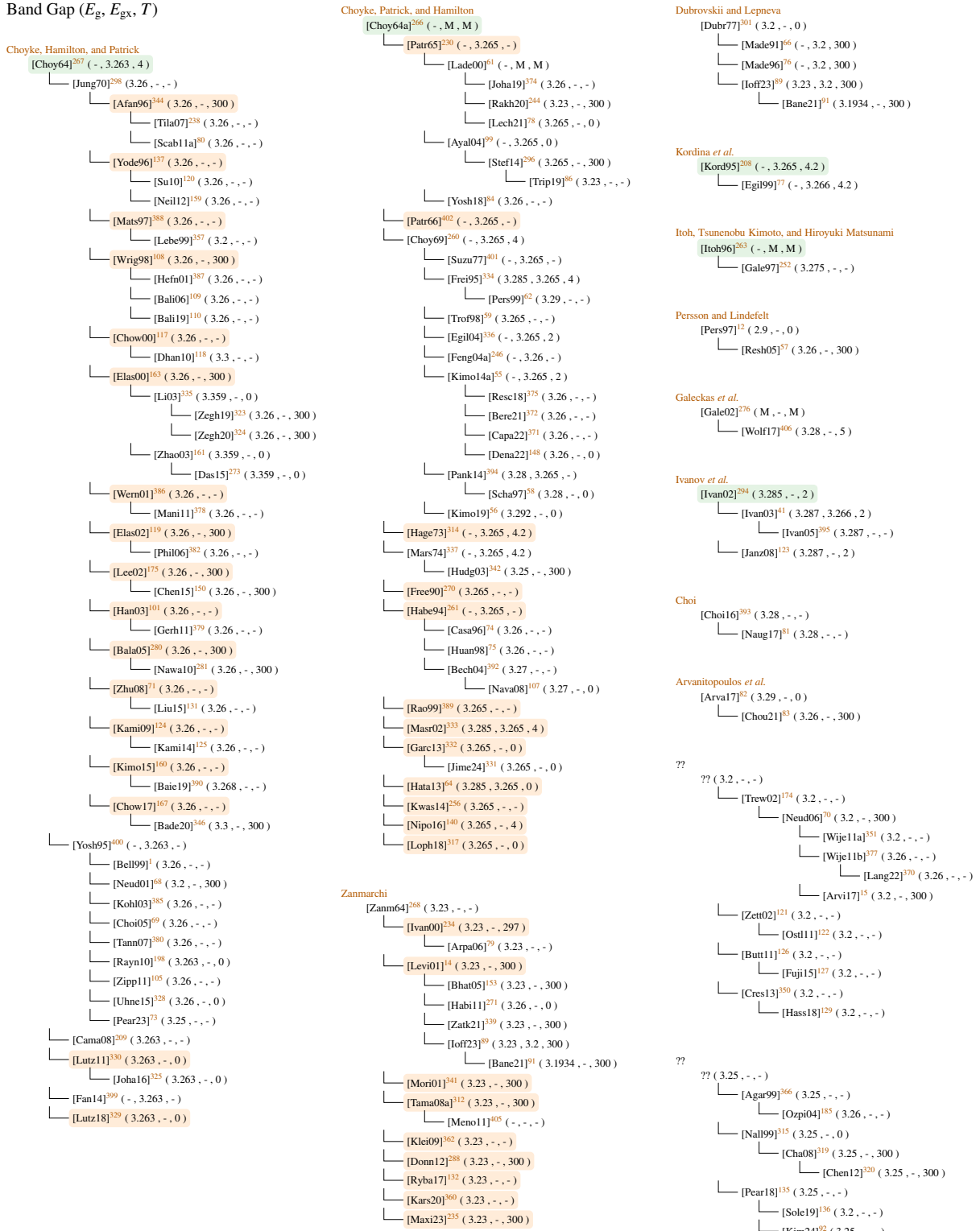


FIG. 14. Citations and values for band gap energies. ■ are fundamental investigations and ■ connections predicted from the used values. We collect publications that share the same value but that do not provide a reference under ??.

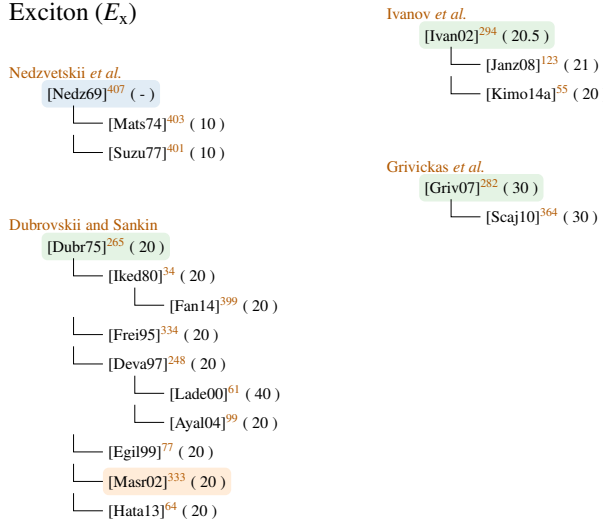


FIG. 15. Citations and values of the free exciton binding energy  $E_x$ .   entries indicate values that have not been determined for 4H-SiC,   are fundamental investigations and   connections predicted from the used values.

we think that the chances that our hypothesis is true is quite high.

Aren't that horrifying news? Well, coincidentally recent measurements by Galeckas *et al.*<sup>276</sup> and Ahuja *et al.*<sup>8</sup> actually suggest that the band gap energy at 300 K is approximately 3.26 eV, whereat it has to be noted that the result by the latter have an uncertainty of 98 meV and thus have to be handled with care. To confirm that  $E_{gx}(0) \approx E_g(300)$  holds, additional verifications are required. In our opinion this also includes an investigation of  $E_x$  versus temperature, which is assumed constant at the moment. The newest models (see Fig. 9), however, suggest an increasing distance between the band gap energies.

An additional avenue for future research would be an investigation of the differences between measurements and calculations. If the latter achieve the actually more accurate results the band gap energy for 4H-SiC might need significant corrections.

#### IV. IMPACT IONIZATION

In high electric fields, charge carriers are able to pick up enough kinetic energy to create an additional electron-hole pair, which is called impact ionization. This effect is sometimes deliberately used, e.g., in avalanche diodes, to increase the responsiveness<sup>3</sup> but often is an undesired effect that leads to breakdown and the destruction of the device. Consequently, impact ionization

simulations are crucial to predict the safe operation regions of a device. In TCAD tools impact ionization is modeled as a (electric field dependent) multiplicative factor that denotes the increase of charge carriers per unit distance.

## A. Theory

The impact ionization is described by the charge carrier generation rate<sup>65,322</sup>

$$G_{II} = \frac{1}{q} (\alpha J_n + \beta J_p) = \frac{1}{q} (\alpha n v_n + \beta p v_p)$$

with  $n$  resp.  $p$  the amount of electron resp. holes,  $v_n$  resp.  $v_p$  their velocity and  $J_n$  resp.  $J_p$  the electron resp. hole current. The impact ionization coefficients for electrons ( $\alpha$ ) and holes ( $\beta$ ) represent the number of secondary carriers a single charge carrier generates per cm in an electric field  $F$ , i.e.,<sup>3</sup>

$$\alpha = \frac{1}{n} \frac{dn}{dx} \text{cm}^{-1} , \quad \beta = \frac{1}{p} \frac{dp}{dx} \text{cm}^{-1} .$$

Many models to describe  $\alpha$  and  $\beta$  were proposed. We will provide a short introduction to the topic, whereat more detailed descriptions are available in literature<sup>3,159,246,408,409</sup>. One of the earliest models is the still very popular empirical Chynoweth's law<sup>410,411</sup>

$$\alpha, \beta(F) = a \exp\left[-\frac{b}{F}\right] , \quad (20)$$

often also called Van Overstraeten-de Man model<sup>412</sup>. This empirical fitting was a necessity at the time of its publication because a physical explanation was only available for strong electric fields as<sup>413</sup>

$$\alpha, \beta(F) = \frac{eF}{E_i} \exp\left[-\frac{3E_p E_i}{(eF\lambda)^2}\right] .$$

This changed with Shockley<sup>414</sup> who modeled the impact ionization coefficient by

$$\alpha, \beta(F) = \frac{eF}{E_i} \exp\left[-\frac{E_i}{eF\lambda}\right] , \quad (21)$$

In this case,  $e$  denotes the electron charge,  $\lambda$  the mean free path and  $E_i$  the ionization energy, i.e., the energy to create an electron-hole pair. The prefactor is the inverse of the length required to gain the ionization energy, i.e., how often per unit length this energy is reached, while the exponential term denotes the chance of doing that without collisions. This model is often called Shockley's "lucky electron"<sup>415</sup>. In Lackner<sup>416</sup> the close relationship between Eq. (20) and Eq. (21), which can

be easily retraced by setting  $a = eF/E_i$  and  $b = E_i/e\lambda$ , is highlighted, leading to a physically based calculation of parameters  $a$  and  $b$ . The author suggests an additional scaling factor, depending on the electric field and the parameter  $b$  for both  $\alpha$  and  $\beta$ , to cover the parameter variations with changing electric field strength.

The low- and high-field cases were finally combined in Baraff's theory<sup>417</sup>, which expresses  $\alpha, \beta \propto \exp[-b/F]$  for low fields and  $\alpha, \beta \propto \exp[-c/F^2]$  for high ones. It was later extended by Thornber<sup>418</sup> to the expression<sup>408</sup>

$$\alpha, \beta(F) = \frac{eF}{\langle E_i \rangle} \exp \left[ -\frac{\langle E_i \rangle}{[(eF\lambda)^2/3E_p] + eF\lambda + E_{k_B T}} \right], \quad (22)$$

with  $\langle E_i \rangle$  the effective ionization threshold<sup>408</sup>,  $E_p$  the optical phonon energy and  $E_{k_B T}$  a temperature contribution that is often neglected in the literature. Konstantinov *et al.*<sup>415</sup> even only used the high-field part for the electrons and dropped the factor  $3E_p$  for the holes in the equation presented in the paper. We assume a typographical error as the division sign is still visible. For the ionization energy  $E_i$  originally a value of  $3/2E_g$  ( $E_g$  the band gap; see Section III) was assumed, which represents the ideal case<sup>165</sup>. Recent measurements, however, revealed for 4H-SiC values between 7.28 and 8.6 eV<sup>255</sup>.

Since Baraff's theory was not able to satisfy all demands<sup>419</sup>, Okuto and Crowell<sup>420</sup> extended Chynoweth's law by adding the electric field as a multiplicative factor, an exponential parameter  $m$  and a temperature dependency via  $c$  and  $d$ . The overall fitting model has the form

$$\alpha, \beta(F) = a\{1 + c(T - 300)\} F^n \exp \left[ -\left( \frac{b\{1 + d(T - 300)\}}{F} \right)^m \right] \quad (23)$$

where  $T$  denotes the temperature in Kelvin. In all investigated publications  $n = 0$  so we will not consider this parameter any further, leading to a simplified model that is often referred to as Selberherr model<sup>409</sup>.

More advanced models were also proposed, which are, however, not yet used in TCAD simulations. These include a more sophisticated temperature dependency in Eq. (23)<sup>421</sup> and models based on multi-stage<sup>422</sup> and inelastic collision events<sup>90</sup>. Other popular methods to investigate the effects of impact ionization are Monte Carlo simulations<sup>10,102–104,114,423–428</sup>, non-localized models<sup>429,430</sup> and the impact of defects<sup>431</sup> in the presence of a magnetic field<sup>432,433</sup>. Some researchers<sup>330,434,435</sup> even combine  $\alpha$  and  $\beta$  to an effective coefficient and model it by a power law, i.e.,  $\alpha, \beta \propto E^n$ , to achieve an analytic expression suitable for calculations.

The impact ionization is anisotropic, meaning that the breakdown field in  $\langle 11\bar{2}0 \rangle$  is about three quarters of the one in  $\langle 0001 \rangle$  direction<sup>436</sup>. For that reason the impact ionization coefficients have

been determined parallel and perpendicular to the c-axis. These can be combined, using a formalism introduced by Hatakeyama<sup>437</sup>, to achieve suitable amplification factors for any desired lattice direction. Jin *et al.*<sup>438</sup> reused the parameter values but introduced a new approach to calculate the "driving force" by considering also the field direction for constant carrier temperature. Nida and Grossner<sup>439</sup> adapted the field strength to an effective  $F^* = (m/m_{\parallel})^{1/2}F$ , with  $m$  resp  $m_{\parallel}$  the effective masses (see Section II).

To depict the changing behavior with temperature either the built-in parameters, as is the case for the Okuto-Crowell model (see Eq. (23)), or a multiplicative factor<sup>440</sup>

$$\gamma = \frac{\tanh\left(\frac{\hbar\omega_{\text{OP}}}{2k_B T_0}\right)}{\tanh\left(\frac{\hbar\omega_{\text{OP}}}{2k_B T_L}\right)} \quad (24)$$

to scale the parameters  $a$  and  $b$  of Eq. (20) is used<sup>61,99,315,437</sup> with  $T_0$  a reference temperature (often 300 K),  $T_L$  the lattice temperature and  $\omega_{\text{OP}}$  the optical phonon energy. We are very confident that the latter corresponds to the longitudinal optical phonon energy  $\omega_{\text{LO}}$  (see Section I) as their respective values match well. Hatakeyama<sup>437</sup>, however, pointed out that for a good fit  $\omega_{\text{OP}} = 190$  meV had to be used, which contradicts experimental results of  $\omega_{\text{LO}} = 120$  meV. Niwa, Suda, and Kimoto<sup>441</sup> use a polynomial of degree two to scale the parameters while Bartsch, Schörner, and Dohnke<sup>434</sup> utilize the ratio  $T/300$  K for this purpose. In contrast, Hamad *et al.*<sup>442</sup> explicitly present parameter values for different temperatures. Nida and Grossner<sup>439</sup> scaled the mean free path by  $\sqrt{\gamma}$  and the ionization energy by the ratio of the bandgap at temperature  $T_L$  and at 300 K.

## B. Results

To measure the impact ionization coefficients an equal amount of charge carriers is generated in a space charge region, either by (pulsed) electron (electron beam induced current (EBIC))<sup>444</sup> or optical beams (optical beam induced current (OBIC))<sup>415,441,442,445–451</sup>. Defects have a significant impact on the coefficients such that EBIC is used to extract parameters at defect-free regions<sup>110</sup>.

The charge carrier generation is executed at varying field strengths. Recording the respective terminal currents enables a comparison against the no-field current and, thus, the determination of the effective amplification. The readout of the current can be executed in DC mode<sup>415,445</sup> (whereat Raghunathan and Baliga<sup>444</sup> state that elimination of leakage current in this case is hard), AC mode<sup>444,448,449</sup> or both combined<sup>446,447</sup>. Additional challenges are the selection of a suitable

test structure, e.g., p-n/n-p diodes or pnp/npn transistors) and the proper separation of electron and hole multiplication phenomena, which we will not further cover in this review. Instead we refer the interested reader to the dedicated literature<sup>415,441,448,450,452,453</sup>.

Monte Carlo simulations are also used for the investigation of the impact ionization. While some are able to extract the impact coefficients as the reciprocal of the average distance<sup>428,454</sup> others solely present simulated values without fitting to any of the earlier presented model<sup>10,102–104,114,423–427,455</sup>. Fitting is, however, crucial to use the results in TCAD simulations tools. For this purpose Stefanakis *et al.*<sup>456</sup> provides fittings to Monte Carlo simulation<sup>114,457</sup>, Nouketcha *et al.*<sup>165</sup> used a genetic algorithm to fit to multiple sources<sup>439,445–447,458,459</sup>, Nida and Grossner<sup>439</sup> fitted their model to values from<sup>415,437,444,446,458</sup> and Stefanakis *et al.*<sup>456</sup> achieved a "global fit" in regard to many 4H investigations<sup>415,446,447,449,451,459</sup>, but also a 6H one<sup>289</sup>, and Monte Carlo simulations<sup>114,457</sup>. Kyuregyan<sup>452</sup> calculated the average of available parameter values without conducting any fitting. According to the authors this is supposed to remove statistical inaccuracies and uncertainties introduced by the characterization methods. Even multiple fittings on the same data were executed. Choi *et al.*<sup>69</sup>, Banerjee<sup>91</sup>, Baliga<sup>110</sup>, Zhao *et al.*<sup>161</sup>, Morisette<sup>341</sup>, Sheridan *et al.*<sup>460</sup> all used the data from Konstantinov *et al.*<sup>415</sup>, however, the ones for Sheridan *et al.*<sup>460</sup> exactly match values achieved for 6H by Ruff, Mitlehner, and Helbig<sup>289</sup>.

TABLE IX. Parameters for fundamental fittings of the Okuto-Crowell model found in literature. If only a single value spanning across two columns is presented the crystal direction was not specified.

ref.	electron							hole							$F$ region
	$a_{\parallel}$	$a_{\perp}$	$b_{\parallel}$	$b_{\perp}$	$c$	$d$	$m$	$a_{\parallel}$	$a_{\perp}$	$b_{\parallel}$	$b_{\perp}$	$c$	$d$	$m$	
	[ $10^6 \text{ cm}^{-1}$ ]	[ $\text{MV cm}^{-1}$ ]	[ $10^{-3}$ ]	[ $10^{-3}$ ]	[1]	[ $10^6 \text{ cm}^{-1}$ ]	[ $\text{MV cm}^{-1}$ ]	[ $10^{-3}$ ]	[ $10^{-3}$ ]	[1]	[ $10^6 \text{ cm}^{-1}$ ]	[ $\text{MV cm}^{-1}$ ]	[ $10^{-3}$ ]	[ $10^{-3}$ ]	[1]
[Ragh99] <sup>444</sup>	-	-	-	-	0	0	1	3.09	17.9	$\pm 0.4$	-3.46	0	1	2.5	3.2
[Bert00] <sup>461j</sup>	0.4	48	15	0	0	1.15	1.8	45	15	0	0	1	-	-	-
[Sher00] <sup>460d</sup>	-	-	-	-	0	0	1	5.18	-	14	-	0	0	1	-
[Moroi01] <sup>341d</sup>	-	-	-	-	0	0	1	-	-	-	-	0	0	1	-
[Ng03] <sup>447</sup>	1.98	9.46	-2.02 <sup>a</sup>	0	1.42	4.38	11.4	-0.913 <sup>a</sup>	0	1.06	1.8-4	-	-	-	-
[Zhao03] <sup>161d</sup>	7.26	23.4	0	0	1	6.85	14.1	0	0	1	-	-	-	-	-
[Hata04] <sup>462</sup>	176	21	33	17	0	0	1	341	29.6	25	16	0	0	1	2-5
[Choi05] <sup>69d</sup>	16.5	25.8	0	0	1	5.5	13.5	0	0	1	1.5-5	-	-	-	-
[Loh08] <sup>446</sup>	2.78	10.5	0	0	1.37	3.51	10.3	0	0	1.09	1-5	-	-	-	-
[Loh09] <sup>463</sup>	-	-	-	-	0	0	1	3.321	10.385	-2.78	0.48 <sup>k</sup>	1.09	1.33-2	-	-
[Nguy11] <sup>448</sup>	0.46	17.8	0	0	1	15.6	17.2	0	0	1	1.5-2.7	-	-	-	-
[Gree12] <sup>453h</sup>	0.019	2.888	0	0	4.828	0.06	1.387	0	0	0.96	1.6-4	-	-	-	-
[Nguy12] <sup>449</sup>	3.36	22.6	0	0	1	8.5	15.97	0	0	1	1.5-4.8	-	-	-	-
[Sun12] <sup>428</sup>	1.803	13.52	0	0	1.2	1.861	9.986	0	0	1.11	1.5-5	-	-	-	-
[Niwa14] <sup>441</sup>	8190	39.4	0	0	1	4.513	12.82	0 <sup>f</sup>	0	1	1.4-2.7	-	-	-	-
[Hama15] <sup>442</sup>	0.99	12.9	0	0	1	1.61	11.5	0	0	1	2.5-7	-	-	-	-
[Niwa15] <sup>458</sup>	0.143	-	4.93	-	0 <sup>e</sup>	0 <sup>e</sup>	2.37	3.14	-	11.8	-	6.3 <sup>c</sup>	1.23 <sup>c</sup>	1.02	1-2.8
[Shar15] <sup>464</sup>	186	-	28	-	0	0	1	301	-	20.5	-	0	0	1	-
[Kyur16] <sup>452i</sup>	38.6	$\pm 15.0$	25.6	$\pm 0.1$	0	0	1	5.31	$\pm 0.30$	13.10	$\pm 0.01$	0	0	1	1-5
[Zhan18] <sup>465</sup>	1.31	13	-1.47	0	1	2.98	13	-1.56	0	1	-	-	-	-	-
[Bali19] <sup>110d</sup>	313	34.5	0	0	1	8.07	15	0	0	1	1.1-5	-	-	-	-
[Zhao19] <sup>451</sup>	0.339	-	5.15	-	0	0	2.37	3.56	-	11.7	-	6.19	1.15	1.02	1-3.2
[Stef20] <sup>450</sup>	-	6.4	-	12.5	0	0	1	-	6	-	13.3	0	0	1	1.3-2
[Bane21] <sup>91d</sup>	100	40.268	0	0	1	41.915	46.428	0	0	1	0.1-1	-	-	-	-
[Chea21] <sup>454g</sup>	0.932	7.19	0	0	1.95	1.75	6.56	0	0	1.45	1.6-10	-	-	-	-
[Stef21] <sup>456e</sup>	2.8	-	20.7	-	-1 <sup>b</sup>	-0.29 <sup>b</sup>	1	2.5	-	12.1	-	1.74 <sup>b</sup>	0.59 <sup>b</sup>	1	-

<sup>a</sup> provided by Cha *et al.*<sup>466</sup>

<sup>b</sup> provided by Steinmann *et al.*<sup>467</sup>

<sup>c</sup> different values suggested by Steinmann *et al.*<sup>467</sup>

<sup>d</sup> values fitted to Konstantinov *et al.*<sup>415</sup>

<sup>e</sup> values fitted to<sup>114,289,415,446,447,449,451,457,459</sup>

<sup>f</sup> temperature dependency stated in the paper that could not be transferred to model formalism

<sup>g</sup>  $a$  and  $b$  presumably stated in  $\text{m}^{-1}$  and  $\text{MV m}^{-1}$  in paper, converted to  $\text{cm}^{-1}$  and  $\text{MV cm}^{-1}$

<sup>h</sup> for  $F > 2.5 \text{ MV cm}^{-1}$  the parameters  $\alpha$  from Ng *et al.*<sup>447</sup> are used

<sup>i</sup> values achieved by averaging of<sup>365,415,441,445-447,453,463</sup>

<sup>j</sup> fitted to Nilsson *et al.*<sup>113</sup>

<sup>k</sup> we changed  $b = 8.9 \times 10^6 - 4.95 \times 10^3 T$  to  $b = 8.9 \times 10^6 + 4.95 \times 10^3 T$  to better match the results in the paper

<sup>l</sup> same values achieved as 6H investigation by Ruff, Mitlehner, and Helbig<sup>289</sup>

TABLE X. Parameters for fundamental fittings of the Thurnber model found in literature. For  $E_{k_B T} = k_B T$  this parameter scales with temperature.

ref.	dir	electron				hole				$F$ region
		$\langle E_i \rangle$	$\lambda$	$E_p$	$E_{k_B T}$	$\langle E_i \rangle$	$\lambda$	$E_p$	$E_{k_B T}$	
		[eV]	[Å]	[meV]	[meV]					
[Kons97] <sup>415f</sup>		10	29.9	120	0	7	32.5	120	0	1.5–10
[Nida19] <sup>439a</sup>		10.61	27	120	$k_B T$	10.87	39.49	85	$k_B T$	1–10
[Nouk20] <sup>165c</sup>	-	7.5	10	92.5	14	6.62	4.8	9	102	0.9–10
[Stei23] <sup>467e</sup>	-	10.6	27	87	$k_B T$	10.9	80	87	$k_B T$	1–10

<sup>a</sup> values picked from specified ranges, fitting to<sup>415,437,444,446,458</sup>

<sup>c</sup>  $3/2 E_g$  instead of  $\langle E_i \rangle$  used in the exponential, fitting to<sup>439,445–447,458,459</sup>

<sup>e</sup> initial values taken from Nida and Grossner<sup>439</sup>

<sup>f</sup> linear term in denominator not used for  $\alpha$

A wide range of Okuto-Crowell (see Table IX) and Thornber (see Table X) model parameters could be identified in literature. In one case we were unable to match the temperature variation of  $\beta$  with  $b = 8.9 \times 10^6 - 4.95 \times 10^3 T^{463}$  with the data presented in the same publication. We achieved much better results with  $d = 8.9 \times 10^6 + 4.95 \times 10^3 T$  with  $T$  the temperature in Kelvin. In Stefanakis *et al.*<sup>450</sup> the fitting for  $\alpha$  also deviates slightly from the plots in the paper. Due to the minor deviation we kept the values as they were. In Cheang, Wong, and Teo<sup>454</sup> the values of parameters  $a$  and  $b$  are two orders of magnitude too high. We suspect that they are specified in m $^{-1}$  resp. MV m $^{-1}$  although in the paper it is explicitly stated as cm $^{-1}$  resp. MV cm $^{-1}$ . Despite these changes we were not able to exactly recreate the plots shown in the paper. We had to exclude the publication by Ng *et al.*<sup>365</sup> as no data are shown in the paper and Cheong *et al.*<sup>468</sup>, Kimoto *et al.*<sup>469</sup> who only specify that SiC is investigated but not the polytype.

A graphical representation of the models describing the impact ionization coefficient for electrons (see Fig. 16) show a spread of approximately one order of magnitude, whereat the deviations increase for low fields. For the crystal direction perpendicular to the c-axis much higher values are determined. This matches qualitatively early estimations, however, the quantities of  $\alpha_{\perp}/\alpha_{\parallel} = 3.5$  used by Lades<sup>61</sup>, Bakowski, Gustafsson, and Lindefelt<sup>65</sup> seems to be too low. For low resp. high fields the fittings of Zhang and You<sup>465</sup> resp. Sharma, Hazdra, and Popelka<sup>464</sup> are too high meaning that the models have to be handled with care in these regions.

For holes (see Fig. 17) the spread in values is much smaller, especially close to a field strength

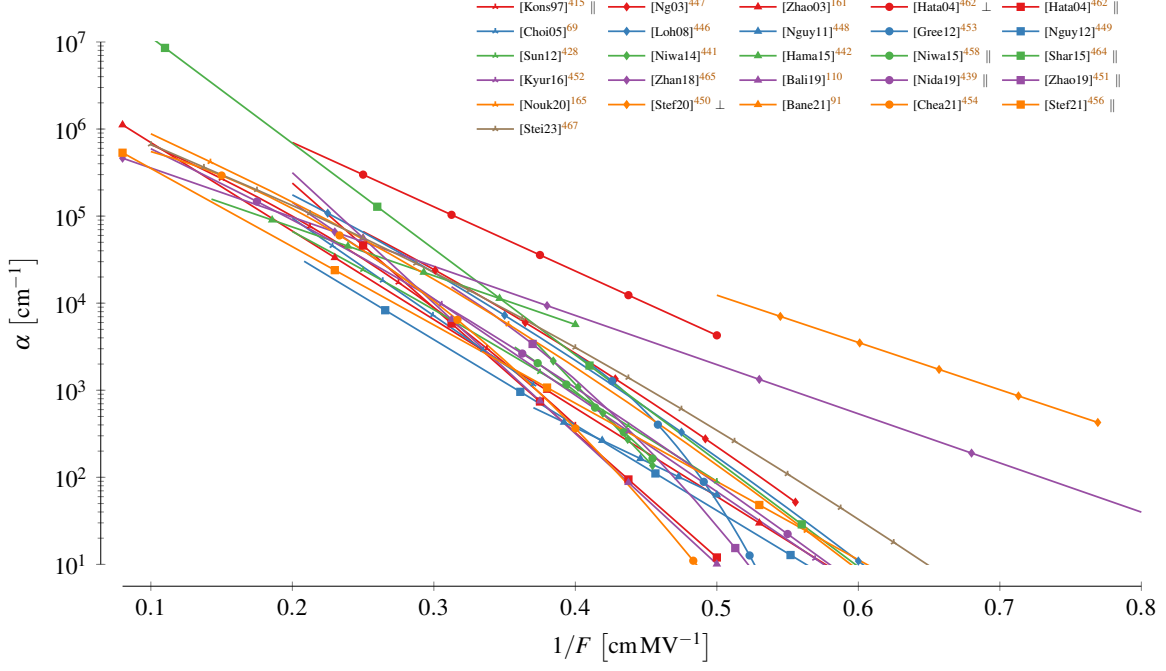


FIG. 16. Impact ionization coefficient  $\alpha$  for electrons. Each model is limited to the interval used for characterization. The colors are altered to increase the readability.

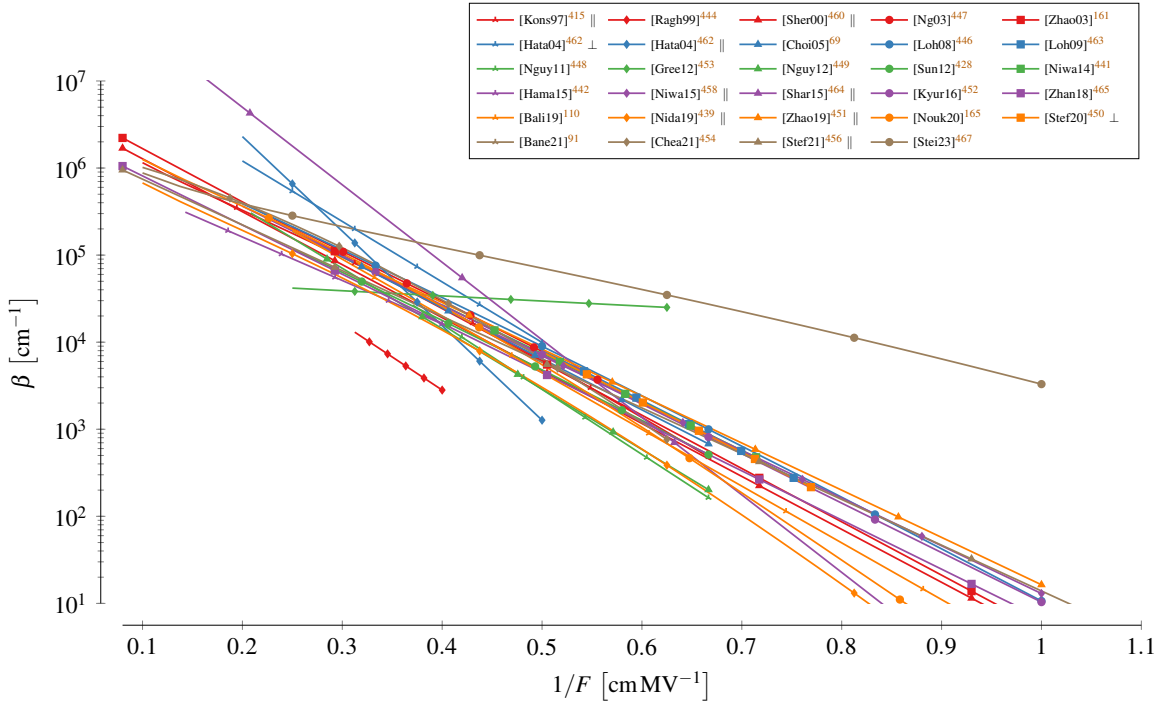


FIG. 17. Impact ionization coefficient  $\beta$  for electrons. Each model is limited to the interval used for characterization. The colors are altered to increase the readability.

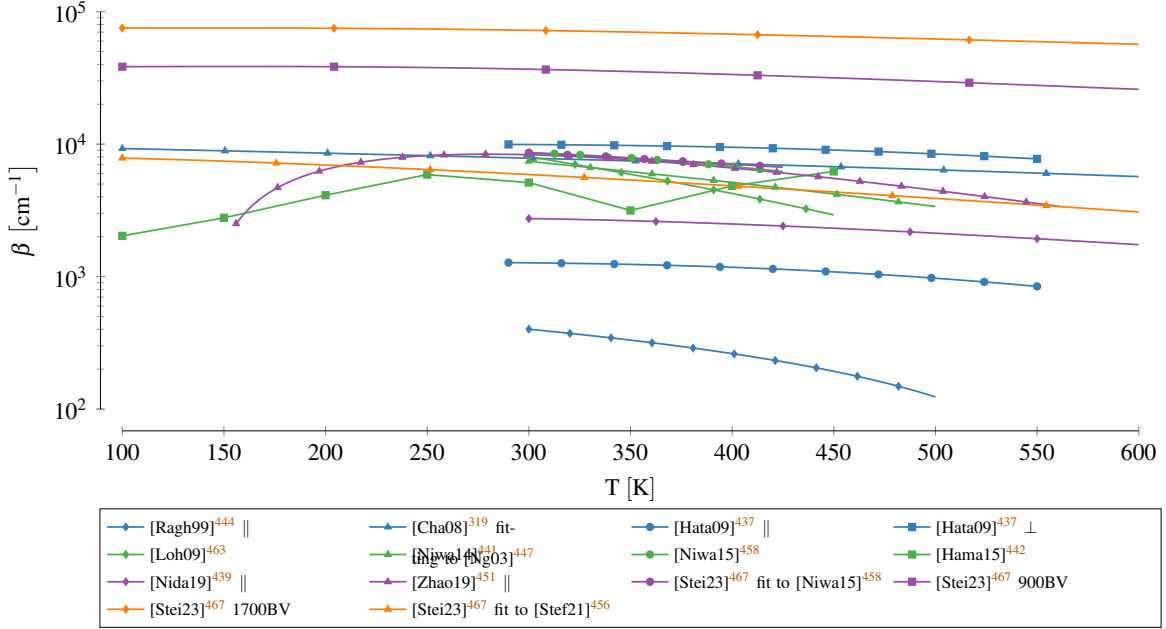


FIG. 18. Temperature dependence of the hole impact ionization coefficient. The single models are evaluated for an electric field of 2 MV cm<sup>-1</sup> and are ordered according to their publication date. The colors simply are used to improve the readability.

around 2 MV cm<sup>-1</sup>. Nevertheless, there are also fittings we want to highlight. The results of Steinmann *et al.*<sup>467</sup> are too high possibly correlating to the fitting of a rather high breakdown voltage. The values from Raghunathan and Baliga<sup>444</sup> are too low, which was attributed to the direction dependency of  $\alpha$ <sup>246,461</sup>, i.e., that the coefficient in the direction perpendicular to the c-axis is much stronger. Feng and Zhao<sup>246</sup> thus conclude that the results in<sup>444</sup> deviate from practical results since the focused beam used in the analyses caused them to miss a large share of the intrinsic defects. Although Fig. 17 supports this statement, the statement that the perpendicular impact ionization of holes is a lot stronger, could not be confirmed. The results suggest rather  $\beta_{\perp} = \beta_{\parallel}$ , which was also used for 6H<sup>65</sup>. Finally, the fittings by Green *et al.*<sup>453</sup> show a significantly slower increase with field than all other models.

Important for TCAD simulations is also the temperature dependency of the impact ionization coefficients. For holes (see Fig. 18) all models predict a decreasing value, which matches the reports of increasing breakdown voltage with increasing temperature<sup>319,470</sup> and prevents thermal runaway. Hatakeyama<sup>437</sup> uses the temperature scaling shown in Eq. (24) (multiplication with  $\gamma$ ), which is also used by Lades<sup>61</sup>, Schröder<sup>144</sup>. Clearly visible is the decline of  $\beta$  with increasing temperature. Steinmann *et al.*<sup>467</sup> proposed two fittings for two different breakdown voltages of

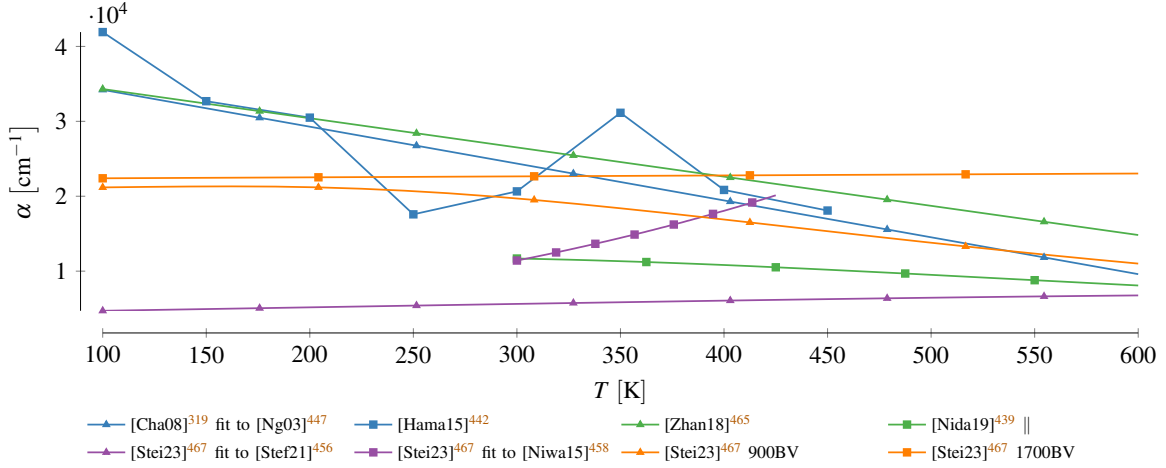


FIG. 19. Temperature dependence of the electron impact ionization coefficient. The single models are evaluated for an electric field of  $3.33 \text{ MV cm}^{-1}$  and are ordered according to their publication date. The colors simply are used to improve the readability.

the investigated device, i.e., 900 V and 1700 V.

For electrons (see Fig. 19) the results are quite inconclusive. Some models even propose an increase of  $\alpha$  with temperature. This is, however, compensated by the decrease in  $\beta$  with increasing temperature due to the relatively small variations of  $\alpha$  compared to  $\beta$  (linear vs. logarithmic y-axis).

### C. Discussion

The majority of the currently utilized impact ionization coefficients are based on 4H measurements (see Fig. 20). Care has to be taken especially for publications prior to the year 2000, as those often are based on 6H<sup>65,289,471,472</sup>. These outdated results have later found their way in various publications<sup>61,108,153,157,159</sup>. In early publications<sup>65</sup> 6H was still used because 4H values were not available or simply<sup>161,473</sup> because the early available fittings from Konstantinov *et al.*<sup>445</sup>, Raghunathan and Baliga<sup>459</sup> deviated significantly. The results from Bakowski, Gustafsson, and Linddefelt<sup>65</sup> were later further changed by Lades<sup>61</sup> who calculated the parameters at 273 K and introduced a typographical error for the hole coefficient  $a$ , which was stated as  $2.24 \times 10^6 \text{ cm}^{-1}$  instead of  $3.24 \times 10^6 \text{ cm}^{-1}$ . We found additional more or less critical inaccuracies, which we all summarize in ??.

The most influential publications are arguably by Raghunathan and Baliga<sup>444,459</sup> and Hatakeyama

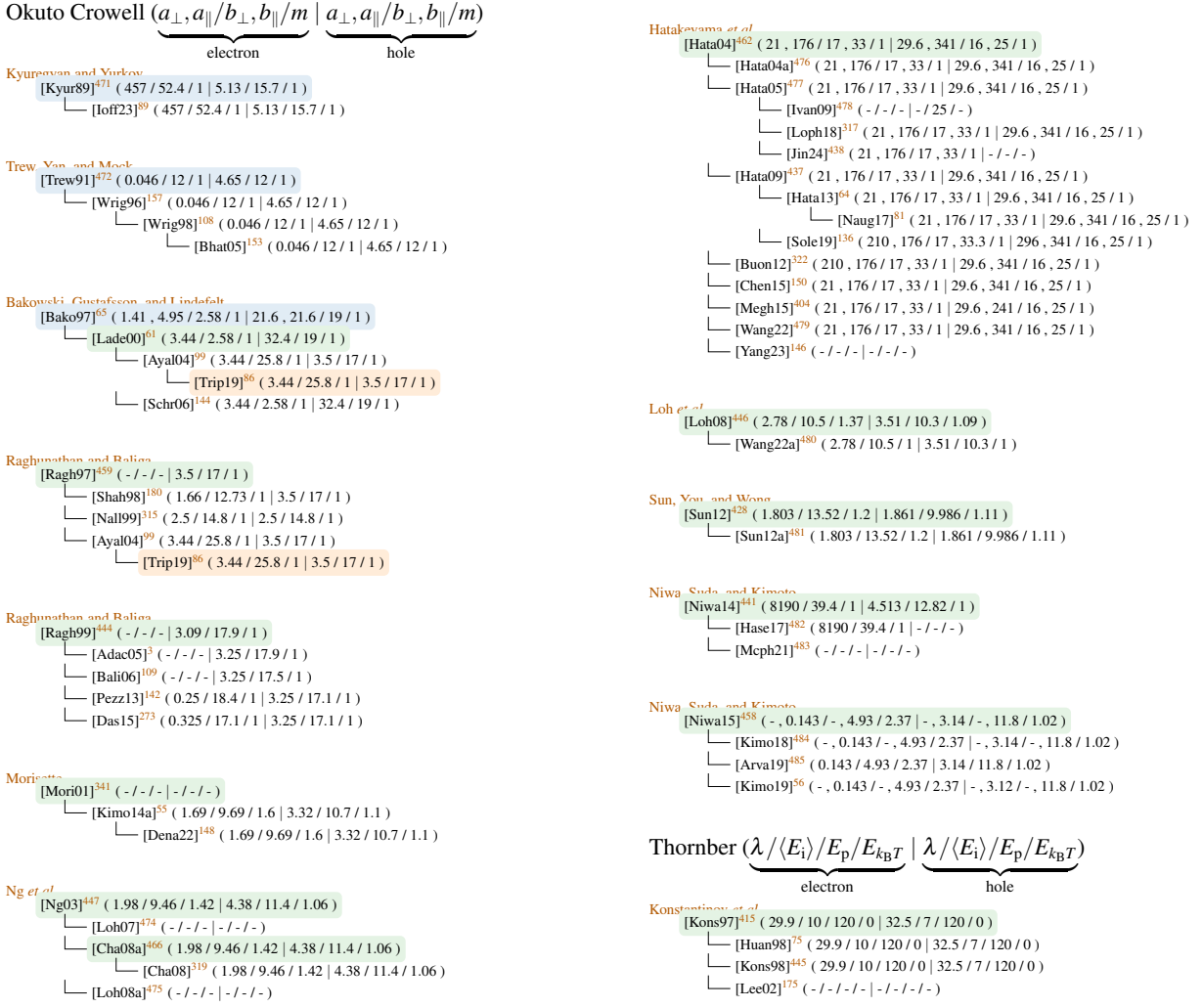


FIG. 20. Reference chain for impact ionization parameters. Publications with blue background are not focused on 4H-SiC, those in green are novel analyses on 4H-SiC and orange color indicates that the reference was guessed based on the values but not explicitly stated in the publication. The values for  $a$  and  $b$  were scaled by  $1 \times 10^6$  for improved readability.

et al.<sup>462</sup>. However, twelve investigations in the last decade indicate that impact ionization is still an active area of research. Nevertheless, only few values for the impact ionization perpendicular to the c-axis are available. Since the available parameters suggest a higher multiplication and thus earlier breakdown in these directions, further in detail investigations are required in the future.

In contrast to Silicon, 4H-SiC shows higher hole than electron current amplification, i.e.,  $\beta > \alpha^{3,178}$ , which is attributed to discontinuities in the electron spectrum<sup>158</sup>. Consequently, the Shockley approximation of the "lucky electron" can only be applied to holes, as the electrons

energy can not continuously increase<sup>415</sup>. Kimoto *et al.*<sup>484</sup> name these "minigaps" as the reason for the low temperature dependence of  $\alpha$ . Temperature analyses are, however, sparsely available. Some of the available data were years after the original publication proposed by other authors, e.g., by Cha and Sandvik<sup>319</sup> or by Steinmann *et al.*<sup>467</sup>, who fitted the linear and quadratic temperature coefficients of the breakdown voltage. Nida and Grossner<sup>439</sup> present the high temperature evolution of some models.

Although models can be used for any arbitrary field strengths, they are most accurate within their often very narrow characterization range. In general, the highest accuracy is required around the critical electric field, i.e., where breakdown occurs. In the literature commonly 2–3 MV cm<sup>-1</sup><sup>23,68,101,119,121,135,137,386,487</sup> are used, whereat some explicitly state a dependence on the doping concentration<sup>56,110,330,345,387,415,436,444,451,458,484,488–490</sup>. Be advised that these values are, most commonly, determined for uniformly doped non-punch through diodes using power law approximations of the impact coefficients<sup>444</sup>. Consequently such values have to be interpreted with a grain of salt and have to be corrected according to the actual structure and doping level<sup>458,491</sup>. Over short distances a higher field is required to achieve breakdown than for thick devices, where charges can multiply over long distances.

## V. INCOMPLETE IONIZATION

It is indispensable to add a doping to a semiconductor, i.e., to introduce impurity atoms, in order to create sophisticated electronic devices. These so-called dopants add energy levels near to the conduction (n-type doping) resp. valence band (p-type doping) such that free charge carrier can be injected at moderate temperatures. In this fashion the electrical characteristics of the material can be altered. Partial overviews on available doping elements and their respective activation energies in 4H-SiC are available<sup>13,14,23,53,68,70,71,118,121,160,246,256,329,330,357,394,492–496</sup>. Uncommon elements were also investigated. Ab initio calculations by Miyata, Higashiguchi, and Hayafuji<sup>497</sup> identified Arsenic<sup>498</sup>, Gallium<sup>499</sup> or Antimony as, energy level wise, fitting. Group IV elements were investigated by Krieger *et al.*<sup>500</sup>, Feng and Zhao<sup>246</sup>, Huang *et al.*<sup>501</sup> focused on Tantalum and Chromium and Dalibor and Schulz<sup>494</sup>, Dalibor *et al.*<sup>502</sup> on Vanadium. Additional factors such as the activation rates<sup>503</sup> or the impact of hydrogen<sup>504</sup> might, however, prevent the deployment of these dopants.

Due to the wide bandgap of 4H-SiC the respective dopant activation energies are large such

that the often used assumption of full ionization is not applicable. Quite the opposite: incomplete ionization has to be carefully considered to correctly predict the amount of free charge carriers and, thus, achieve a realistic conductivity<sup>505,506</sup>.

In this section we will, thus, review measurements, models and TCAD parameters used to described the amount of ionized dopants depending on temperature and doping concentration. We focus on the four most common doping species in 4H-SiC<sup>80,152,507</sup>: Aluminum (analysis by Darmody and Goldsman<sup>133</sup>) and Boron for p-type resp. Nitrogen and Phosphorous for n-type doping. We limit ourselves to simple model, e.g., a single energy level per lattice site (cubic or hexagonal). Depending on various parameters, e.g., binding type and location<sup>134,392,508,509</sup> or whether the impurity is located in a non-neutral regions or not<sup>506</sup>, rather elaborate descriptions would be necessary to account otherwise<sup>232</sup>.

## A. Theory

A good overview on the the physical descriptions of incomplete ionization is provided by<sup>80</sup>. In brief, the amount of ionized dopants can be modeled by the Fermi-Dirac distribution<sup>169,271,328,330,510</sup>, also known as steady-state Gibbs distribution<sup>506</sup>, as

$$\begin{aligned} N_D^+ &= \frac{N_D}{1 + g_D \exp\left(\frac{E_{F,n} - E_D}{k_B T}\right)} \\ N_A^- &= \frac{N_A}{1 + g_A \exp\left(\frac{E_A - E_{F,p}}{k_B T}\right)} \end{aligned} \quad (25)$$

where  $N_A$  resp.  $N_D$  are the active acceptor resp. donor concentrations,  $E_A$  resp.  $E_D$  the acceptor resp. donor energy levels,  $E_{F,n}$  resp.  $E_{F,p}$  the electron resp. hole Fermi level and  $g_D$  resp.  $g_A$  the degeneracy factors. The latter denote the degeneracy of the energy levels<sup>199</sup>, whereat in the literature commonly the values  $g_A = 4$  (spin up and spin down plus two valence bands) and  $g_D = 2$  (spin up and down)<sup>505,511</sup> are used. There are, however, exception: Troffer<sup>59</sup> used  $g_D = 6$ , Scaburri<sup>80</sup>, Laube *et al.*<sup>512</sup> a spin degeneracy of  $g_D = 4$  for Phosphorous, Balachandran, Chow, and Agarwal<sup>280</sup>, Nawaz<sup>281</sup>  $g_A = g_D = 3$ , Persson and Lindefelt<sup>396</sup>  $g_A = 2$ , Lv *et al.*<sup>513</sup>  $g_A = g_D = 2$  and Pernot *et al.*<sup>236</sup>  $g_k = 6$  resp.  $g_h = 2$  for the cubic resp. hexagonal site of Nitrogen. There were also efforts to introduce a temperature dependency as  $G_A(T)$  and  $G_D(T)$ <sup>23,49,58,59,80,514,515</sup>, whereat the description by Lophitis *et al.*<sup>317</sup> (equ. (11)) deviates significantly.

If solely Boltzmann statistics are considered Eq. (25) can be simplified to<sup>64,80,99,121,322</sup>

$$\begin{aligned} N_D^+ &= \frac{N_D}{1 + g_D \frac{n}{N_C} \exp\left(\frac{\Delta E_D}{k_B T}\right)}, & n &= N_C \exp\left(\frac{E_F - E_C}{k_B T}\right) \\ N_A^- &= \frac{N_A}{1 + g_A \frac{p}{N_V} \exp\left(\frac{\Delta E_A}{k_B T}\right)}, & p &= N_V \exp\left(\frac{E_V - E_F}{k_B T}\right) \end{aligned} \quad (26)$$

with  $N_C$  resp.  $N_V$  the effective density of states in the conduction resp. valence band (see Section II) and  $\Delta E_D = E_C - E_D$  resp.  $\Delta E_A = E_A - E_V$  the ionization energies of donors and acceptors relative to the conduction ( $E_C$ ) and valence band ( $E_V$ ). This representation is often preferred in TCAD simulation tools, which commonly operate on charge carrier concentrations.

For completeness we want to highlight that using the neutrality equation<sup>80</sup>

$$N_D^+(E_F) + p(E_F) = N_A^-(E_F) + n(E_F) \quad (27)$$

it is possible to even get rid of the carrier concentration. If we assume a highly donor doped material ( $p(E_F)$  can be neglected) and no compensation ( $N_A^-(E_F) = 0$ ) Eq. (27) results, by inserting Eq. (26) for  $N_D^+$ , in a quadratic equation for  $n$  which can be solved to<sup>152,175,179,289,323,324,516</sup>

$$N_D^+ = N_D \frac{-1 + \sqrt{1 + 4 g_D \frac{N_D}{N_C} \exp\left(\frac{\Delta E_D}{k_B T}\right)}}{2 g_D \frac{N_D}{N_C} \exp\left(\frac{\Delta E_D}{k_B T}\right)}.$$

We have to highlight that the solution of the quadratic expression for  $n$  by Scaburri<sup>80</sup> is incorrect, which makes it impossible to retrace the presented, correct, equation for  $N_D^+$ . Accordingly an expression for  $N_A^-$  can be achieved.

The ionization energies also depend on the doping concentration. This can be explained by the changing potential energy of the charge carriers when they are closer to the ionized atoms, effectively shielding them<sup>517</sup>. To model the decrease in the ionization energy the Pearson-Bardeen<sup>517</sup> expression

$$\Delta E(N) = \Delta E_0 - \alpha N^{1/3} \quad (28)$$

is used.

The literature is inconsistent on what dopants should be included into the overall doping concentration  $N$  in Eq. (28). Some authors include both donors and acceptors  $N_A + N_D$ <sup>64,322</sup>, others only the respective donor concentration ( $N_A$  or  $N_D$ )<sup>15,50,514,518–520</sup>, while a third group just uses the ionized ones<sup>52</sup>. Kajikawa<sup>521</sup> even argues that the compensating dopants, i.e., donors for the

acceptor levels and vice versa, have the bigger impact and should be used instead of the overall donor and acceptor concentrations. There have also been proposals to include the compensating dopants into the factor  $\alpha$ <sup>80,522</sup>. Finally, a completely different approach focuses on the degree of compensation depicted by a screening of free charge carriers<sup>80,523</sup>, which introduces an additional temperature dependency.

An alternative approach to the Pearson-Bardeen expression in Eq. (28) is given by Altermatt, Schenk, and Heiser<sup>524</sup>, Altermatt *et al.*<sup>525</sup>, who used the logistic equation

$$\Delta E(N) = \frac{\Delta E_0}{1 + (N/N_E)^c} \quad (29)$$

to model the decrease in ionization energy. It is based around the idea of charge carrier hopping between the non-ionized dopants<sup>84,92,133,496,521</sup>? ?, also referred to as nearest-neighbor-hopping (NNH) conduction and variable-range-hopping (VRH) conduction. Darmody and Goldsman<sup>133</sup> argue that with Eq. (28) it is possible to shift the dopant level into the conduction/valence band and thus ionizing all dopants immediately, which is not possible with Eq. (29). The described approach has not yet found its way into the major simulation tools.

Dopants have differing ionization energies depending on whether they are located in a hexagonal or a cubic lattice site<sup>34</sup> (see ??). Consequently Eq. (26) has to be adapted to<sup>64,498</sup>

$$N_D^+ = \frac{\frac{1}{2}N_D}{1 + g_D \frac{p}{N_C} \left( \frac{\Delta E_{Dh}}{k_B T} \right)} + \frac{\frac{1}{2}N_D}{1 + g_D \frac{p}{N_C} \left( \frac{\Delta E_{Dc}}{k_B T} \right)}$$

$$N_A^- = \frac{\frac{1}{2}N_A}{1 + g_A \frac{p}{N_V} \left( \frac{\Delta E_{Ah}}{k_B T} \right)} + \frac{\frac{1}{2}N_A}{1 + g_A \frac{p}{N_V} \left( \frac{\Delta E_{Ac}}{k_B T} \right)}$$

where the factors 1/2 denote that both lattice sites are equally probable<sup>99</sup>. In TCAD simulations it is often the case that these separate values are merged to an effective energy level, ending up once again in a description as shown in Eq. (26)<sup>65,153,289,322,329</sup>. The effects of such simplifications have been investigated by Lades<sup>61</sup>, Ayalew *et al.*<sup>526</sup>.

For more accurate approximation of dynamic processes around the dopant, i.e., (de)trapping of charge carriers, the electron and hole cross sections are crucial (see ??). There are multiple description available in literature, which differ in their temperature scaling<sup>527</sup>. The multi-phonon capture model is independent of temperature<sup>528–530</sup> while the cascade capture model is proportional to  $T^{-2}$ <sup>253,531,532</sup>. Kaindl *et al.*<sup>533</sup> argue that the latter delivers a better fit. A scaling with  $T^{-3}$  was used by Kuznetsov and Zubrilov<sup>241</sup>. Note that we discovered large discrepancies between the single tools regarding which models are supported.

## B. Results

The most commonly method to determine the ionization energy of dopants in literature is to fit the neutrality equation, i.e., for p-type doping

$$p + N_K = \frac{N_A}{1 + \frac{g_{AP}}{N_V} \exp\left(\frac{\Delta E_A}{k_B T}\right)}.$$

to Hall measurements, e.g., conductivity or charge carrier concentration, for varying temperature<sup>15,49–51,58,59,200,228,236,253,389,499,509,511,516,520,521,535–559</sup>. The compensation doping density  $N_K$  is only required for fitting purposes, such that we solely use  $N_A$  as the doping density to present our results. Due to the anisotropy of the Hall effect it is possible to achieve direction dependent ionization energies this way<sup>58</sup>. Other approaches based on Hall measurements include the fitting to the activation ratio<sup>560</sup> or free carrier concentration spectroscopy (FCCS)<sup>514,518,561</sup>. Further used electrical measurements are (thermal)<sup>292,562</sup> admittance spectroscopy (AS)<sup>57–59,253,499,520,533,542</sup>, electron spin resonance (ESR) measurement<sup>565</sup>, DLTS<sup>58,241,566</sup> and minority carrier transient spectroscopy (MCTS)<sup>566</sup>, which are often combined with Hall measurements for more accurate results. Troffer<sup>59</sup> notes that DLTS is more sensitive but admittance spectroscopy allows to depict time constants below 1  $\mu$ s.

These electrical methods are complemented by optical ones, e.g., (fourier transform infrared) photothermal ionization spectroscopy (PTIS)<sup>247</sup>, donor-acceptor pair (DAP) luminescence<sup>34,41,248,395</sup>, free to acceptor (FTA) spectroscopy<sup>34</sup>, infrared absorption (IA)<sup>200</sup>, photoluminescence (PL)<sup>314,401,403,542,568</sup>, time-resolved spectroscopy (TRS)<sup>314</sup> or delay measurements (DM)<sup>314</sup>. In these cases electrons are empowered and the resulting photon emission is recorded. The latter can be cause by transitions among traps or between traps and the conduction/valence band<sup>58</sup>. Note that different methods lead to slightly deviating results, even when applied to the same device<sup>200</sup>. Also possible are calculations, e.g., Faulkner model (FM) calculations<sup>42</sup>, density functional theory (DFT)<sup>217,497</sup>, effective mass approximation (EMA)<sup>221</sup>, first principles calculations (FPC)<sup>134,501,504</sup> or *ab initio* supercell calculations (AISC)<sup>569</sup>. Finally, some authors define a value range based on measurements in literature<sup>61,99,152</sup>, calculate an average values<sup>570</sup> or fit to existing data<sup>64,78,133</sup>.

In the sequel we are going to present the ionization energies  $\Delta E_D$  resp.  $\Delta E_A$  found in literature with their respective doping concentration. In order to draw the measurements we dropped uncertainties and replaced the sometimes stated exciton energy  $E_x$  with 20 meV (see Section III). We had to discard results where the samples were solely described as "high purity" or "unintentional

doping<sup>401,403,537,568</sup> and Laube *et al.*<sup>512</sup>, which was superseded by a publication of the same authors. We mark results for the hexagonal lattice site by a trailing “h” and result for the cubic one by a trailing “c”. The latter is often also denoted by the letter “k”, which, most probably, corresponds to the german word “kubisch” for cubic. In fact, some of the literature is written in german<sup>58,59</sup>, making it hard to retrace the results for the international community.

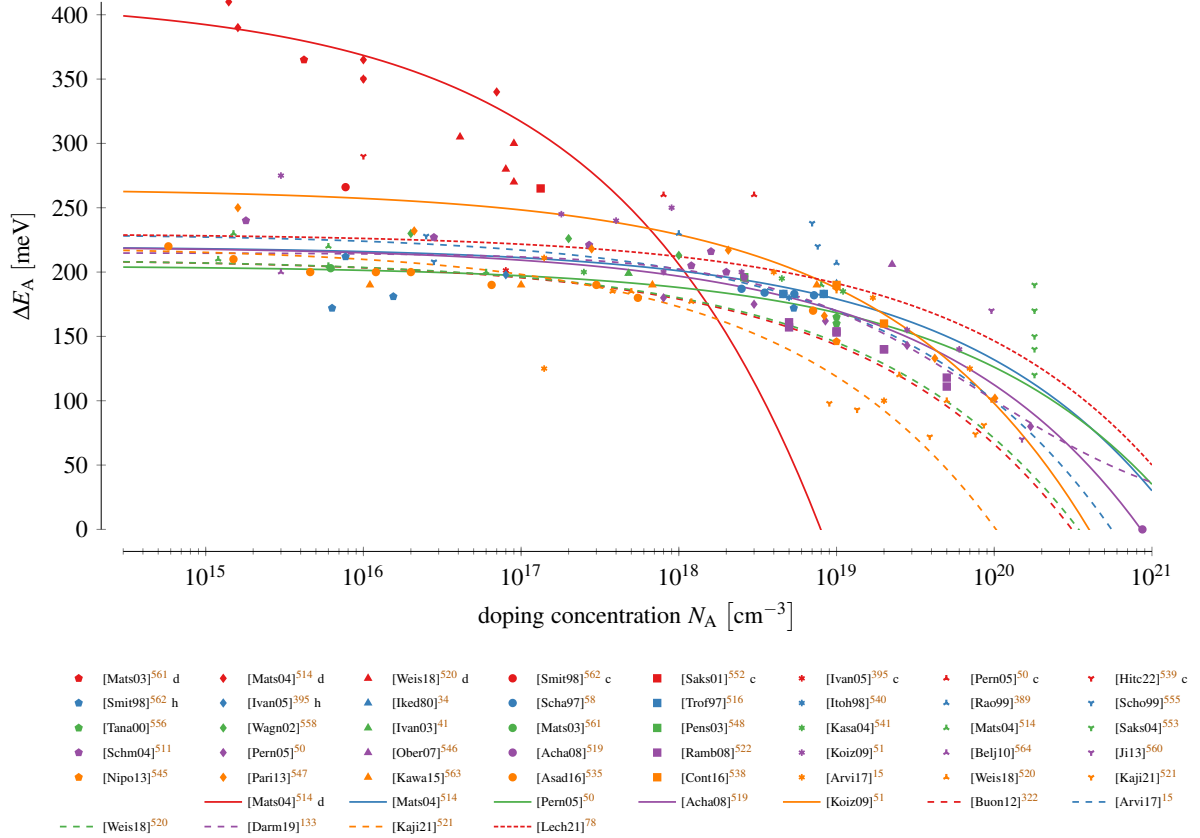


FIG. 21. Aluminum ionization levels. Marks refer to measurements and lines to fittings. The letter ‘d’ after the reference indicates a deep level whose origin is still discussed (see text). Colors are used solely to increase the readability.

For Aluminum (see Fig. 21) many measurements and model fittings have been proposed. The values are equally distributed across the last three decades, meaning that the improvements in material quality did not result in significant changes. The model proposed by Achatz *et al.*<sup>519</sup> uses the critical aluminum concentration for the doping-induced metal-insulator transition to set  $\Delta E_A = 0$  and then fit the parameters. This is in contrast to the logistic equation in Eq. (29) used by Darmody and Goldsman<sup>133</sup>, where a much slower decrease of  $\Delta E_A$  below 100 meV can be observed.

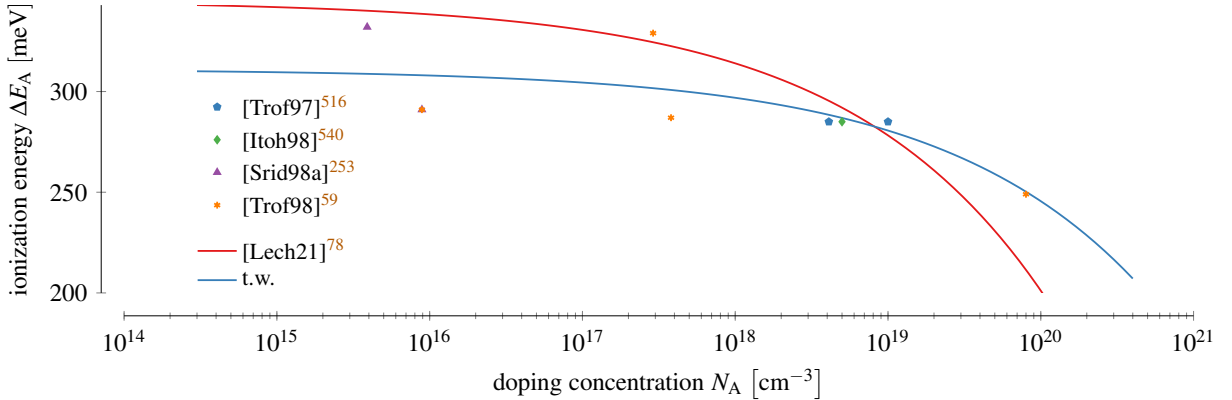


FIG. 22. Boron ionization levels. Marks refer to measurements and lines to fittings. Colors are used solely to increase the readability.

For low-doped and compensated devices a second energy level is required to properly describe the measurements<sup>50</sup>. The origin of this deep level is still discussed in literature. Matsuura *et al.*<sup>514,561</sup> were not able to provide any explanation, Weiße *et al.*<sup>520</sup> suspect excited states of the aluminum ground state and Pernot, Contreras, and Camassel<sup>50</sup>, Smith, Evvaraye, and Mitchel<sup>562</sup> describe them as the cubic lattice site. In fact, Smith, Evvaraye, and Mitchel<sup>562</sup> states that for higher concentration only the hexagonal site is measured. Nevertheless, in our plots we show the data as presented by the original authors, with the exceptions of the ones by Saks *et al.*<sup>552</sup>, which Pernot, Contreras, and Camassel<sup>50</sup> pointed out to denote the cubic lattice site.

The available measurements for Boron (see Fig. 22) are very few and date back to the last millennium. We suspect the main cause in the deep D-center<sup>59,133,134</sup> that comes with a Boron doping. It introduces an energy level in a range of 495–630 meV<sup>34,59,241,248,253,566</sup>, which results in a very effective recombination center. In some publications and also in some simulation tools the D-center level is used as the actual Boron one<sup>34,66,89,248,256,399,401,571</sup>. Since only a single fitting according to Eq. (28) is available for Boron we used all the available data to generate an additional one (t.w.).

For the n-type donor Nitrogen (shown in Fig. 23) almost all publications distinguish between cubic and hexagonal site. However, there is also a big spread in the data, especially towards higher doping concentrations. The results suggest that the ionization energy does not decrease (especially for the cubic lattice site) even as the solubility limit ( $1 \times 10^{19} \text{ cm}^3$  for annealing at 1700 K up to  $3 \times 10^{20} \text{ cm}^3$  for annealing at 2500 K<sup>56,66,394,395,572</sup>) is approached.

For Nitrogen only fittings according to Eq. (28) are available. Kagamihara *et al.*<sup>518</sup> provided

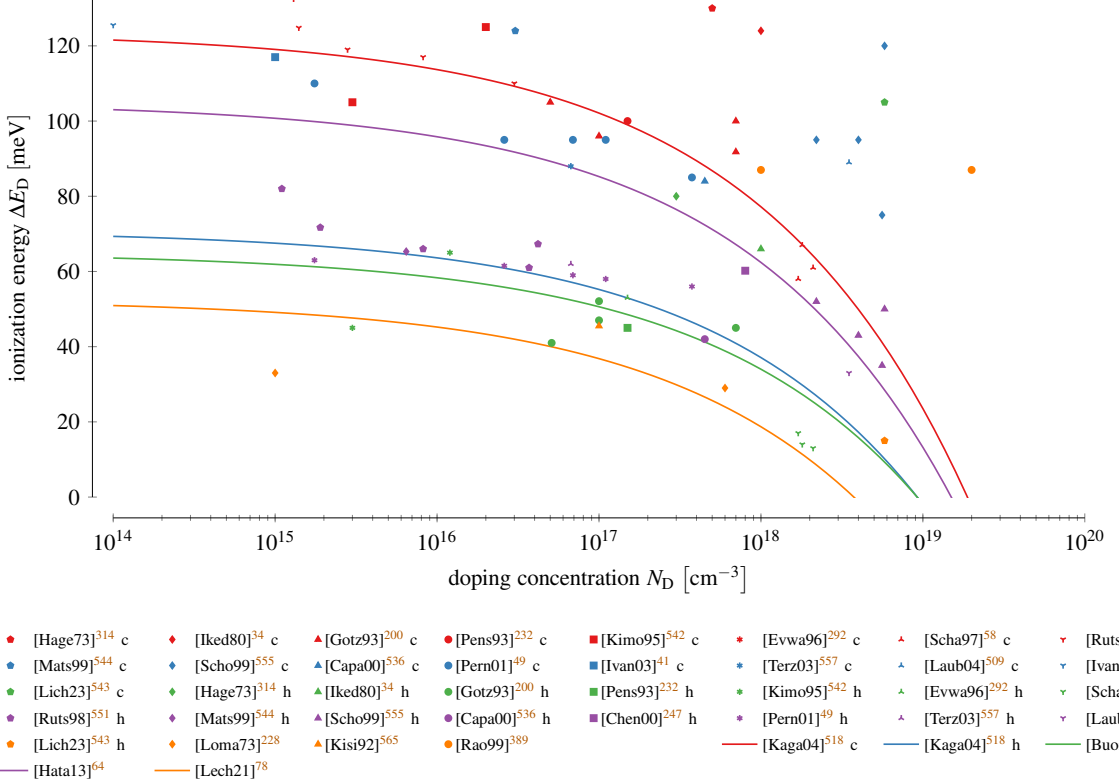


FIG. 23. Nitrogen ionization levels. Marks refer to measurements and lines to fittings. Colors are used solely to increase the readability.

a fitting for both hexagonal and cubic lattice site, which were combined by Hatakeyama, Fukuda, and Okumura<sup>64</sup> to an effective ionization energy model. The remaining fittings also represent effective levels but are surprisingly low. In the case of Buono<sup>322</sup> this can be explained by the selection of  $\Delta E_0$ , which was picked as the effective value of 65 meV determined by Bakowski, Gustafsson, and Lindefelt<sup>65</sup> based on the values from Götz *et al.*<sup>200</sup>. The latter, as can be seen in the figure, were, however, determined for a doping of  $1 \times 10^{17} \text{ cm}^{-3}$  resp.  $1 \times 10^{18} \text{ cm}^{-3}$ .

Compared to Nitrogen a lot less measurements are available for Phosphorous (see Fig. 24), all roughly two decades old. Again, hexagonal and cubic lattice site are always distinguished, but the results especially for the latter largely deviate. Due to the lack of fittings according to Eq. (28) we used the available data to generate very crude fittings. Even as the solubility limit ( $6 \times 10^{18} \text{ cm}^3$  for annealing at 1700 K up to  $2 \times 10^{20} \text{ cm}^3$  for annealing at 2500 K<sup>56,66,394,395,572</sup>) is reached high ionization energies for the cubic lattice site are observable.

The parameters for the Pearson-Bardeen model (see Eq. (28)) fittings, which were shown in Figs. 21 to 24, are summarized in Table XI. We also added our own fitting parameters (t.w.). To

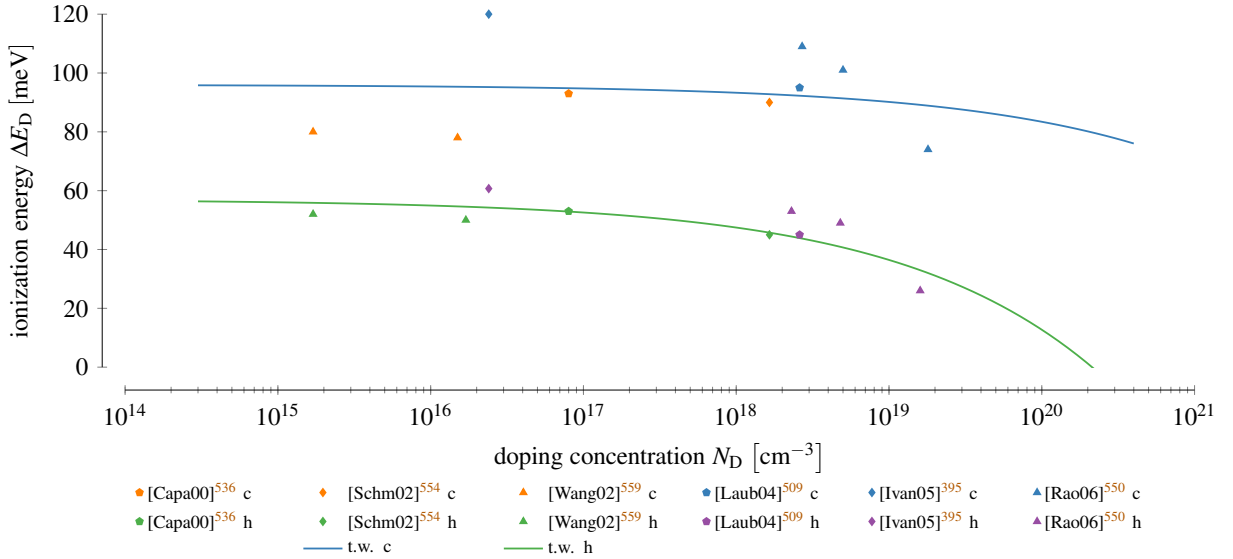


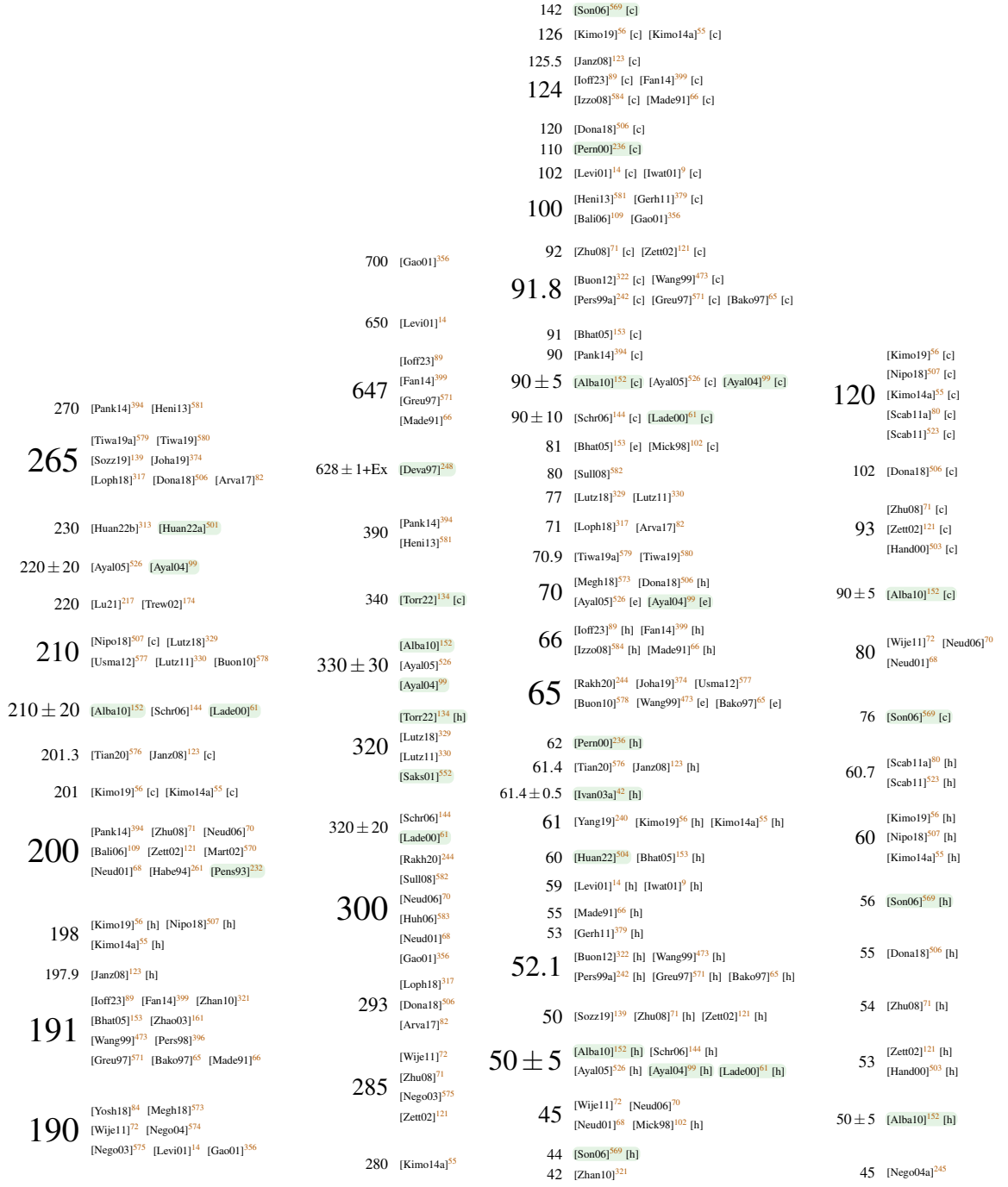
FIG. 24. Phosphorous ionization levels. Marks refer to measurements and lines to fittings. Colors are used solely to increase the readability.

take the described inconsistency for  $N$  in Eq. (28) into account column N denotes either the total doping (tot), the n- resp. p-type doping (dop), the compensation (comp) or fitting (fit). For the figures we used uniformly the specific doping concentration  $N_A$  resp.  $N_D$  (x-axis).

Cross-sections with varying temperature were heavily investigated at the end of the last century (see Table XII). The column  $\sigma$  denotes the cross section with the charge carrier in the energetically closer band (conduction or valence) because the interaction with the other band is significantly lower<sup>59,533</sup>.

Finally we also investigated single energy values used in overviews or in TCAD simulations (see Fig. 25). We do not show fundamental values here as these are always linked to a specific doping concentration. For Aluminum many publications use a value that corresponds to the deeper (cubic site?) energy level. Also for Boron some values refer to the deep D-center. Altogether, a wide range of values is used, especially for Nitrogen, where again hexagonal and cubic sites are almost always distinguished. We want to highlight that for the Boron ionization energy of 293 meV<sup>82,317,506</sup> no direct connection to any fundamental investigation could be inferred.

In some publications the dopant is not clearly specified. Instead only the acceptor and donor energy level are provided (see Fig. 26). While the acceptor values clearly correspond to Aluminum the n-type values could belong to both Nitrogen and Phosphorous.



Al

B

N

P

FIG. 25. Energy levels used in literature for each investigated dopant shown at the bottom. [c] marks cubic, [h] hexagonal and [e] effective values, i.e., a combination of hexagonal and cubic. Nodes with green background indicate a fundamental publication.

TABLE XI. Parameters for the Pearson-Bardeen model (see Eq. (28)). Column N denotes how the factor  $N$  is interpreted: either as active dopants (dop), all dopants (tot), just the compensating ones (comp) or simply used in a fitting (fit). The site denotes besides hexagonal and cubic also a combined effective energy level (eff) and the deep level for Aluminium (deep). If left blank no information were stated in the paper.

ref.	N	site	$\Delta E$	$\alpha$
			[meV]	[meV cm]
<b>Nitrogen</b>				
[Kaga04] <sup>518</sup>	dop	hex	70.9	$3.38 \times 10^{-5}$
		cubic	123.7	$4.65 \times 10^{-5}$
[Buon12] <sup>322</sup>	tot	eff	65	$3.1 \times 10^{-5}$
[Hata13] <sup>64</sup>	tot	eff	105	$4.26 \times 10^{-5}$
[Lech21] <sup>78</sup>	tot		52.5	$3.38 \times 10^{-5}$
<b>Phosphorous</b>				
t.w.	fit	hex	57	$9.54 \times 10^{-6}$
		cubic	96	$2.71 \times 10^{-6}$
<b>Aluminum</b>				
[Mats04] <sup>514</sup>	dop		220	$1.9 \times 10^{-5}$
[Pern05] <sup>50</sup>	dop		205	$1.7 \times 10^{-5}$
[Acha08] <sup>519</sup>	dop		220	$2.32 \times 10^{-5}$
[Koiz09] <sup>51</sup>	dop		265	$3.6 \times 10^{-5}$
[Buon12] <sup>322</sup>	tot	eff	210	$3.1 \times 10^{-5}$
[Arvi17] <sup>15</sup>	dop		$230 \pm 10$	$(2.8 \pm 0.3) \times 10^{-5}$
[Weis18] <sup>520</sup>	dop		210	$3 \times 10^{-5}$
[Kaji21] <sup>521</sup>	comp		220	$4.7 \times 10^{-5}$
[Lech21] <sup>78</sup>	tot		230	$1.8 \times 10^{-5}$
<b>Boron</b>				
[Lech21] <sup>78</sup>	tot		345	$3.1 \times 10^{-5}$
t.w.	fit		311	$1.41 \times 10^{-5}$

TABLE XII. Dopants and their respective cross sections with the charge carriers in the energetically closer band (conduction or valence). Different temperature dependencies are indicated in the column  $T^\alpha$ . We found no data for Nitrogen.

ref.	site	$T^\alpha$	$\Delta E$	$\sigma$
			[meV]	[cm <sup>2</sup> ]
<b>Nitrogen</b>				
[Kain99] <sup>533</sup>	cubic	$T^0$	77	$7.92 \times 10^{-15}$
		$T^{-2}$	90	$3.57 \times 10^{-10}$
<b>Aluminum</b>				
[Kuzn95] <sup>241</sup>		$T^{-3}$	229	$8 \times 10^{-13}$
[Scha97] <sup>58</sup>		$T^0$	164–179	$2.2\text{--}7.6 \times 10^{-13}$
		$T^{-2}$	189–202	$1.7\text{--}5.6 \times 10^{-12}$
[Kain99] <sup>533</sup>		$T^0$	189	$2.58 \times 10^{-13}$
		$T^{-2}$	208	$2.57 \times 10^{-8}$
[Resh05] <sup>57</sup>		$T^0$	185	$1 \times 10^{-14}$
		$T^{-2}$	210	$1 \times 10^{-13}$
[Belj10] <sup>564</sup>		$T^0$	200	$1 \times 10^{-12}$
[Kawa15] <sup>563</sup>		$T^0$	190	$1.4 \times 10^{-13}$
[Kato22] <sup>567</sup>		$T^0$	120–170	$1\text{--}100 \times 10^{-17}$
<b>Boron</b>				
[Srid98a] <sup>253</sup>		$T^0$	259–262	-
		$T^{-2}$	284–295	-
[Trof98] <sup>59</sup>		$T^0$	292	$6 \times 10^{-15}$
		$T^{-2}$	314	$5 \times 10^{-14}$
[Kain99] <sup>533</sup>		$T^0$	312	$2.1 \times 10^{-14}$
		$T^{-2}$	375	$9.69 \times 10^{-9}$
[Zhan03] <sup>566</sup>		$T^0$	230–280	$2\text{--}30 \times 10^{-14}$

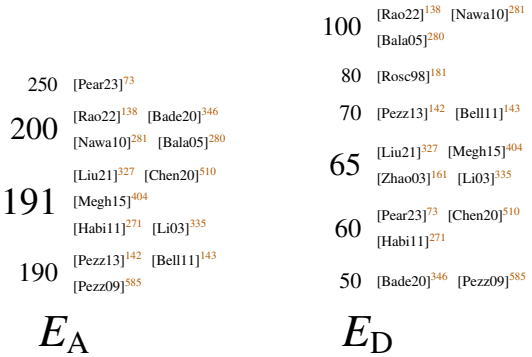


FIG. 26. Energy levels used in literature for acceptors and donors without closer specification of dopant element.

### C. Discussion

In contrast to other properties that have been investigated within this review, there exist a lot of fundamental studies and measurements for incomplete ionization. Nevertheless, the results acquired over the last decades deviate sometimes significantly, making it impossible to distill them to common values. This is, by the way, not caused by less mature samples in the past. Even by limiting our analysis to the last two decades we did reveal a large spread in measurement results. The situation is worsened by the fact that values for hexagonal and cubic lattice sites are often used without appropriate notation. In this fashion significant errors can be introduced, especially for Boron where the deep levels is approximately twice the shallow one.

Overall, almost all publications utilize values determined from 4H-SiC measurements. Only seldomly 6H data were used<sup>244,583</sup>, whereat the values match those from 4H publications<sup>82,317,506</sup>. However, since the latter did not provide a reference for the picked values it is impossible to retrace where and how these values have been determined. Nevertheless we tried to create causality chains for n-type (see Fig. 27) p-type (see Fig. 28) values, whereat quite some values had to be inferred due to missing information.

For n-type doping the values published by Ikeda, Matsunami, and Tanaka<sup>34</sup> are widely used up until this day. Similarly, for p-type doping Götz *et al.*<sup>200</sup> provided for some time the values. However, recently the values by Ivanov, Magnusson, and Janzén<sup>42</sup>, Ivanov, Henry, and Janzén<sup>395</sup> are dominantly cited.

The most research has been clearly directed towards Aluminum. Overall, future research should be denoted to (i) gather additional data for Phosphorous and Boron and (ii) condense the already

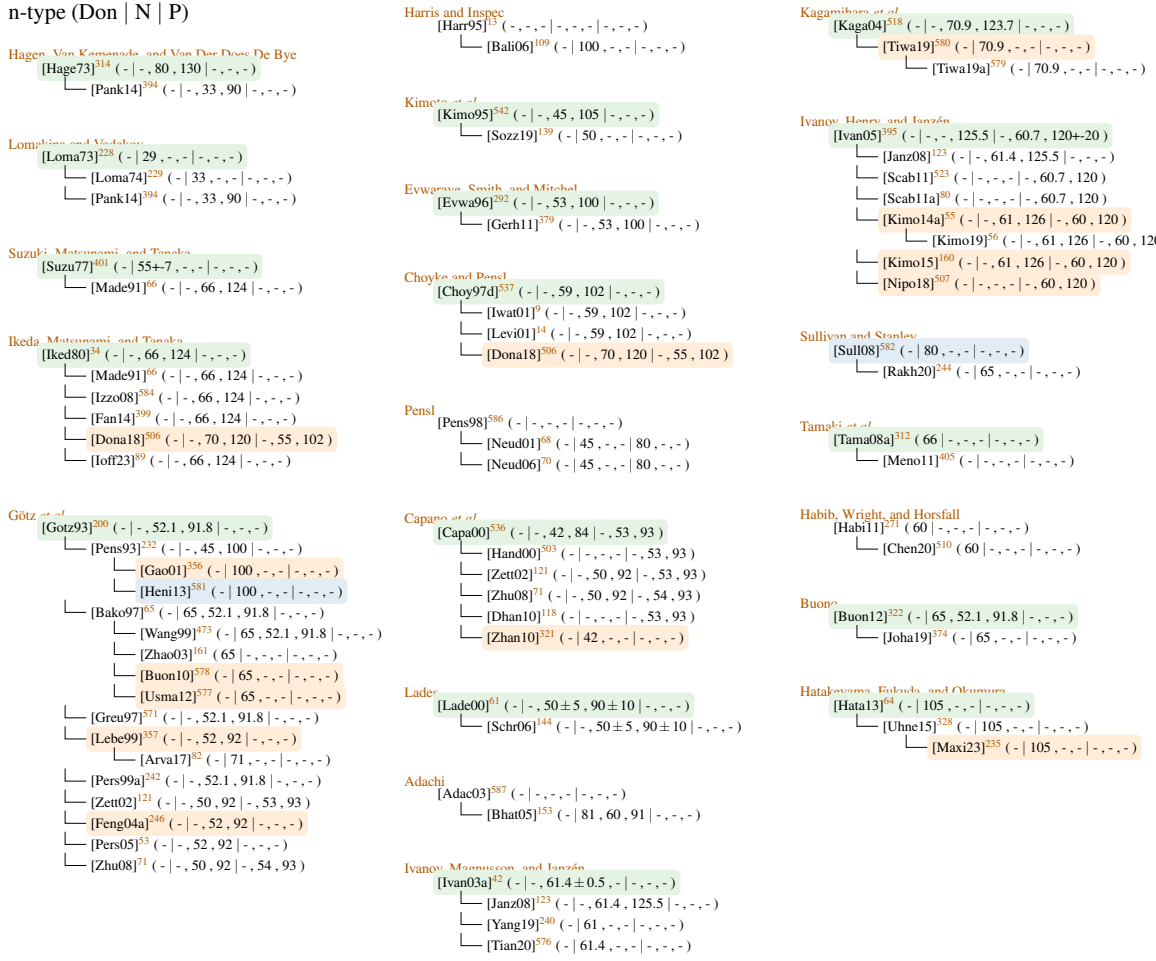


FIG. 27. Reference chain for n-type doping. Entries with green background show fundamental investigations, orange references we inferred based on the used data and blue investigation based not on 4H.

achieved values. For this purpose we added our own fittings based on the gathered data for cubic and hexagonal lattice site as well as for all values together (effective value).



FIG. 28. Reference chain for p-type doping. Entries with green background show fundamental investigations, orange references we inferred based on the used data and blue investigation based not on 4H.

## REFERENCES

- <sup>1</sup>E. Bellotti, *Advanced Modeling of Wide Band Gap Semiconductor Materials and Devices*, Ph.D. thesis, Georgia Institute of Technology (1999).

<sup>2</sup>V. Komarov, S. Wang, and J. Tang, in *Encyclopedia of RF and Microwave Engineering*, edited by K. Chang (Wiley, 2005) 1st ed.

<sup>3</sup>S. Adachi, *Properties of Group-IV, III-V and II-VI Semiconductors* (John Wiley, Chichester, England, 2005).

<sup>4</sup>J. Olivares, M. DeMiguel-Ramos, E. Iborra, M. Clement, T. Mirea, M. Moreira, and I. Katard-

jiev, in *2013 Joint European Frequency and Time Forum & International Frequency Control Symposium (EFTF)* (IEEE, Prague, Czech Republic, 2013) pp. 118–121.

<sup>5</sup>W. Ching, Y.-N. Xu, P. Rulis, and L. Ouyang, *Materials Science and Engineering: A* **422**, 147 (2006).

<sup>6</sup>L. Patrick and W. J. Choyke, *Physical Review B* **2**, 2255 (1970).

<sup>7</sup>R. H. Lyddane, R. G. Sachs, and E. Teller, *Physical Review* **59**, 673 (1941).

<sup>8</sup>R. Ahuja, A. Ferreira Da Silva, C. Persson, J. M. Osorio-Guillén, I. Pepe, K. Järrendahl, O. P. A. Lindquist, N. V. Edwards, Q. Wahab, and B. Johansson, *Journal of Applied Physics* **91**, 2099 (2002).

<sup>9</sup>H. Iwata and K. M. Itoh, *Journal of Applied Physics* **89**, 6228 (2001).

<sup>10</sup>M. Hjelm, H.-E. Nilsson, A. Martinez, K. F. Brennan, and E. Bellotti, *Journal of Applied Physics* **93**, 1099 (2003).

<sup>11</sup>R. Mickevičius and J. H. Zhao, *Materials Science Forum* **264–268**, 291 (1998).

<sup>12</sup>C. Persson and U. Lindefelt, *Journal of Applied Physics* **82**, 5496 (1997).

<sup>13</sup>G. L. Harris and Inspec, eds., *Properties of Silicon Carbide*, EMIS Datareviews Series No. 13 (INSPEC, the Inst. of Electrical Engineers, London, 1995).

<sup>14</sup>M. E. Levinshtein, S. L. Rumyantsev, and M. Shur, eds., *Properties of Advanced Semiconductor Materials: GaN, AlN, InN, BN, SiC, SiGe* (Wiley, New York, 2001).

<sup>15</sup>I.-R. Arvinte, *Investigation of Dopant Incorporation in Silicon Carbide Epilayers Grown by Chemical Vapor Deposition*, Ph.D. thesis, Universite Cote d'Azur (2017).

<sup>16</sup>H. Harima, S.-i. Nakashima, and T. Uemura, *Journal of Applied Physics* **78**, 1996 (1995).

<sup>17</sup>H. Harima, T. Hosoda, and S. Nakashima, *Materials Science Forum* **264–268**, 449 (1998).

<sup>18</sup>D. W. Feldman, J. H. Parker, W. J. Choyke, and L. Patrick, *Physical Review* **173**, 787 (1968).

<sup>19</sup>K. Karch, F. Bechstedt, P. Pavone, and D. Strauch, *Physical Review B* **53**, 13400 (1996).

<sup>20</sup>G. Wellenhofer, K. Karch, P. Pavone, U. Rössler, and D. Strauch, *Physical Review B* **53**, 6071 (1996).

<sup>21</sup>B. Adolph, K. Tenelsen, V. I. Gavrilenko, and F. Bechstedt, *Physical Review B* **55**, 1422 (1997).

<sup>22</sup>X. Peng-Shou, X. Chang-Kun, P. Hai-Bin, and X. Fa-Qiang, *Chinese Physics* **13**, 2126 (2004).

<sup>23</sup>G. Pensl, F. Ciobanu, T. Frank, M. Krieger, S. Reshanov, F. Schmid, and M. Weidner, *International Journal of High Speed Electronics and Systems* **15**, 705 (2005).

<sup>24</sup>J. Coutinho, V. J. B. Torres, K. Demmouche, and S. Öberg,

[Physical Review B](#) **96**, 174105 (2017).

<sup>25</sup>I. G. Ivanov, A. Stelmach, M. Kleverman, and E. Janzén, [Physical Review B](#) **73**, 045205 (2006).

<sup>26</sup>J. G. Hartnett, D. Mouneyrac, J. Krupka, J.-M. Le Floch, M. E. Tobar, and D. Cros, [Journal of Applied Physics](#) **109**, 064107 (2011).

<sup>27</sup>C. R. Jones, J. Dutta, G. Yu, and Y. Gao, [Journal of Infrared, Millimeter, and Terahertz Waves](#) **32**, 838 (2011).

<sup>28</sup>L. Li, S. Reyes, M. J. Asadi, X. Wang, G. Fabi, E. Ozdemir, W. Wu, P. Fay, and J. C. M. Hwang, in [2023 100th ARFTG Microwave Measurement Conference \(ARFTG\)](#) (IEEE, Las Vegas, NV, USA, 2023) pp. 1–4.

<sup>29</sup>M. Naftaly, J. F. Molloy, B. Magnusson, Y. M. Andreev, and G. V. Lanskii, [Optics Express](#) **24**, 2590 (2016).

<sup>30</sup>A. T. Tarekegne, B. Zhou, K. Kaltenecker, K. Iwaszczuk, S. Clark, and P. U. Jepsen, [Optics Express](#) **27**, 3618 (2019).

<sup>31</sup>M.-m. Gao, L.-y. Fan, X.-y. Gong, J.-l. You, and Z.-z. Chen, [Journal of Applied Physics](#) **132**, 135702 (2022).

<sup>32</sup>S. Ninomiya and S. Adachi, [Japanese Journal of Applied Physics](#) **33**, 2479 (1994).

<sup>33</sup>L. Cheng, J.-Y. Yang, and W. Zheng, [ACS Applied Electronic Materials](#) **4**, 4140 (2022).

<sup>34</sup>M. Ikeda, H. Matsunami, and T. Tanaka, [Physical Review B](#) **22**, 2842 (1980).

<sup>35</sup>Q. Yang, Q. Liu, W. Xu, D. Zhou, F. Ren, R. Zhang, Y. Zheng, and H. Lu, [Solid-State Electronics](#) **187**, 108196 (2022).

<sup>36</sup>J. M. Dutta, G. Yu, and C. R. Jones, in [2006 Joint 31st International Conference on Infrared Millimeter Waves](#) (IEEE, Shanghai, China, 2006) pp. 411–411.

<sup>37</sup>S. Chen, M. Afsar, and D. Sakdatorn, [IEEE Transactions on Instrumentation and Measurement](#) **57**, 706 (2008).

<sup>38</sup>L. Li, S. Reyes, M. J. Asadi, P. Fay, and J. C. M. Hwang, [Applied Physics Letters](#) **123**, 012105 (2023).

<sup>39</sup>T. Li, L. Li, X. Wang, J. C. M. Hwang, S. Yanagimoto, and Y. Yanagimoto, [IEEE Journal of Microwaves](#) , 1 (2024).

<sup>40</sup>Y. Yanagimoto, S. Yanagimoto, T. Li, and J. C. M. Hwang, in [2024 103rd ARFTG Microwave Measurement Conference \(ARFTG\)](#) (IEEE, Washington, DC, USA, 2024) pp. 1–4.

<sup>41</sup>I. G. Ivanov, B. Magnusson, and E. Janzén, [Physical Review B](#) **67**, 165211 (2003).

<sup>42</sup>I. G. Ivanov, B. Magnusson, and E. Janzén, [Physical Review B](#) **67**, 165212 (2003).

- <sup>43</sup>A. Agarwal, S.-H. Ryu, and J. Palmour, in *Silicon Carbide*, edited by W. J. Choyke, H. Matsunami, and G. Pensl (Springer Berlin Heidelberg, Berlin, Heidelberg, 2004) pp. 785–811.
- <sup>44</sup>D. Hofman, J. Lely, and J. Volger, *Physica* **23**, 236 (1957).
- <sup>45</sup>A. Schöner, in *Silicon Carbide*, edited by W. J. Choyke, H. Matsunami, and G. Pensl (Springer Berlin Heidelberg, Berlin, Heidelberg, 2004) pp. 229–250.
- <sup>46</sup>I. Polaert, N. Benamara, J. Tao, T.-H. Vuong, M. Ferrato, and L. Estel, *Chemical Engineering and Processing: Process Intensification* **122**, 339 (2017).
- <sup>47</sup>J. Chen, Z. H. Levine, and J. W. Wilkins, *Physical Review B* **50**, 11514 (1994).
- <sup>48</sup>U. Lindefelt, *Journal of Applied Physics* **84**, 2628 (1998).
- <sup>49</sup>J. Pernot, W. Zawadzki, S. Contreras, J. L. Robert, E. Neyret, and L. Di Cioccio, *Journal of Applied Physics* **90**, 1869 (2001).
- <sup>50</sup>J. Pernot, S. Contreras, and J. Camassel, *Journal of Applied Physics* **98**, 023706 (2005).
- <sup>51</sup>A. Koizumi, J. Suda, and T. Kimoto, *Journal of Applied Physics* **106**, 013716 (2009).
- <sup>52</sup>H. Tanaka, S. Asada, T. Kimoto, and J. Suda, *Journal of Applied Physics* **123**, 245704 (2018).
- <sup>53</sup>C. Persson and A. Ferreira Da Silva, in *Optoelectronic Devices: III Nitrides* (Elsevier, 2005) pp. 479–559.
- <sup>54</sup>P. T. B. Shaffer, *Applied Optics* **10**, 1034 (1971).
- <sup>55</sup>T. Kimoto and J. A. Cooper, *Fundamentals of Silicon Carbide Technology: Growth, Characterization, Devices* 1st ed. (Wiley, 2014).
- <sup>56</sup>T. Kimoto, in *Wide Bandgap Semiconductor Power Devices* (Elsevier, 2019) pp. 21–42.
- <sup>57</sup>S. Reshanov, *Device-Relevant Defect Centers and Minority Carrier Lifetime in 3C-, 4H- and 6H-SiC*, Ph.D. thesis, Erlangen-Nürnberg, Germany (2005).
- <sup>58</sup>M. Schadt, *Transporteigenschaften von Elektronen Und Löchern in Siliciumkarbid*, Ph.D. thesis, FriedrichAlexander-Universität (1997).
- <sup>59</sup>T. Troffer, *Elektrische Und Optische Charakterisierung Bauelementrelevanter Dotierstoffe in Siliciumkarbid*, Ph.D. thesis, FriedrichAlexander-Universität (1998).
- <sup>60</sup>N. W. Thibault, American Mineralogist **29**, 327 (1944), <https://pubs.geoscienceworld.org/msa/ammin/article-pdf/29/9-10/327/4243453/am-1944-327.pdf>.
- <sup>61</sup>M. Lades, *Modeling and Simulation of Wide Bandgap Semiconductor Devices: 4H/6H-SiC*, Ph.D. thesis, Technische Universität München (2000).
- <sup>62</sup>C. Persson, U. Lindefelt, and B. E. Sernelius, *Journal of Applied Physics* **86**, 4419 (1999).
- <sup>63</sup>N. T. Son, C. Persson, U. Lindefelt, W. M. Chen, B. K. Meyer, D. M. Hofmann, and E. Janzén,

in *Silicon Carbide*, edited by W. J. Choyke, H. Matsunami, and G. Pensl (Springer Berlin Heidelberg, Berlin, Heidelberg, 2004) pp. 437–460.

<sup>64</sup>T. Hatakeyama, K. Fukuda, and H. Okumura, *IEEE Transactions on Electron Devices* **60**, 613 (2013).

<sup>65</sup>M. Bakowski, U. Gustafsson, and U. Lindefelt, *physica status solidi (a)* **162**, 421 (1997).

<sup>66</sup>O. Madelung and R. Poerschke, eds., *Semiconductors: Group IV Elements and III-V Compounds*, Data in Science and Technology (Springer Berlin Heidelberg, Berlin, Heidelberg, 1991).

<sup>67</sup>B. Wenzien, P. Käckell, F. Bechstedt, and G. Cappellini, *Physical Review B* **52**, 10897 (1995).

<sup>68</sup>P. Neudeck, in *Encyclopedia of Materials: Science and Technology* (Elsevier, 2001) pp. 8508–8519.

<sup>69</sup>Y. Choi, H.-Y. Cha, L. Eastman, and M. Spencer, *IEEE Transactions on Electron Devices* **52**, 1940 (2005).

<sup>70</sup>P. G. Neudeck (CRC Press, 2006).

<sup>71</sup>X. Zhu, *ALTERNATIVE GROWTH AND INTERFACE PASSIVATION TECHNIQUES FOR SiO<sub>2</sub> ON 4H-SiC*, Ph.D. thesis, Auburn University (2008).

<sup>72</sup>M. B. Wijesundara and R. Azevedo, *Silicon Carbide Microsystems for Harsh Environments*, MEMS Reference Shelf, Vol. 22 (Springer New York, New York, NY, 2011).

<sup>73</sup>S. J. Pearton, X. Xia, F. Ren, M. A. J. Rasel, S. Stepanoff, N. Al-Mamun, A. Haque, and D. E. Wolfe, *Journal of Vacuum Science & Technology B* **41**, 030802 (2023).

<sup>74</sup>J. Casady and R. Johnson, *Solid-State Electronics* **39**, 1409 (1996).

<sup>75</sup>M. Huang, N. Goldsman, C.-H. Chang, I. Mayergoyz, J. M. McGarrity, and D. Woolard, *Journal of Applied Physics* **84**, 2065 (1998).

<sup>76</sup>O. Madelung, ed., *Semiconductors — Basic Data* (Springer Berlin Heidelberg, Berlin, Heidelberg, 1996).

<sup>77</sup>T. Egilsson, J. P. Bergman, I. G. Ivanov, A. Henry, and E. Janzén, *Physical Review B* **59**, 1956 (1999).

<sup>78</sup>B. Lechner, *Behaviour of 4H-SiC Power Semiconductor Devices under Extreme Operating Conditions*, Ph.D. thesis, Technische Universität München (2021).

<sup>79</sup>N. Arpatzanis, A. Tsormpatzoglou, C. A. Dimitriadis, K. Zekentes, N. Camara, and M. Godlewski, *physica status solidi (a)* **203**, 2551 (2006).

<sup>80</sup>R. Scaburri, *The Incomplete Ionization of Substitutional Dopants in Silicon Carbide*, Ph.D. thesis, Università di Bologna, Bologna (2011).

<sup>81</sup>A. Naugarhiya, P. Wakhradkar, P. N. Kondekar, G. C. Patil, and R. M. Patrikar,

Journal of Computational Electronics **16**, 190 (2017).

- <sup>82</sup>A. Arvanitopoulos, N. Lophitis, S. Perkins, K. N. Gyftakis, M. Belanche Guadas, and M. Antoniou, in *2017 IEEE 11th International Symposium on Diagnostics for Electrical Machines, Power Electronics and* (IEEE, Tinos, Greece, 2017) pp. 565–571.
- <sup>83</sup>R. Choudhary, M. Mehta, R. Singh Shekhawat, S. Singh, and D. Singh, *Materials Today: Proceedings* **46**, 5889 (2021).
- <sup>84</sup>H. Yoshioka and K. Hirata, *AIP Advances* **8**, 045217 (2018).
- <sup>85</sup>C. Miccoli and F. Iucolano, *Materials Science in Semiconductor Processing* **97**, 40 (2019).
- <sup>86</sup>S. Tripathi, C. Upadhyay, C. Nagaraj, A. Venkatesan, and K. Devan, *Nuclear Instruments and Methods in Physics Research Section A: Accelerators, Spectrometers, Detectors and Targets* **920**, 165001 (2019).
- <sup>87</sup>W. M. Klahold, W. J. Choyke, and R. P. Devaty, *Physical Review B* **102**, 205203 (2020).
- <sup>88</sup>A. Kovalchuk, J. Wozny, Z. Lisik, J. Podgorski, L. Ruta, A. Kubiak, and A. Boiadzhian, *Journal of Physics: Conference Series* **1534**, 012006 (2020).
- <sup>89</sup>I. Institute, “Silicon Carbide,” <http://www.ioffe.ru/SVA/NSM/Semicond/SiC/index.html> (2023).
- <sup>90</sup>A. Acharyya, *Applied Physics A* **123**, 629 (2017).
- <sup>91</sup>S. Banerjee, in *Advances in Terahertz Technology and Its Applications*, edited by S. Das, N. Anveshkumar, J. Dutta, and A. Biswas (Springer Singapore, Singapore, 2021) pp. 153–172.
- <sup>92</sup>H. Kim, *Transactions on Electrical and Electronic Materials* **25**, 141 (2024).
- <sup>93</sup>M. Bhatnagar and B. Baliga, *IEEE Transactions on Electron Devices* **40**, 645 (1993).
- <sup>94</sup>C. Codreanu, M. Avram, E. Carbunescu, and E. Iliescu, *Materials Science in Semiconductor Processing* **3**, 137 (2000).
- <sup>95</sup>T. Chow and R. Tyagi, in *[1993] Proceedings of the 5th International Symposium on Power Semiconductor Devices and ICs* (IEEE, Monterey, CA, USA, 1993) pp. 84–88.
- <sup>96</sup>C. Weitzel, J. Palmour, C. Carter, K. Moore, K. Nordquist, S. Allen, C. Thero, and M. Bhatnagar, *IEEE Transactions on Electron Devices* **43**, 1732 (Oct./1996).
- <sup>97</sup>H. Morkoç, S. Strite, G. B. Gao, M. E. Lin, B. Sverdlov, and M. Burns, *Journal of Applied Physics* **76**, 1363 (1994).
- <sup>98</sup>A. Burk, M. O’Loughlin, R. Siergiej, A. Agarwal, S. Sriram, R. Clarke, M. MacMillan, V. Balakrishna, and C. Brandt, *Solid-State Electronics* **43**, 1459 (1999).

- <sup>99</sup>T. Ayalew, *SiC Semiconductor Devices Technology, Modeling, and Simulation*, Ph.D. thesis, TU Wien (2004).
- <sup>100</sup>S. Sriram, R. R. Siergiej, R. C. Clarke, A. K. Agarwal, and C. D. Brandt, *physica status solidi (a)* **162**, 441 (1997).
- <sup>101</sup>R. Han, X. Xu, X. Hu, N. Yu, J. Wang, Y. Tian, and W. Huang, *Optical Materials* **23**, 415 (2003).
- <sup>102</sup>R. Mickevičius and J. H. Zhao, *Journal of Applied Physics* **83**, 3161 (1998).
- <sup>103</sup>J. H. Zhao, V. Gruzinskis, Y. Luo, M. Weiner, M. Pan, P. Shiktorov, and E. Starikov, *Semiconductor Science and Technology* **15**, 1093 (2000).
- <sup>104</sup>A. Akturk, N. Goldsman, S. Potbhare, and A. Lelis, *Journal of Applied Physics* **105**, 033703 (2009).
- <sup>105</sup>B. Zippelius, *Elektrische Charakterisierung Bauelement-relevanter Defekte in 3C- Und 4H-Siliziumkarbid*, Ph.D. thesis, Friedrich-Alexander-Universität Erlangen-Nürnberg (2011).
- <sup>106</sup>C. Weitzel, *Materials Science Forum* **264–268**, 907 (1998).
- <sup>107</sup>F. Nava, G. Bertuccio, A. Cavallini, and E. Vittone, *Measurement Science and Technology* **19**, 102001 (2008).
- <sup>108</sup>N. G. Wright, D. Morrison, C. M. Johnson, and A. G. O'Neill, *Materials Science Forum* **264–268**, 917 (1998).
- <sup>109</sup>B. J. Baliga, *Silicon Carbide Power Devices* (WORLD SCIENTIFIC, 2006).
- <sup>110</sup>B. J. Baliga, *Fundamentals of Power Semiconductor Devices* (Springer International Publishing, Cham, 2019).
- <sup>111</sup>J. Y. Tsao, S. Chowdhury, M. A. Hollis, D. Jena, N. M. Johnson, K. A. Jones, R. J. Kaplar, S. Rajan, C. G. Van De Walle, E. Bellotti, C. L. Chua, R. Collazo, M. E. Coltrin, J. A. Cooper, K. R. Evans, S. Graham, T. A. Grotjohn, E. R. Heller, M. Higashiwaki, M. S. Islam, P. W. Juodawlkis, M. A. Khan, A. D. Koehler, J. H. Leach, U. K. Mishra, R. J. Nemanich, R. C. N. Pilawa-Podgurski, J. B. Shealy, Z. Sitar, M. J. Tadjer, A. F. Witulski, M. Wraback, and J. A. Simmons, *Advanced Electronic Materials* **4**, 1600501 (2018).
- <sup>112</sup>I. N. Jiya and R. Gouws, *Micromachines* **11**, 1116 (2020).
- <sup>113</sup>H.-E. Nilsson, E. Bellotti, M. Hjelm, K. F. Brennan, and C. Petersson, **Proceedings of the IMACS Conference, Sofia, Bulgaria, June 1999** (1999).
- <sup>114</sup>E. Bellotti, H.-E. Nilsson, K. F. Brennan, P. P. Ruden, and R. Trew, *Journal of Applied Physics* **87**, 3864 (2000).

- <sup>115</sup>J. L. Vasconcelos, C. G. Rodrigues, and R. Luzzi, *Materials Science and Engineering: B* **249**, 114426 (2019).
- <sup>116</sup>C. G. Rodrigues, *Semiconductors* **55**, 625 (2021).
- <sup>117</sup>T. P. Chow, *Materials Science Forum* **338–342**, 1155 (2000).
- <sup>118</sup>G. Dhanaraj, K. Byrappa, V. Prasad, and M. Dudley, eds., *Springer Handbook of Crystal Growth* (Springer Berlin Heidelberg, Berlin, Heidelberg, 2010).
- <sup>119</sup>A. Elasser and T. Chow, *Proceedings of the IEEE* **90**, 969 (2002).
- <sup>120</sup>M. Su, *Power Devices and Integrated Circuits Based on 4H-SiC Lateral JFETs*, Ph.D. thesis, New Brunswick Rutgers, New Jersey (2010).
- <sup>121</sup>C.-M. Zetterling, ed., *Process Technology for Silicon Carbide Devices*, EMIS Processing Series No. 2 (Institution of Electrical Engineers, London, 2002).
- <sup>122</sup>M. Östling, *Science China Information Sciences* **54**, 1087 (2011).
- <sup>123</sup>E. Janzén, A. Gali, A. Henry, I. G. Ivanov, B. Magnusson, and N. T. Son, in *Defects in Micro-electronic Materials and Devices* (CRC Press, 2008) pp. 615–669.
- <sup>124</sup>N. Kaminski, 2009 13th European Conference on Power Electronics and Applications **8** (2009).
- <sup>125</sup>N. Kaminski and O. Hilt, *IET Circuits, Devices & Systems* **8**, 227 (2014).
- <sup>126</sup>C. Buttay, D. Planson, B. Allard, D. Bergogne, P. Bevilacqua, C. Joubert, M. Lazar, C. Martin, H. Morel, D. Tournier, and C. Raynaud, *Materials Science and Engineering: B* **176**, 283 (2011).
- <sup>127</sup>S. Fujita, *Japanese Journal of Applied Physics* **54**, 030101 (2015).
- <sup>128</sup>P. G. Neudeck, in *Extreme Environment Electronics* (CRC Press, Taylor & Francis Group, 2013) pp. 225–232.
- <sup>129</sup>A. Hassan, Y. Savaria, and M. Sawan, *IEEE Access* **6**, 78790 (2018).
- <sup>130</sup>M. Higashiwaki, K. Sasaki, A. Kuramata, T. Masui, and S. Yamakoshi, *physica status solidi (a)* **211**, 21 (2014).
- <sup>131</sup>G. Liu, B. R. Tuttle, and S. Dhar, *Applied Physics Reviews* **2**, 021307 (2015).
- <sup>132</sup>S. Rybalka, E.Yu. Krayushkina, A. Demidov, O. Shishkina, and B. Surin, *International Journal of Physical Research* **5**, 11 (2017).
- <sup>133</sup>C. Darmody and N. Goldsman, *Journal of Applied Physics* **126**, 145701 (2019).
- <sup>134</sup>V. J. B. Torres, I. Capan, and J. Coutinho, *Physical Review B* **106**, 224112 (2022).
- <sup>135</sup>S. J. Pearton, J. Yang, P. H. Cary, F. Ren, J. Kim, M. J. Tadjer, and M. A. Mastro,

Applied Physics Reviews **5**, 011301 (2018).

- <sup>136</sup>V. Soler, *Design and Process Developments towards an Optimal 6.5 kV SiC Power MOSFET*, Ph.D. thesis, Universitat Politècnica de Catalunya (2019).
- <sup>137</sup>M. Yoder, IEEE Transactions on Electron Devices **43**, 1633 (Oct./1996).
- <sup>138</sup>S. Rao, E. D. Mallemace, and F. G. Della Corte, Electronics **11**, 1839 (2022).
- <sup>139</sup>G. Sozzi, M. Puzzanghera, R. Menozzi, and R. Nipoti, IEEE Transactions on Electron Devices **66**, 3028 (2019).
- <sup>140</sup>R. Nipoti, G. Sozzi, M. Puzzanghera, and R. Menozzi, MRS Advances **1**, 3637 (2016).
- <sup>141</sup>M. Usman and M. Nawaz, Solid-State Electronics **92**, 5 (2014).
- <sup>142</sup>F. Pezzimenti, IEEE Transactions on Electron Devices **60**, 1404 (2013).
- <sup>143</sup>S. Bellone, F. G. Della Corte, L. F. Albanese, and F. Pezzimenti, IEEE Transactions on Power Electronics **26**, 2835 (2011).
- <sup>144</sup>D. Schröder, *Leistungselektronische Bauelemente* (Springer Berlin Heidelberg, Berlin, Heidelberg, 2006).
- <sup>145</sup>X. Dong, M. Huang, Y. Ma, C. Fu, M. He, Z. Yang, Y. Li, and M. Gong, IEEE Transactions on Nuclear Science , 1 (2024).
- <sup>146</sup>T. Yang, C. Fu, W. Song, Y. Tan, S. Xiao, C. Wang, K. Liu, X. Zhang, and X. Shi, Nuclear Instruments and Methods in Physics Research Section A: Accelerators, Spectrometers, Detectors and Associated Equipment **940**, 165202 (2020).
- <sup>147</sup>T. Yang, Y. Tan, C. Wang, X. Zhang, and X. Shi, "Simulation of the 4H-SiC Low Gain Avalanche Diode," (2022), arXiv:2206.10191 [physics].
- <sup>148</sup>M. De Napoli, Frontiers in Physics **10**, 898833 (2022).
- <sup>149</sup>M. Cabello, V. Soler, G. Rius, J. Montserrat, J. Rebollo, and P. Godignon, Materials Science in Semiconductor Processing **78**, 22 (2018).
- <sup>150</sup>Q. Chen, L. Yang, S. Wang, Y. Zhang, Y. Dai, and Y. Hao, Applied Physics A **118**, 1219 (2015).
- <sup>151</sup>H. A. Mantooth, in *Extreme Environment Electronics* (CRC Press, Taylor & Francis Group, 2013) pp. 243–252.
- <sup>152</sup>L. F. Albanese, *Characterization, Modeling and Simulation of 4H-SiC Power Diodes*, Ph.D. thesis, Università degli Studi di Salerno (2010).
- <sup>153</sup>P. Bhatnagar, A. B. Horsfall, N. G. Wright, C. M. Johnson, K. V. Vassilevski, and A. G. O'Neill, Solid-State Electronics **49**, 453 (2005).
- <sup>154</sup>M. W. Cole and P. Joshi, in *Silicon Carbide*, edited by Z. C. Feng and J. H. Zhao (Springer

- Berlin Heidelberg, Berlin, Heidelberg, 2004) pp. 517–536.
- <sup>155</sup>H. Iwata and K. M. Itoh, *Materials Science Forum* **338–342**, 729 (2000).
- <sup>156</sup>H. Iwata, K. M. Itoh, and G. Pensl, *Journal of Applied Physics* **88**, 1956 (2000).
- <sup>157</sup>N. Wright, in *IEE Colloquium on New Developments in Power Semiconductor Devices*, Vol. 1996 (IEE, London, UK, 1996) pp. 6–6.
- <sup>158</sup>H.-E. Nilsson, U. Sannemo, and C. S. Petersson, *Journal of Applied Physics* **80**, 3365 (1996).
- <sup>159</sup>I. Neila Inglesias, “APPLYING NUMERICAL SIMULATION TO MODELS SiC SEMICONDUCTOR DEVICES,” (2012).
- <sup>160</sup>T. Kimoto, *Japanese Journal of Applied Physics* **54**, 040103 (2015).
- <sup>161</sup>J. Zhao, X. Li, K. Tone, P. Alexandrov, M. Pan, and M. Weiner, *Solid-State Electronics* **47**, 377 (2003).
- <sup>162</sup>A. Elasser, M. Kheraluwala, M. Ghezzo, R. Steigerwald, N. Evers, J. Kretchmer, and T. Chow, *IEEE Transactions on Industry Applications* **39**, 915 (2003).
- <sup>163</sup>A. Elasser, M. Ghezzo, N. Krishnamurthy, J. Kretchmer, A. Clock, D. Brown, and T. Chow, *Solid-State Electronics* **44**, 317 (2000).
- <sup>164</sup>V. Chelnokov and A. Syrkin, *Materials Science and Engineering: B* **46**, 248 (1997).
- <sup>165</sup>F. L. L. Nouketcha, Y. Cui, A. Lelis, R. Green, C. Darmody, J. Schuster, and N. Goldsman, *IEEE Transactions on Electron Devices* **67**, 3999 (2020).
- <sup>166</sup>A. A. Lebedev, *Radiation Effects in Silicon Carbide*, Materials Research Foundations No. volume 6 (2017) (Materials Research Forum LLC, Millersville, PA, USA, 2017).
- <sup>167</sup>T. P. Chow, I. Omura, M. Higashiwaki, H. Kawarada, and V. Pala, *IEEE Transactions on Electron Devices* **64**, 856 (2017).
- <sup>168</sup>J. A. Pellish and L. M. Cohn, in *Extreme Environment Electronics* (CRC Press, Taylor & Francis Group, 2013) pp. 49–58.
- <sup>169</sup>S. M. Sze and K. K. Ng, *Physics of Semiconductor Devices*, 3rd ed. (Wiley-Interscience, Hoboken, N.J, 2007).
- <sup>170</sup>J. Millán, *IET Circuits, Devices & Systems* **1**, 372 (2007).
- <sup>171</sup>A. Pérez-Tomás, P. Brosselard, P. Godignon, J. Millán, N. Mestres, M. R. Jennings, J. A. Covington, and P. A. Mawby, *Journal of Applied Physics* **100**, 114508 (2006).
- <sup>172</sup>T. P. Chow, N. Ramungul, J. Fedison, and Y. Tang, in *Silicon Carbide*, edited by W. J. Choyke, H. Matsunami, and G. Pensl (Springer Berlin Heidelberg, Berlin, Heidelberg, 2004) pp. 737–767.

- <sup>173</sup>N. Zhang, *High Voltage GaN HEMTs with Low On-Resistance for Switching Applications*, Ph.D. thesis, UNIVERSITY of CALIFORNIA, Santa Barbara (2002).
- <sup>174</sup>R. Trew, *Proceedings of the IEEE* **90**, 1032 (2002).
- <sup>175</sup>S. K. Lee, *Processing and Characterization of Silicon Carbide (6H-SiC and 4H-SiC) Contacts for High Power and h...* (Mikroelektronik och informationsteknik, Kista, 2002).
- <sup>176</sup>R. Kemerley, H. Wallace, and M. Yoder, *Proceedings of the IEEE* **90**, 1059 (2002).
- <sup>177</sup>V. Dmitriev, T. P. Chow, S. P. DenBaars, M. S. Shur, and M. G. Spencer, “*High-Temperature Electronics in Europe;*” Tech. Rep. (Defense Technical Information Center, Fort Belvoir, VA, 2000).
- <sup>178</sup>T. Chow, V. Khemka, J. Fedison, N. Ramungul, K. Matocha, Y. Tang, and R. Gutmann, *Solid-State Electronics* **44**, 277 (2000).
- <sup>179</sup>C. M. Zetterling, M. Östling, C. I. Harris, N. Nordell, K. Wongchotigul, and M. G. Spencer, *Materials Science Forum* **264–268**, 877 (1998).
- <sup>180</sup>P. B. Shah and K. A. Jones, *Journal of Applied Physics* **84**, 4625 (1998).
- <sup>181</sup>M. Roschke, F. Schwierz, G. Paasch, and D. Schipanski, *Materials Science Forum* **264–268**, 965 (1998).
- <sup>182</sup>E. Danielsson, C. I. Harris, C. M. Zetterling, and M. Östling, *Materials Science Forum* **264–268**, 805 (1998).
- <sup>183</sup>T. P. Chow, N. Ramungul, and M. Ghezzo, *MRS Proceedings* **483**, 89 (1997).
- <sup>184</sup>T. P. Chow and M. Ghezzo, *MRS Proceedings* **423**, 9 (1996).
- <sup>185</sup>B. Ozpineci, “*Comparison of Wide-Bandgap Semiconductors for Power Electronics Applications,*” Tech. Rep. ORNL/TM-2003/257, 885849 (Oak Ridge National Laboratory, 2004).
- <sup>186</sup>F. Bechstedt, *Materials Science Forum* **264–268**, 265 (1998).
- <sup>187</sup>W. M. Chen, N. T. Son, E. Janzén, D. M. Hofmann, and B. K. Meyer, *physica status solidi (a)* **162**, 79 (1997).
- <sup>188</sup>Y. M. Tairov and Y. A. Vodakov, in *Electroluminescence*, Vol. 17, edited by J. I. Pankove (Springer Berlin Heidelberg, Berlin, Heidelberg, 1977) pp. 31–61.
- <sup>189</sup>G. Wellenhofer and U. Rössler, *physica status solidi (b)* **202**, 107 (1997).
- <sup>190</sup>N. T. Son, P. N. Hai, W. M. Chen, C. Hallin, B. Monemar, and E. Janzén, *Physical Review B* **61**, R10544 (2000).
- <sup>191</sup>C. Persson and U. Lindefelt, *Physical Review B* **54**, 10257 (1996).
- <sup>192</sup>K. Karch, G. Wellenhofer, P. Pavone, U. Rössler, and D. Strauch, “*Structural and electronic*

- properties of SiC polytypes,” (1995).
- <sup>193</sup>J. Dong and A.-B. Chen, in *SiC Power Materials*, Vol. 73, edited by R. Hull, R. M. Osgood, J. Parisi, H. Warlimont, and Z. C. Feng (Springer Berlin Heidelberg, Berlin, Heidelberg, 2004) pp. 63–87.
- <sup>194</sup>H. P. Iwata, U. Lindefelt, S. Öberg, and P. R. Briddon, *Physical Review B* **68**, 245309 (2003).
- <sup>195</sup>S. Nakashima and H. Harima, *physica status solidi (a)* **162**, 39 (1997).
- <sup>196</sup>Y. Kuroiwa, Y.-i. Matsushita, K. Harada, and F. Oba, *Applied Physics Letters* **115**, 112102 (2019).
- <sup>197</sup>W. Lambrecht, S. Limpijumnong, S. Rashkeev, and B. Segall, *physica status solidi (b)* **202**, 5 (1997).
- <sup>198</sup>C. Raynaud, D. Tournier, H. Morel, and D. Planson, *Diamond and Related Materials* **19**, 1 (2010).
- <sup>199</sup>J. Blakemore, *Semiconductor Statistics* (Elsevier, 1962).
- <sup>200</sup>W. Götz, A. Schöner, G. Pensl, W. Sutrop, W. J. Choyke, R. Stein, and S. Leibenzeder, *Journal of Applied Physics* **73**, 3332 (1993).
- <sup>201</sup>C. Hemmingsson, N. T. Son, O. Kordina, J. P. Bergman, E. Janzén, J. L. Lindström, S. Savage, and N. Nordell, *Journal of Applied Physics* **81**, 6155 (1997).
- <sup>202</sup>P. Ščajev, M. Karaliūnas, E. Kuokštis, and K. Jarašiūnas, *Journal of Luminescence* **134**, 588 (2013).
- <sup>203</sup>V. K. Khanna, *Extreme-Temperature and Harsh-Environment Electronics: Physics, Technology and Applications*, second edition ed. (IOP Publishing, Bristol [England] (Temple Circus, Temple Way, Bristol BS1 6HG, UK), 2023).
- <sup>204</sup>R. Ishikawa, M. Hara, H. Tanaka, M. Kaneko, and T. Kimoto, *Applied Physics Express* **14**, 061005 (2021).
- <sup>205</sup>R. Ishikawa, H. Tanaka, M. Kaneko, and T. Kimoto, *Journal of Applied Physics* **135**, 075704 (2024).
- <sup>206</sup>H. P. Iwata, *Applied Physics Letters* **82**, 598 (2003).
- <sup>207</sup>T. Kinoshita, K. M. Itoh, J. Muto, M. Schadt, G. Pensl, and K. Takeda, *Materials Science Forum* **264–268**, 295 (1998).
- <sup>208</sup>O. Kordina, A. Henry, J. P. Bergman, N. T. Son, W. M. Chen, C. Hallin, and E. Janzén, *Applied Physics Letters* **66**, 1373 (1995).
- <sup>209</sup>J. Camassel and S. Juillaguet, *physica status solidi (b)* **245**, 1337 (2008).

- <sup>210</sup>J. T. Devreese, in *Digital Encyclopedia of Applied Physics*, edited by Wiley-VCH Verlag GmbH & Co. KGaA (Wiley, 2003) 1st ed.
- <sup>211</sup>G. D. Mahan, *Many-Particle Physics* (Springer US, Boston, MA, 1990).
- <sup>212</sup>H. Fröhlich, *Advances in Physics* **3**, 325 (1954).
- <sup>213</sup>K. Takahashi, A. Yoshikawa, and A. Sandhu, eds., *Wide Bandgap Semiconductors* (Springer Berlin Heidelberg, Berlin, Heidelberg, 2007).
- <sup>214</sup>K. Mikami, M. Kaneko, and T. Kimoto, *IEEE Electron Device Letters* , 1 (2024).
- <sup>215</sup>N. T. Son, W. M. Chen, O. Kordina, A. O. Konstantinov, B. Monemar, E. Janzén, D. M. Hofman, D. Volm, M. Drechsler, and B. K. Meyer, *Applied Physics Letters* **66**, 1074 (1995).
- <sup>216</sup>P. Käckell, B. Wenzien, and F. Bechstedt, *Physical Review B* **50**, 10761 (1994).
- <sup>217</sup>L. Lu, H. Zhang, X. Wu, J. Shi, and Y.-Y. Sun, *Chinese Physics B* **30**, 096806 (2021).
- <sup>218</sup>C. Persson and U. Lindefelt, *Journal of Applied Physics* **86**, 5036 (1999).
- <sup>219</sup>G. L. Zhao and D. Bagayoko, *New Journal of Physics* **2**, 16 (2000).
- <sup>220</sup>W. R. L. Lambrecht and B. Segall, *Physical Review B* **52**, R2249 (1995).
- <sup>221</sup>A.-B. Chen and P. Srichaikul, *physica status solidi (b)* **202**, 81 (1997).
- <sup>222</sup>G. Pennington and N. Goldsman, *Physical Review B* **64**, 045104 (2001).
- <sup>223</sup>D. Volm, B. K. Meyer, D. M. Hofmann, W. M. Chen, N. T. Son, C. Persson, U. Lindefelt, O. Kordina, E. Sörman, A. O. Konstantinov, B. Monemar, and E. Janzén, *Physical Review B* **53**, 15409 (1996).
- <sup>224</sup>C. Persson and U. Lindefelt, *Journal of Applied Physics* **83**, 266 (1998).
- <sup>225</sup>G. Ng, *Computational Studies of 4H and 6H Silicon Carbide*, Ph.D. thesis, Arizona State University (2010).
- <sup>226</sup>G. Ng, D. Vasileska, and D. Schroder, *Superlattices and Microstructures* **49**, 109 (2011).
- <sup>227</sup>N. T. Son, P. Hai, W. Chen, C. Hallin, B. Monemar, and E. Janzén, *Materials Science Forum* **338–342**, 563 (2000).
- <sup>228</sup>G. Lomakina and Y. A. Vodakov, **15**, 83 (1973).
- <sup>229</sup>G. Lomakina, in *In: Silicon Carbide-1973; Proceedings of the Third International Conference* (1974) pp. 520–526.
- <sup>230</sup>L. Patrick, W. J. Choyke, and D. R. Hamilton, *Physical Review* **137**, A1515 (1965).
- <sup>231</sup>M. Schadt, G. Pensl, R. P. Devaty, W. J. Choyke, R. Stein, and D. Stephani, *Applied Physics Letters* **65**, 3120 (1994).
- <sup>232</sup>G. Pensl and W. Choyke, *Physica B: Condensed Matter* **185**, 264 (1993).

- <sup>233</sup>A. Itoh, T. Kimoto, and H. Matsunami, *IEEE Electron Device Letters* **16**, 280 (1995).
- <sup>234</sup>P. A. Ivanov, M. E. Levenshtein, J. W. Palmour, S. L. Rumyantsev, and R. Singh, *Semiconductor Science and Technology* **15**, 908 (2000).
- <sup>235</sup>S. I. Maximenko, *AIP Advances* **13**, 105021 (2023).
- <sup>236</sup>J. Pernot, S. Contreras, J. Camassel, J. L. Robert, W. Zawadzki, E. Neyret, and L. Di Cioccio, *Applied Physics Letters* **77**, 4359 (2000).
- <sup>237</sup>G. Pennington and N. Goldsman, *Journal of Applied Physics* **95**, 4223 (2004).
- <sup>238</sup>V. Tilak, K. Matocha, and G. Dunne, *IEEE Transactions on Electron Devices* **54**, 2823 (2007).
- <sup>239</sup>R. A. Faulkner, *Physical Review* **184**, 713 (1969).
- <sup>240</sup>A. Yang, K. Murata, T. Miyazawa, T. Tawara, and H. Tsuchida, *Journal of Applied Physics* **126**, 055103 (2019).
- <sup>241</sup>N. Kuznetsov and A. Zubrilov, *Materials Science and Engineering: B* **29**, 181 (1995).
- <sup>242</sup>C. Persson, U. Lindefelt, and B. E. Sernelius, *Physical Review B* **60**, 16479 (1999).
- <sup>243</sup>R. P. Joshi, *Journal of Applied Physics* **78**, 5518 (1995).
- <sup>244</sup>S. Rakheja, L. Huang, S. Hau-Riege, S. E. Harrison, L. F. Voss, and A. M. Conway, *IEEE Journal of the Electron Devices Society* **8**, 1118 (2020).
- <sup>245</sup>Y. Negoro, K. Katsumoto, T. Kimoto, and H. Matsunami, *Journal of Applied Physics* **96**, 224 (2004).
- <sup>246</sup>Z. C. Feng and J. H. Zhao, eds., *Silicon Carbide: Materials, Processing, and Devices*, Opto-electronic Properties of Semiconductors and Superlattices No. v. 20 (Taylor & Francis, New York, 2004).
- <sup>247</sup>C. Q. Chen, J. Zeman, F. Engelbrecht, C. Peppermüller, R. Helbig, Z. H. Chen, and G. Martínez, *Journal of Applied Physics* **87**, 3800 (2000).
- <sup>248</sup>R. P. Devaty and W. J. Choyke, *physica status solidi (a)* **162**, 5 (1997).
- <sup>249</sup>K. Neimontas, T. Malinauskas, R. Aleksiejūnas, M. Sūdžius, K. Jarašiūnas, L. Storasta, J. P. Bergman, and E. Janzen, *Semiconductor Science and Technology* **21**, 952 (2006).
- <sup>250</sup>M. Flores, F. Maia, V. Freire, J. Da Costa, and E. Da Silva, *Microelectronics Journal* **34**, 717 (2003).
- <sup>251</sup>H. Van Daal, W. Knippenberg, and J. Wasscher, *Journal of Physics and Chemistry of Solids* **24**, 109 (1963).
- <sup>252</sup>A. Galeckas, J. Linnros, V. Grivickas, U. Lindefelt, and C. Hallin, *Applied Physics Letters* **71**, 3269 (1997).

- <sup>253</sup>S. G. Sridhara, L. L. Clemen, R. P. Devaty, W. J. Choyke, D. J. Larkin, H. S. Kong, T. Troffer, and G. Pensl, *Journal of Applied Physics* **83**, 7909 (1998).
- <sup>254</sup>F. C. Beyer, *Deep Levels in SiC*, Ph.D. thesis, Linköping University (2011).
- <sup>255</sup>A. Gsponer, M. Knopf, P. Gaggl, J. Burin, S. Waid, and T. Bergauer, *Nuclear Instruments and Methods in Physics Research Section A: Accelerators, Spectrometers, Detectors and Associated Equipment* **623**, 103 (2010).
- <sup>256</sup>P. Kwasnicki, *Evaluation of Doping in 4H-SiC by Optical Spectroscopies*, Ph.D. thesis, UNIVERSITE MONTPELLIER II (2014).
- <sup>257</sup>D. K. Schroder, *Semiconductor Material and Device Characterization*, 1st ed. (Wiley, 2005).
- <sup>258</sup>J. P. Wolfe and A. Mysyrowicz, *Scientific American* **250**, 98 (1984), 24969326.
- <sup>259</sup>R. J. Elliott, *Physical Review* **108**, 1384 (1957).
- <sup>260</sup>W. Choyke, in *Silicon Carbide–1968* (Elsevier, 1969) pp. S141–S152.
- <sup>261</sup>Ch. Haberstroh, R. Helbig, and R. A. Stein, *Journal of Applied Physics* **76**, 509 (1994).
- <sup>262</sup>A. Itoh, H. Akita, T. Kimoto, and H. Matsunami, *Applied Physics Letters* **65**, 1400 (1994).
- <sup>263</sup>A. Itoh, T. K. Tsunenobu Kimoto, and H. M. Hiroyuki Matsunami, *Japanese Journal of Applied Physics* **35**, 4373 (1996).
- <sup>264</sup>M. Ikeda and H. Matsunami, *Physica Status Solidi (a)* **58**, 657 (1980).
- <sup>265</sup>G. B. Dubrovskii and V. I. Sankin, *Sov. Phys. Solid State* **17**, 1847 (1975).
- <sup>266</sup>W. J. Choyke, L. Patrick, and D. Hamilton, 7th in conference on semicond. physics paris 1964, **7**, 751 (1964).
- <sup>267</sup>W. J. Choyke, D. R. Hamilton, and L. Patrick, *Physical Review* **133**, A1163 (1964).
- <sup>268</sup>G. Zanmarchi, 7th in conference on semicond. physics paris 1964, **7**, 57 (1964).
- <sup>269</sup>W. J. Choyke, H. Matsunami, and G. Pensl, eds., *Silicon Carbide: Recent Major Advances*, Advanced Texts in Physics (Springer Berlin Heidelberg, Berlin, Heidelberg, 2004).
- <sup>270</sup>R. Freer, ed., *The Physics and Chemistry of Carbides, Nitrides and Borides* (Springer Netherlands, Dordrecht, 1990).
- <sup>271</sup>H. Habib, N. G. Wright, and A. B. Horsfall, *Advanced Materials Research* **413**, 229 (2011).
- <sup>272</sup>H. Y. Fan, *Physical Review* **82**, 900 (1951).
- <sup>273</sup>A. Das and S. P. Duttagupta, *Radiation Protection Dosimetry* **167**, 443 (2015).
- <sup>274</sup>R. Pässler, *physica status solidi (b)* **200**, 155 (1997).
- <sup>275</sup>R. Pässler, *Journal of Applied Physics* **83**, 3356 (1998).
- <sup>276</sup>A. Galeckas, P. Grivickas, V. Grivickas, V. Bikbajevs, and J. Linnros, *physica status solidi (a)* **191**, 613 (2002).

- <sup>277</sup>R. Pässler, *Physical Review B* **66**, 085201 (2002).
- <sup>278</sup>K. P. O'Donnell and X. Chen, *Applied Physics Letters* **58**, 2924 (1991).
- <sup>279</sup>Y. P. Varshni, *Physica* **34**, 149 (1967).
- <sup>280</sup>S. Balachandran, T. P. Chow, and A. K. Agarwal, *Materials Science Forum* **483–485**, 909 (2005).
- <sup>281</sup>M. Nawaz, *Microelectronics Journal* **41**, 801 (2010).
- <sup>282</sup>P. Grivickas, V. Grivickas, J. Linnros, and A. Galeckas, *Journal of Applied Physics* **101**, 123521 (2007).
- <sup>283</sup>R. Pässler, *physica status solidi (b)* **216**, 975 (1999).
- <sup>284</sup>L. Viña, S. Logothetidis, and M. Cardona, *Physical Review B* **30**, 1979 (1984).
- <sup>285</sup>R. Pässler, *physica status solidi (b)* **236**, 710 (2003).
- <sup>286</sup>E. F. Schubert, *Doping in III-V Semiconductors*, Cambridge Studies in Semiconductor Physics and Microelectronic Engineering No. 1 (Cambridge University Press, Cambridge [England] ; New York, NY, USA, 1993).
- <sup>287</sup>S. Jain and D. Roulston, *Solid-State Electronics* **34**, 453 (1991).
- <sup>288</sup>G. Donnarumma, V. Palankovski, and S. Selberherr, in *Proceedings of the International Conference on Simulation of Semiconductor Processes and Devices (SISPAD)* (2012) pp. 125–128.
- <sup>289</sup>M. Ruff, H. Mitlehner, and R. Helbig, *IEEE Transactions on Electron Devices* **41**, 1040 (1994).
- <sup>290</sup>M. K. Mainali, P. Dulal, B. Shrestha, E. Amonette, A. Shan, and N. J. Podraza, *Surface Science Spectra* **31**, 026003 (2024).
- <sup>291</sup>W. J. Choyke and L. Patrick, *Physical Review* **105**, 1721 (1957).
- <sup>292</sup>A. O. Ewvaraye, S. R. Smith, and W. C. Mitchel, *Journal of Applied Physics* **79**, 7726 (1996).
- <sup>293</sup>I. G. Ivanov, U. Lindefelt, A. Henry, O. Kordina, C. Hallin, M. Aroyo, T. Egilsson, and E. Janzén, *Physical Review B* **58**, 13634 (1998).
- <sup>294</sup>I. G. Ivanov, J. Zhang, L. Storasta, and E. Janzén, *Materials Science Forum* **389–393**, 613 (2002).
- <sup>295</sup>S. Sridhara, S. Bai, O. Shigiltchoff, R. P. Devaty, and W. J. Choyke, *Materials Science Forum* **338–342**, 567 (2000).
- <sup>296</sup>D. Stefanakis and K. Zekentes, *Microelectronic Engineering* **116**, 65 (2014).
- <sup>297</sup>W. H. Backes, P. A. Bobbert, and W. Van Haeringen, *Physical Review B* **49**, 7564 (1994).
- <sup>298</sup>H.-g. Junginger and W. Van Haeringen, *physica status solidi (b)* **37**, 709 (1970).
- <sup>299</sup>W. Van Haeringen, P. Bobbert, and W. Backes, *physica status solidi (b)* **202**, 63 (1997).

- <sup>300</sup>K. Yamaguchi, D. Kobayashi, T. Yamamoto, and K. Hirose, *Physica B: Condensed Matter* **532**, 99 (2018).
- <sup>301</sup>G. B. Dubrovskii and A. A. Lepneva, Sov. Phys. Solid State **19**, 729 (1977).
- <sup>302</sup>I. Shalish, I. B. Altfeder, and V. Narayanamurti, *Physical Review B* **65**, 073104 (2002).
- <sup>303</sup>Explanation see text.
- <sup>304</sup>According to shown band gap the data were extract from a 21R-SiC device although in<sup>65</sup> argued that it was 6H.
- <sup>305</sup>Solely measurement for lowest temperature shown.
- <sup>306</sup>V. I. Gavrilenko, A. V. Postnikov, N. I. Klyui, and V. G. Litovchenko, *physica status solidi (b)* **162**, 477 (1990).
- <sup>307</sup>C. H. Park, B.-H. Cheong, K.-H. Lee, and K. J. Chang, *Physical Review B* **49**, 4485 (1994).
- <sup>308</sup>J. Käckel, *Siliziumkarbid - Strukturelle und elektronische Eigenschaften verschiedener Polytypen*, Ph.D. thesis, Friedrich-Schiller-Universität Jena (1996).
- <sup>309</sup>Model fitted to 6H-SiC results in<sup>7</sup>.
- <sup>310</sup>Model fitted to results in<sup>260</sup>.
- <sup>311</sup>Origin of Varshni parameters unknown.
- <sup>312</sup>T. Tamaki, G. G. Walden, Y. Sui, and J. A. Cooper, *IEEE Transactions on Electron Devices* **55**, 1920 (2008).
- <sup>313</sup>Y. Huang, R. Wang, Y. Zhang, D. Yang, and X. Pi, *Journal of Applied Physics* **131**, 185703 (2022).
- <sup>314</sup>S. Hagen, A. Van Kemenade, and J. Van Der Does De Bye, *Journal of Luminescence* **8**, 18 (1973).
- <sup>315</sup>F. Nallet, D. Planson, K. Isoird, M. Locatelli, and J. Chante, in *CAS '99 Proceedings. 1999 International Semiconductor Conference (Cat. No.99TH8389)*, Vol. 1 (IEEE, Sinaia, Romania, 1999) pp. 195–198.
- <sup>316</sup>R. Weingärtner, P. J. Wellmann, M. Bickermann, D. Hofmann, T. L. Straubinger, and A. Winacker, *Applied Physics Letters* **80**, 70 (2002).
- <sup>317</sup>N. Lophitis, A. Arvanitopoulos, S. Perkins, and M. Antoniou, in *Disruptive Wide Bandgap Semiconductors, Related Technologies, and Their Applications*, edited by Y. K. Sharma (InTech, 2018).
- <sup>318</sup>P. Wellmann, S. Bushevoy, and R. Weingärtner, *Materials Science and Engineering: B* **80**, 352 (2001).
- <sup>319</sup>H.-Y. Cha and P. M. Sandvik, *Japanese Journal of Applied Physics* **47**, 5423 (2008).

- <sup>320</sup>B. Chen, Y. Yang, X. Xie, N. Wang, Z. Ma, K. Song, and X. Zhang, *Chinese Science Bulletin* **57**, 4427 (2012).
- <sup>321</sup>Y.-R. Zhang, B. Zhang, Z.-J. Li, and X.-C. Deng, *Chinese Physics B* **19**, 067102 (2010).
- <sup>322</sup>B. Buono, *Simulation and Characterization of Silicon Carbide Power Bipolar Junction Transistors*, Ph.D. thesis, KTH Royal Institute of Technology (2012).
- <sup>323</sup>K. Zeghdar, L. Dehimi, F. Pezzimenti, S. Rao, and F. G. Della Corte, *Japanese Journal of Applied Physics* **58**, 014002 (2019).
- <sup>324</sup>K. Zeghdar, L. Dehimi, F. Pezzimenti, M. L. Megherbi, and F. G. Della Corte, *Journal of Electronic Materials* **49**, 1322 (2020).
- <sup>325</sup>D. Johannesson and M. Nawaz, *IEEE Transactions on Power Electronics* **31**, 4517 (2016).
- <sup>326</sup>H. Lanyon and R. Tuft, *IEEE Transactions on Electron Devices* **26**, 1014 (1979).
- <sup>327</sup>H. Liu, J. Wang, S. Liang, H. Yu, and W. Deng, *Semiconductor Science and Technology* **36**, 025009 (2021).
- <sup>328</sup>V. Uhnevionak, *Simulation and Modeling of Silicon-Carbide Devices*, Ph.D. thesis, Friedrich-Alexander-Universität (2015).
- <sup>329</sup>J. Lutz, U. Scheuermann, H. Schlangenotto, and R. De Doncker, “Power Semiconductor Devices—Key Components for Efficient Electrical Energy Conversion Systems,” in *Semiconductor Power Devices* (Springer International Publishing, Cham, 2018) pp. 1–20.
- <sup>330</sup>J. Lutz, H. Schlangenotto, U. Scheuermann, and R. De Doncker, *Semiconductor Power Devices: Physics, Characteristics, Reliability* (Springer Berlin Heidelberg, Berlin, Heidelberg, 2011).
- <sup>331</sup>M. Jiménez-Ramos, A. García Osuna, M. Rodriguez-Ramos, E. Viezzer, G. Pellegrini, P. Godignon, J. Rafí, G. Rius, and J. García López, *Radiation Physics and Chemistry* **214**, 111283 (2024).
- <sup>332</sup>T. R. Garcia, A. Kumar, B. Reinke, T. E. Blue, and W. Windl, *Applied Physics Letters* **103**, 152108 (2013).
- <sup>333</sup>P. Masri, *Surface Science Reports* **48**, 1 (2002).
- <sup>334</sup>J. A. Freitas, in *Properties of Silicon Carbide*, EMIS Datareviews Series No. 13, edited by G. L. Harris and Inspec (INSPEC, the Inst. of Electrical Engineers, London, 1995) pp. 29–41.
- <sup>335</sup>X. Li, Y. Luo, L. Fursin, J. Zhao, M. Pan, P. Alexandrov, and M. Weiner, *Solid-State Electronics* **47**, 233 (2003).
- <sup>336</sup>T. Egilsson, I. G. Ivanov, N. T. Son, G. Henry, A., J. P. Bergman, and E. Janzén, in

- Silicon Carbide*, edited by Z. C. Feng and J. H. Zhao (Springer Berlin Heidelberg, Berlin, Heidelberg, 2004) pp. 517–536.
- <sup>337</sup>R. C. Marshall, J. W. Faust, C. E. Ryan, A. F. C. R. L. (U.S.), and University of South Carolina, eds., *Silicon Carbide—1973: Proceedings*, 1st ed. (University of South Carolina Press, Columbia, 1974).
- <sup>338</sup>S. Sandeep and R. Komaragiri, in *India International Conference on Power Electronics 2010 (IICPE2010)* (IEEE, New Delhi, India, 2011) pp. 1–5.
- <sup>339</sup>B. Zat’ko, L. Hrubčín, A. Šagátová, J. Osvald, P. Boháček, E. Kováčová, Y. Halahovets, S. V. Rozov, and V. Sandukovskij, *Applied Surface Science* **536**, 147801 (2021).
- <sup>340</sup>G. Rescher, G. Pobegen, T. Aichinger, and T. Grasser, *IEEE Transactions on Electron Devices* **65**, 1419 (2018).
- <sup>341</sup>D. T. Morisette, *Development of Robust Power Schottky Barrier Diodes in Silicon Carbide*, Ph.D. thesis, Purdue University (2001).
- <sup>342</sup>J. Hudgins, G. Simin, E. Santi, and M. Khan, *IEEE Transactions on Power Electronics* **18**, 907 (2003).
- <sup>343</sup>K. C. Mandal, P. G. Muzykov, R. M. Krishna, and J. R. Terry, *IEEE Transactions on Nuclear Science* **59**, 1591 (2012).
- <sup>344</sup>V. V. Afanas’ev, M. Bassler, G. Pensl, M. J. Schulz, and E. Stein Von Kamienski, *Journal of Applied Physics* **79**, 3108 (1996).
- <sup>345</sup>M. Shur, S. L. Rumyantsev, and M. E. Levinshtein, eds., *SiC Materials and Devices, Selected Topics in Electronics and Systems* No. v. 40 (World Scientific, New Jersey ; London, 2006).
- <sup>346</sup>S. J. Bader, H. Lee, R. Chaudhuri, S. Huang, A. Hickman, A. Molnar, H. G. Xing, D. Jena, H. W. Then, N. Chowdhury, and T. Palacios, *IEEE Transactions on Electron Devices* **67**, 4010 (2020).
- <sup>347</sup>D. Mukherjee and M. Neto, *Recent Advances in SiC/Diamond Composite Devices* (IOP Publishing, 2023).
- <sup>348</sup>X. Guo, Q. Xun, Z. Li, and S. Du, *Micromachines* **10**, 406 (2019).
- <sup>349</sup>H. A. Mantooth, K. Peng, E. Santi, and J. L. Hudgins, *IEEE Transactions on Electron Devices* **62**, 423 (2015).
- <sup>350</sup>J. D. Cressler and H. A. Mantooth, *Extreme Environment Electronics* (CRC Press, Taylor & Francis Group, Boca Raton, 2013).
- <sup>351</sup>M. B. J. Wijesundara and R. G. Azevedo, “System Integration,” in *Silicon Carbide Microsystems for Harsh Environments*, Vol. 22 (Springer New York, New

- York, NY, 2011) pp. 189–230.
- <sup>352</sup>V. Cimalla, J. Pezoldt, and O. Ambacher, *Journal of Physics D: Applied Physics* **40**, S19 (2007).
- <sup>353</sup>M. J. Kumar and V. Parihar, *Microelectronic Engineering* **81**, 90 (2005).
- <sup>354</sup>K. Bertilsson, *Simulation and Optimization of SiC Field Effect Transistors*, Ph.D. thesis, Mikroelektronik och informationsteknik / KTH, Microelectronics and Information Technology, IMIT / KTH, Microelectronics and Information Technology, IMIT (2004).
- <sup>355</sup>A. Powell and L. Rowland, *Proceedings of the IEEE* **90**, 942 (2002).
- <sup>356</sup>Y. Gao, S. I. Soloviev, T. S. Sudarshan, and C.-C. Tin, *Journal of Applied Physics* **90**, 5647 (2001).
- <sup>357</sup>A. A. Lebedev, *Semiconductors* **33**, 107 (1999).
- <sup>358</sup>R. J. Trew, *physica status solidi (a)* **162**, 409 (1997).
- <sup>359</sup>P. G. Neudeck, *Journal of Electronic Materials* **24**, 283 (1995).
- <sup>360</sup>R. Karsthof, M. E. Bathen, A. Galeckas, and L. Vines, *Physical Review B* **102**, 184111 (2020).
- <sup>361</sup>G. Lioliou, M. Mazzillo, A. Sciuto, and A. Barnett, *Optics Express* **23**, 21657 (2015).
- <sup>362</sup>P. B. Klein, *physica status solidi (a)* **206**, 2257 (2009).
- <sup>363</sup>D. Werber, P. Borthen, and G. Wachutka, *Materials Science Forum* **556–557**, 905 (2007).
- <sup>364</sup>P. Ščajev, V. Gudelis, K. Jarašiūnas, and P. B. Klein, *Journal of Applied Physics* **108**, 023705 (2010).
- <sup>365</sup>B. Ng, J. David, D. Massey, R. Tozer, G. Rees, F. Yan, J. H. Zhao, and M. Weiner, *Materials Science Forum* **457–460**, 1069 (2004).
- <sup>366</sup>A. Agarwal, S. Seshadri, J. Casady, S. Mani, M. MacMillan, N. Saks, A. Burk, G. Augustine, V. Balakrishna, P. Sanger, C. Brandt, and R. Rodrigues, *Diamond and Related Materials* **8**, 295 (1999).
- <sup>367</sup>J. Shenoy, J. Cooper, and M. Melloch, *IEEE Electron Device Letters* **18**, 93 (1997).
- <sup>368</sup>A. Agarwal, G. Augustine, V. Balakrishna, C. Brandt, A. Burk, Li-Shu Chen, R. Clarke, P. Eseker, H. Hobgood, R. Hopkins, A. Morse, L. Rowland, S. Seshadri, R. Siergiej, T. Smith, and S. Sriram, in *International Electron Devices Meeting. Technical Digest* (IEEE, San Francisco, CA, USA, 1996) pp. 225–230.
- <sup>369</sup>Wolfspeed, “Silicon Carbide and Nitride Materials Catalog,” (2023).
- <sup>370</sup>C. Langpoklakpam, A.-C. Liu, K.-H. Chu, L.-H. Hsu, W.-C. Lee, S.-C. Chen, C.-W. Sun, M.-H. Shih, K.-Y. Lee, and H.-C. Kuo, *Crystals* **12**, 245 (2022).
- <sup>371</sup>I. Capan, *Electronics* **11**, 532 (2022).

- <sup>372</sup>J. V. Berens, *Carrier Mobility and Reliability of 4H-SiC Trench MOSFETs*, Ph.D. thesis, TU Wien (2021).
- <sup>373</sup>H. Matsunami, *Proceedings of the Japan Academy, Series B* **96**, 235 (2020).
- <sup>374</sup>D. Johannesson, M. Nawaz, and H. P. Nee, *Materials Science Forum* **963**, 670 (2019).
- <sup>375</sup>G. Rescher, *Behavior of SiC-MOSFETs under Temperature and Voltage Stress*, Ph.D. thesis, TU Wien (2018).
- <sup>376</sup>S. Chowdhury, C. Hitchcock, R. Dahal, I. B. Bhat, and T. P. Chow, in *2015 IEEE 27th International Symposium on Power Semiconductor Devices & IC's (ISPSD)* (IEEE, Hong Kong, China, 2015) pp. 353–356.
- <sup>377</sup>M. B. J. Wijesundara and R. G. Azevedo, “Introduction,” in *Silicon Carbide Microsystems for Harsh Environments*, Vol. 22 (Springer New York, New York, NY, 2011) pp. 1–32.
- <sup>378</sup>V. R. Manikam and Kuan Yew Cheong, *IEEE Transactions on Components, Packaging and Manufacturing* **28**, 1 (2005).
- <sup>379</sup>R. Gerhardt, ed., *Properties and Applications of Silicon Carbide* (IntechOpen, 2011).
- <sup>380</sup>C. M. Tanner, J. Choi, and J. P. Chang, *Journal of Applied Physics* **101**, 034108 (2007).
- <sup>381</sup>M. Willander, M. Friesel, Q.-u. Wahab, and B. Straumal, *Journal of Materials Science: Materials in Electronics* **17**, 1 (2006).
- <sup>382</sup>M. Philip and A. O'Neill, in *2006 Conference on Optoelectronic and Microelectronic Materials and Device* (IEEE, Perth, Australia, 2006) pp. 137–140.
- <sup>383</sup>T. P. Chow, *Microelectronic Engineering* **83**, 112 (2006).
- <sup>384</sup>S. Dhar, Y. W. Song, L. C. Feldman, T. Isaacs-Smith, C. C. Tin, J. R. Williams, G. Chung, T. Nishimura, D. Starodub, T. Gustafsson, and E. Garfunkel, *Applied Physics Letters* **84**, 1498 (2004).
- <sup>385</sup>J. Kohlscheen, Y. N. Emirov, M. M. Beerbom, J. T. Wolan, S. E. Saddow, G. Chung, M. F. MacMillan, and R. Schlaf, *Journal of Applied Physics* **94**, 3931 (2003).
- <sup>386</sup>M. Werner and W. Fahrner, *IEEE Transactions on Industrial Electronics* **48**, 249 (2001).
- <sup>387</sup>A. Hefner, R. Singh, Jih-Sheg Lai, D. Berning, S. Bouche, and C. Chapuy, *IEEE Transactions on Power Electronics* **16**, 273 (2001).
- <sup>388</sup>H. Matsunami and T. Kimoto, *Materials Science and Engineering: R: Reports* **20**, 125 (1997).
- <sup>389</sup>M. V. Rao, J. B. Tucker, M. C. Ridgway, O. W. Holland, N. Papanicolaou, and J. Mittereder, *Journal of Applied Physics* **86**, 752 (1999).
- <sup>390</sup>D. Baierhofer, in *ESSDERC 2019 - 49th European Solid-State Device Research Conference (ESSDERC)* (ESSDERC, 2019) pp. 1–4.

- (IEEE, Cracow, Poland, 2019) pp. 31–34.
- <sup>391</sup>J. W. Kleppinger, S. K. Chaudhuri, O. Karadavut, and K. C. Mandal, *Journal of Applied Physics* **129**, 244501 (2021).
- <sup>392</sup>F. Bechstedt, J. Furthmüller, U. Grossner, and C. Raffy, in *Silicon Carbide*, edited by W. J. Choyke, H. Matsunami, and G. Pensl (Springer Berlin Heidelberg, Berlin, Heidelberg, 2004) pp. 3–25.
- <sup>393</sup>H. Choi, “Overview of Silicon Carbide Power Devices,” (2016).
- <sup>394</sup>J. I. Pankove, ed., *Electroluminescence*, softcover reprint of the original 1st ed. 1977 ed. (Springer Berlin, Berlin, 2014).
- <sup>395</sup>I. G. Ivanov, A. Henry, and E. Janzén, *Physical Review B* **71**, 241201 (2005).
- <sup>396</sup>C. Persson and U. Lindefelt, *Materials Science Forum* **264–268**, 275 (1998).
- <sup>397</sup>A. Aditya, S. Khandelwal, C. Mukherjee, A. Khan, S. Panda, and B. Maji, in *2015 International Conference on Recent Developments in Control, Automation and Power Engineering (ICDCAPE)* (IEEE, Noida, India, 2015) pp. 61–65.
- <sup>398</sup>S. Zollner, J. G. Chen, E. Duda, T. Wetteroth, S. R. Wilson, and J. N. Hilfiker, *Journal of Applied Physics* **85**, 8353 (1999).
- <sup>399</sup>J. Fan and P. K. Chu, “General Properties of Bulk SiC,” in *Silicon Carbide Nanostructures* (Springer International Publishing, Cham, 2014) pp. 7–114.
- <sup>400</sup>S. Yoshida, in *Properties of Silicon Carbide*, EMIS Datareviews Series No. 13, edited by G. L. Harris and Inspec (INSPEC, the Inst. of Electrical Engineers, London, 1995) pp. 29–41.
- <sup>401</sup>A. Suzuki, H. Matsunami, and T. Tanaka, *Journal of The Electrochemical Society* **124**, 241 (1977).
- <sup>402</sup>L. Patrick, D. R. Hamilton, and W. J. Choyke, *Physical Review* **143**, 526 (1966).
- <sup>403</sup>H. Matsunami, A. Suzuki, and T. Tanaka, in *In: Silicon Carbide-1973; Proceedings of the Third International Conference* (1974) pp. 618–625.
- <sup>404</sup>M. L. Megherbi, L. Dehimi, W. terghini, F. Pezzimenti, and F. G. Della Corte, *Courrier du Savoir* **19**, 71 (2015).
- <sup>405</sup>K. G. Menon, A. Nakajima, L. Ngwendson, and E. M. Sankara Narayanan, *IEEE Electron Device Letters* **32**, 1272 (2011).
- <sup>406</sup>G. Wolfowicz, C. P. Anderson, A. L. Yeats, S. J. Whiteley, J. Niklas, O. G. Poluektov, F. J. Heremans, and D. D. Awschalom, *Nature Communications* **8**, 1876 (2017).
- <sup>407</sup>B. Nedzvetskii, B. V. Novikov, N. K. Prokof’eva, and M. B. Reifman, *Sov. Phys. Solid State* **2**, 914 (1969).

- <sup>408</sup>F. Capasso, in *Semiconductors and Semimetals*, Vol. 22 (Elsevier, 1985) pp. 1–172.
- <sup>409</sup>S. Selberherr, *Analysis and Simulation of Semiconductor Devices* (Springer Vienna, Vienna, 1984).
- <sup>410</sup>A. G. Chynoweth, *Physical Review* **109**, 1537 (1958).
- <sup>411</sup>A. G. Chynoweth, *Journal of Applied Physics* **31**, 1161 (1960).
- <sup>412</sup>R. Van Overstraeten and H. De Man, *Solid-State Electronics* **13**, 583 (1970).
- <sup>413</sup>P. A. Wolff, *Physical Review* **95**, 1415 (1954).
- <sup>414</sup>W. Shockley, *Solid-State Electronics* **2**, 35 (1961).
- <sup>415</sup>A. O. Konstantinov, Q. Wahab, N. Nordell, and U. Lindefelt, *Applied Physics Letters* **71**, 90 (1997).
- <sup>416</sup>T. Lackner, *Solid-State Electronics* **34**, 33 (1991).
- <sup>417</sup>G. A. Baraff, *Physical Review* **128**, 2507 (1962).
- <sup>418</sup>K. K. Thornber, *Journal of Applied Physics* **52**, 279 (1981).
- <sup>419</sup>Y. Okuto and C. R. Crowell, *Physical Review B* **6**, 3076 (1972).
- <sup>420</sup>Y. Okuto and C. Crowell, *Solid-State Electronics* **18**, 161 (1975).
- <sup>421</sup>M. Valdinoci, D. Ventura, M. Vecchi, M. Rudan, G. Bacarani, F. Illien, A. Stricker, and L. Zullino, in *1999 International Conference on Simulation of Semiconductor Processes and Devices. SISPAD'99 (IEEE)* (Japan Soc. Appl. Phys, Kyoto, Japan, 1999) pp. 27–30.
- <sup>422</sup>A. Acharyya and J. P. Banerjee, *Journal of Computational Electronics* **13**, 917 (2014).
- <sup>423</sup>K. Brennan, E. Bellotti, M. Farahmand, H.-E. Nilsson, P. Ruden, and Yumin Zhang, *IEEE Transactions on Electron Devices* **47**, 1882 (Oct./2000).
- <sup>424</sup>R. Fujita, K. Konaga, Y. Ueoka, Y. Kamakura, N. Mori, and T. Kotani, in *2017 International Conference on Simulation of Semiconductor Processes and Devices (SISPAD)* (IEEE, Kamakura, Japan, 2017) pp. 289–292.
- <sup>425</sup>H.-E. Nilsson, E. Bellotti, K. Brennan, and M. Hjelm, *Materials Science Forum* **338–342**, 765 (2000).
- <sup>426</sup>C. C. Sun, A. H. You, and E. K. Wong, in *MALAYSIA ANNUAL PHYSICS CONFERENCE 2010 (PERFIK-2010)* (Damai Laut, (Malaysia), 2011) pp. 277–280.
- <sup>427</sup>H. Tanaka, T. Kimoto, and N. Mori, *Journal of Applied Physics* **131**, 225701 (2022).
- <sup>428</sup>C. Sun, A. You, and E. Wong, *The European Physical Journal Applied Physics* **60**, 10204 (2012).
- <sup>429</sup>A. Concannon, F. Piccinini, A. Mathewson, and C. Lombardi, in

*Proceedings of International Electron Devices Meeting* (IEEE, Washington, DC, USA, 1995) pp. 289–292.

<sup>430</sup>K. Katayama and T. Toyabe, in *International Technical Digest on Electron Devices Meeting* (IEEE, Washington, DC, USA, 1989) pp. 135–138.

<sup>431</sup>R. Raghunathan and B. J. Baliga, *Applied Physics Letters* **72**, 3196 (1998).

<sup>432</sup>P. Mukherjee, S. K. R. Hossain, A. Acharyya, and A. Biswas, *Applied Physics A* **126**, 127 (2020).

<sup>433</sup>P. Mukherjee, D. Chatterjee, and A. Acharyya, *Journal of Computational Electronics* **16**, 503 (2017).

<sup>434</sup>W. Bartsch, R. Schörner, and K. O. Dohnke, *Materials Science Forum* **645–648**, 909 (2010).

<sup>435</sup>Z. Stum, Y. Tang, H. Naik, and T. P. Chow, *Materials Science Forum* **778–780**, 467 (2014).

<sup>436</sup>S.-i. Nakamura, H. Kumagai, T. Kimoto, and H. Matsunami, *Applied Physics Letters* **80**, 3355 (2002).

<sup>437</sup>T. Hatakeyama, *physica status solidi (a)* **206**, 2284 (2009).

<sup>438</sup>S. Jin, K. Lee, W. Choi, C. Park, S. Yi, H. Fujii, J. Yoo, Y. Park, J. Jeong, and D. S. Kim, *IEEE Transactions on Electron Devices* , 1 (2024).

<sup>439</sup>S. Nida and U. Grossner, *IEEE Transactions on Electron Devices* **66**, 1899 (2019).

<sup>440</sup>C. R. Crowell and S. M. Sze, *Applied Physics Letters* **9**, 242 (1966).

<sup>441</sup>H. Niwa, J. Suda, and T. Kimoto, *Materials Science Forum* **778–780**, 461 (2014).

<sup>442</sup>H. Hamad, C. Raynaud, P. Bevilacqua, S. Scharnholz, and D. Planson, *Materials Science Forum* **821–823**, 223 (2015).

<sup>443</sup>C. Banc, E. Bano, T. Ouisse, O. Noblanc, and C. Brylinski, *Materials Science Forum* **389–393**, 1371 (2002).

<sup>444</sup>R. Raghunathan and B. Baliga, *Solid-State Electronics* **43**, 199 (1999).

<sup>445</sup>A. O. Konstantinov, Q. Wahab, N. Nordell, and U. Lindefelt, *Journal of Electronic Materials* **27**, 335 (1998).

<sup>446</sup>W. S. Loh, B. K. Ng, J. S. Ng, S. I. Soloviev, H.-Y. Cha, P. M. Sandvik, C. M. Johnson, and J. P. R. David, *IEEE Transactions on Electron Devices* **55**, 1984 (2008).

<sup>447</sup>B. Ng, J. David, R. Tozer, G. Rees, Feng Yan, Jian H. Zhao, and M. Weiner, *IEEE Transactions on Electron Devices* **50**, 1724 (2003).

<sup>448</sup>D. Nguyen, C. Raynaud, N. Dheilly, M. Lazar, D. Tournier, P. Brosselard, and D. Planson, *Diamond and Related Materials* **20**, 395 (2011).

<sup>449</sup>D. Nguyen, C. Raynaud, M. Lazar, G. Pâques, S. Scharnholz, N. Dheilly, D. Tournier, and

- D. Planson, *Materials Science Forum* **717–720**, 545 (2012).
- <sup>450</sup>D. Stefanakis, X. Chi, T. Maeda, M. Kaneko, and T. Kimoto, *IEEE Transactions on Electron Devices* **67**, 3740 (2020).
- <sup>451</sup>Y. Zhao, H. Niwa, and T. Kimoto, *Japanese Journal of Applied Physics* **58**, 018001 (2019).
- <sup>452</sup>A. S. Kyuregyan, *Semiconductors* **50**, 289 (2016).
- <sup>453</sup>J. E. Green, W. S. Loh, A. R. J. Marshall, B. K. Ng, R. C. Tozer, J. P. R. David, S. I. Soloviev, and P. M. Sandvik, *IEEE Transactions on Electron Devices* **59**, 1030 (2012).
- <sup>454</sup>P. L. Cheang, E. K. Wong, and L. L. Teo, *Journal of Electronic Materials* **50**, 5259 (2021).
- <sup>455</sup>L. Zhu, P. A. Losee, T. P. Chow, K. A. Jones, C. Scozzie, M. H. Ervin, P. B. Shah, M. A. Derenge, R. Vispute, T. Venkatesan, and A. K. Agarwal, *Materials Science Forum* **527–529**, 1367 (2006).
- <sup>456</sup>D. Stefanakis, N. Makris, K. Zekentes, and D. Tassis, *IEEE Transactions on Electron Devices* **68**, 2582 (2021).
- <sup>457</sup>H.-E. Nilsson, A. Martinez, U. Sannemo, M. Hjelm, E. Bellotti, and K. Brennan, *Physica B: Condensed Matter* **314**, 68 (2002).
- <sup>458</sup>H. Niwa, J. Suda, and T. Kimoto, *IEEE Transactions on Electron Devices* **62**, 3326 (2015).
- <sup>459</sup>R. Raghunathan and B. Baliga, in *Proceedings of 9th International Symposium on Power Semiconductor Devices* (IEEE, Weimar, Germany, 1997) pp. 173–176.
- <sup>460</sup>D. C. Sheridan, G. Niu, J. Merrett, J. D. Cressler, C. Ellis, and C.-C. Tin, *Solid-State Electronics* **44**, 1367 (2000).
- <sup>461</sup>K. Bertilsson, H.-E. Nilsson, and C. Petersson, in *COMPEL 2000. 7th Workshop on Computers in Power Electronics. Proceedings (Cat. No.00TH8535)* (IEEE, Blacksburg, VA, USA, 2000) pp. 118–120.
- <sup>462</sup>T. Hatakeyama, T. Watanabe, T. Shinohe, K. Kojima, K. Arai, and N. Sano, *Applied Physics Letters* **85**, 1380 (2004).
- <sup>463</sup>W. Loh, J. David, B. Ng, S. I. Soloviev, P. M. Sandvik, J. Ng, and C. M. Johnson, *Materials Science Forum* **615–617**, 311 (2009).
- <sup>464</sup>R. K. Sharma, P. Hazdra, and S. Popelka, *IEEE Transactions on Nuclear Science* **62**, 534 (2015).
- <sup>465</sup>X. Zhang and N. You, in *2018 IEEE 3rd International Conference on Integrated Circuits and Microsystems* (IEEE, Shanghai, 2018) pp. 60–63.
- <sup>466</sup>H.-Y. Cha, S. Soloviev, S. Zelakiewicz, P. Waldrab, and P. M. Sandvik, *IEEE Sensors Journal* **8**, 233 (2008).

- <sup>467</sup>P. Steinmann, B. Hull, I.-H. Ji, D. Lichtenwalner, and E. Van Brunt, *Journal of Applied Physics* **133**, 235705 (2023).
- <sup>468</sup>J. S. Cheong, M. M. Hayat, Xinxin Zhou, and J. P. R. David, *IEEE Transactions on Electron Devices* **62**, 1946 (2015).
- <sup>469</sup>T. Kimoto, M. Kaneko, K. Tachiki, K. Ito, R. Ishikawa, X. Chi, D. Stefanakis, T. Kobayashi, and H. Tanaka, in *2021 IEEE International Electron Devices Meeting (IEDM)* (IEEE, San Francisco, CA, USA, 2021) pp. 36.1.1–36.1.4.
- <sup>470</sup>X. Guo, A. Beck, Xiaowei Li, J. Campbell, D. Emerson, and J. Sumakeris, *IEEE Journal of Quantum Electronics* **41**, 562 (2005).
- <sup>471</sup>A. Kyuregyan and S. Yurkov, *23*, **10**, 1126 (1989).
- <sup>472</sup>R. Trew, J.-B. Yan, and P. Mock, *Proceedings of the IEEE* **79**, 598 (1991).
- <sup>473</sup>J. Wang and B. W. Williams, *Semiconductor Science and Technology* **14**, 1088 (1999).
- <sup>474</sup>W. Loh, C. M. Johnson, J. Ng, P. M. Sandvik, S. Arthur, S. I. Soloviev, and J. David, *Materials Science Forum* **556–557**, 339 (2007).
- <sup>475</sup>W. S. Loh, E. Z. J. Goh, K. Vassilevski, I. Nikitina, J. P. R. David, N. G. Wright, and C. M. Johnson, *MRS Proceedings* **1069**, 1069 (2008).
- <sup>476</sup>T. Hatakeyama, T. Watanabe, K. Kojima, N. Sano, T. Shinohe, and K. Arai, *MRS Proceedings* **815**, J9.3 (2004).
- <sup>477</sup>T. Hatakeyama, J. Nishio, C. Ota, and T. Shinohe, in *2005 International Conference On Simulation of Semiconductor Processes and Devices* (IEEE, Tokyo, Japan, 2005) pp. 171–174.
- <sup>478</sup>A. Ivanov, M. Mynbaeva, A. Sadokhin, N. Strokan, and A. Lebedev, *Nuclear Instruments and Methods in Physics Research Section A: Accelerators, Spectrometers, Detectors and Associated Equipment* **908**, 165 (2018).
- <sup>479</sup>C. Wang, X. Li, L. Li, X. Deng, W. Zhang, L. Zheng, Y. Zou, W. Qian, Z. Li, and B. Zhang, *IEEE Electron Device Letters* **43**, 2025 (2022).
- <sup>480</sup>Y. Wang, J.-c. Zhou, M. Lin, X.-j. Li, J.-Q. Yang, and F. Cao, *IEEE Journal of the Electron Devices Society* **10**, 373 (2022).
- <sup>481</sup>C. C. Sun, A. H. You, and E. K. Wong, in *2012 10th IEEE International Conference on Semiconductor Electronics (ICSE)* (IEEE, Kuala Lumpur, Malaysia, 2012) pp. 366–369.
- <sup>482</sup>J. Hasegawa, L. Pace, L. V. Phung, M. Hatano, and D. Planson, *IEEE Transactions on Electron Devices* **64**, 1203 (2017).
- <sup>483</sup>J. A. McPherson, C. W. Hitchcock, T. Paul Chow, W. Ji, and A. A. Woodworth, *IEEE Transactions on Electron Devices* **64**, 1203 (2017).

- IEEE Transactions on Nuclear Science **68**, 651 (2021).
- <sup>484</sup>T. Kimoto, H. Niwa, T. Okuda, E. Saito, Y. Zhao, S. Asada, and J. Suda, *Journal of Physics D: Applied Physics* **51**, 363001 (2018).
- <sup>485</sup>A. E. Arvanitopoulos, M. Antoniou, S. Perkins, M. Jennings, M. B. Guadas, K. N. Gyftakis, and N. Lophitis, *IEEE Transactions on Industry Applications* **55**, 4080 (2019).
- <sup>486</sup>B. Ng, F. Yan, J. David, R. Tozer, G. Rees, C. Qin, and J. Zhao, *IEEE Photonics Technology Letters* **14**, 1342 (2002).
- <sup>487</sup>P. G. Neudeck, *Journal of Electronic Materials* **27**, 317 (1998).
- <sup>488</sup>J. Palmour, R. Singh, R. Glass, O. Kordina, and C. Carter, in *Proceedings of 9th International Symposium on Power Semiconductor Devices and IC's* (IEEE, Weimar, Germany, 1997) pp. 25–32.
- <sup>489</sup>D. Peters, P. Friedrichs, H. Mitlehner, R. Schoerner, U. Weinert, B. Weis, and D. Stephani, in *12th International Symposium on Power Semiconductor Devices & ICs. Proceedings (Cat. No.00CH37094)* (IEEE, Toulouse, France, 2000) pp. 241–244.
- <sup>490</sup>R. Singh, J. Cooper, M. Melloch, T. Chow, and J. Palmour, *IEEE Transactions on Electron Devices* **49**, 665 (2002).
- <sup>491</sup>O. Slobodyan, J. Flicker, J. Dickerson, J. Shoemaker, A. Binder, T. Smith, S. Goodnick, R. Kaplar, and M. Hollis, *Journal of Materials Research* **37**, 849 (2022).
- <sup>492</sup>I. G. Atabaev, Kh. N. Juraev, and M. U. Hajiev, *Journal of Spectroscopy* **2018**, 1 (2018).
- <sup>493</sup>J. M. Bluet, J. Pernot, J. Camassel, S. Contreras, J. L. Robert, J. F. Michaud, and T. Billon, *Journal of Applied Physics* **88**, 1971 (2000).
- <sup>494</sup>T. Dalibor and M. Schulz, eds., *Numerical Data and Functional Relationships in Science and Technology. Subvol. A2: Gruppe 3: Kristall- Und Festkörperphysik = Group 3: Crystal and Solid State Physics Vol. 41, Semiconductors Impurities and Defects in Group IV Elements, IV-IV and III-V Compounds. Part Beta: Group IV-IV and III-V Compounds / Ed. by M. Schulz; Authors: T. Dalibor*, Vol. 41 (Springer, Berlin Heidelberg, 2003).
- <sup>495</sup>V. Heera, D. Panknin, and W. Skorupa, *Applied Surface Science* **184**, 307 (2001).
- <sup>496</sup>R. Wang, Y. Huang, D. Yang, and X. Pi, *Applied Physics Letters* **122**, 180501 (2023).
- <sup>497</sup>M. Miyata, Y. Higashiguchi, and Y. Hayafuji, *Journal of Applied Physics* **104**, 123702 (2008).
- <sup>498</sup>J. Senzaki, K. Fukuda, Y. Ishida, Y. Tanaka, H. Tanoue, N. Kobayashi, T. Tanaka, and K. Arai, *MRS Proceedings* **622**, T6.7.1 (2000).
- <sup>499</sup>T. Troffer, G. Pensl, A. Schöner, A. Henry, C. Hallin, Kordina, and E. Janzén,

- Materials Science Forum **264–268** (1998), 10.4028/www.scientific.net/MSF.264-268.557.
- <sup>500</sup>M. Krieger, M. Rühl, T. Sledziewski, G. Ellrott, T. Palm, H. B. Weber, and M. Bockstedte, Materials Science Forum **858**, 301 (2016).
- <sup>501</sup>Y. Huang, R. Wang, Y. Qian, Y. Zhang, D. Yang, and X. Pi, Chinese Physics B **31**, 046104 (2022).
- <sup>502</sup>T. Dalibor, G. Pensl, H. Matsunami, T. Kimoto, W. J. Choyke, A. Schöner, and N. Nordell, physica status solidi (a) **162**, 199 (1997).
- <sup>503</sup>E. M. Handy, M. V. Rao, O. W. Holland, K. A. Jones, M. A. Derenge, and N. Papanicolaou, Journal of Applied Physics **88**, 5630 (2000).
- <sup>504</sup>Y. Huang, R. Wang, Y. Zhang, D. Yang, and X. Pi, Chinese Physics B **31**, 056108 (2022).
- <sup>505</sup>G. Xiao, J. Lee, J. Liou, and A. Ortiz-Conde, Microelectronics Reliability **39**, 1299 (1999).
- <sup>506</sup>N. Donato and F. Udrea, IEEE Transactions on Electron Devices **65**, 4469 (2018).
- <sup>507</sup>R. Nipoti, H. M. Ayedh, and B. G. Svensson, Materials Science in Semiconductor Processing **78**, 13 (2018).
- <sup>508</sup>N. T. Son, Mt. Wagner, C. G. Hemmingsson, L. Storasta, B. Magnusson, W. M. Chen, S. Greulich-Weber, J.-M. Spaeth, and E. Janzén, in *Silicon Carbide*, edited by W. J. Choyke, H. Matsunami, and G. Pensl (Springer Berlin Heidelberg, Berlin, Heidelberg, 2004) pp. 461–492.
- <sup>509</sup>M. Laube, F. Schmid, K. Semmelroth, G. Pensl, R. P. Devaty, W. J. Choyke, G. Wagner, and M. Maier, in *Silicon Carbide*, edited by W. J. Choyke, H. Matsunami, and G. Pensl (Springer Berlin Heidelberg, Berlin, Heidelberg, 2004) pp. 493–515.
- <sup>510</sup>Q. Chen, W. He, C. Cheng, and Y. Xue, Journal of Physics: Conference Series **1649**, 012048 (2020).
- <sup>511</sup>F. Schmid, M. Krieger, M. Laube, G. Pensl, and G. Wagner, in *Silicon Carbide*, edited by W. J. Choyke, H. Matsunami, and G. Pensl (Springer Berlin Heidelberg, Berlin, Heidelberg, 2004) pp. 517–536.
- <sup>512</sup>M. Laube, F. Schmid, G. Pensl, G. Wagner, M. Linnarsson, and M. Maier, Journal of Applied Physics **92**, 549 (2002).
- <sup>513</sup>Z. Lv, J. Li, L. Dong, and J. Zang, in *2023 International Conference on Telecommunications, Electronics and Computer Engineering (ICTEC)* (IEEE, Lisbon, Portugal, 2023) pp. 269–273.
- <sup>514</sup>H. Matsuura, M. Komeda, S. Kagamihara, H. Iwata, R. Ishihara, T. Hatakeyama, T. Watanabe, K. Kojima, T. Shinohe, and K. Arai, Journal of Applied Physics **96**, 2708 (2004).
- <sup>515</sup>H. Matsuura, Materials Science Forum **389–393**, 679 (2002).
- <sup>516</sup>T. Troffer, M. Schadt, T. Frank, H. Itoh, G. Pensl, J. Heindl, H. P. Strunk, and M. Maier,

- physica status solidi (a) **162**, 277 (1997).
- <sup>517</sup>G. L. Pearson and J. Bardeen, *Physical Review* **75**, 865 (1949).
- <sup>518</sup>S. Kagamihara, H. Matsuura, T. Hatakeyama, T. Watanabe, M. Kushibe, T. Shinohe, and K. Arai, *Journal of Applied Physics* **96**, 5601 (2004).
- <sup>519</sup>P. Achatz, J. Pernot, C. Marcenat, J. Kacmarcik, G. Ferro, and E. Bustarret, *Applied Physics Letters* **92**, 072103 (2008).
- <sup>520</sup>J. Weiße, M. Hauck, T. Sledziewski, M. Tschiesche, M. Krieger, A. J. Bauer, H. Mitlehner, L. Frey, and T. Erlbacher, *Materials Science Forum* **924**, 184 (2018).
- <sup>521</sup>Y. Kajikawa, *Journal of Electronic Materials* **50**, 1247 (2021).
- <sup>522</sup>M. Rambach, A. J. Bauer, and H. Ryssel, *physica status solidi (b)* **245**, 1315 (2008).
- <sup>523</sup>R. Scaburri, A. Desalvo, and R. Nipoti, *Materials Science Forum* **679–680**, 397 (2011).
- <sup>524</sup>P. P. Altermatt, A. Schenk, and G. Heiser, *Journal of Applied Physics* **100**, 113714 (2006).
- <sup>525</sup>P. P. Altermatt, A. Schenk, B. Schmithüsen, and G. Heiser, *Journal of Applied Physics* **100**, 113715 (2006).
- <sup>526</sup>T. Ayalew, T. Grasser, H. Kosina, and S. Selberherr, *Materials Science Forum* **483–485**, 845 (2005).
- <sup>527</sup>I. D. Booker, *Carrier Lifetime Relevant Deep Levels in SiC*, Linköping Studies in Science and Technology. Dissertations, Vol. 1714 (Linköping University Electronic Press, Linköping, 2015).
- <sup>528</sup>P. T. Landsberg, *physica status solidi (b)* **41**, 457 (1970).
- <sup>529</sup>B. K. Ridley, *Journal of Physics C: Solid State Physics* **11**, 2323 (1978).
- <sup>530</sup>M. Lades, W. Kaindl, N. Kaminski, E. Niemann, and G. Wachutka, *IEEE Transactions on Electron Devices* **46**, 598 (1999).
- <sup>531</sup>M. Lax, *Physical Review* **119**, 1502 (1960).
- <sup>532</sup>V. N. Abakumov, V. I. Perel, and I. N. Yassievich, *Nonradiative Recombination in Semiconductors*, Modern Problems in Condensed Matter Sciences No. v. 33 (North-Holland ; Sole distributors for the USA and Canada, Elsevier Science Pub. Co, Amsterdam ; New York : New York, NY, USA, 1991).
- <sup>533</sup>W. Kaindl, M. Lades, N. Kaminski, E. Niemann, and G. Wachutka, *Journal of Electronic Materials* **28**, 154 (1999).
- <sup>534</sup>I. S. Gorban, A. P. Krokhmal', V. I. Levin, A. S. Skirda, Yu. M. Tairov, and V. F. Tsetkov, Sov. Phys. Semiconductors **21**, 119 (1987).

- <sup>535</sup>S. Asada, T. Okuda, T. Kimoto, and J. Suda, *Applied Physics Express* **9**, 041301 (2016).
- <sup>536</sup>M. A. Capano, J. A. Cooper, M. R. Melloch, A. Saxler, and W. C. Mitchel, *Journal of Applied Physics* **87**, 8773 (2000).
- <sup>537</sup>W. Choyke and G. Pensl, *MRS Bulletin* **22**, 25 (1997).
- <sup>538</sup>S. Contreras, L. Konczewicz, P. Kwasnicki, R. Arvinte, H. Peyre, T. Chassagne, M. Zielinski, M. Kayambaki, S. Juillaguet, and K. Zekentes, *Materials Science Forum* **858**, 249 (2016).
- <sup>539</sup>C. Hitchcock, R. Ghandi, P. Deeb, S. Kennerly, M. Torky, and T. P. Chow, *Materials Science Forum* **1062**, 422 (2022).
- <sup>540</sup>H. Itoh, T. Troffer, and G. Pensl, *Materials Science Forum* **264–268**, 685 (1998).
- <sup>541</sup>L. Kasamakova-Kolaklieva, L. Storasta, I. G. Ivanov, B. Magnusson, S. Contreras, C. Consejo, J. Pernot, M. Zielinski, and E. Janzén, *Materials Science Forum* **457–460**, 677 (2004).
- <sup>542</sup>T. Kimoto, A. Itoh, H. Matsunami, S. Sridhara, L. L. Clemen, R. P. Devaty, W. J. Choyke, T. Dalibor, C. Peppermüller, and G. Pensl, *Applied Physics Letters* **67**, 2833 (1995).
- <sup>543</sup>D. J. Lichtenwalner, J. H. Park, S. Rogers, H. Dixit, A. Scholtze, S. Bubel, and S. H. Ryu, *Materials Science Forum* **1089**, 3 (2023).
- <sup>544</sup>H. Matsuura, T. K. Tsunenobu Kimoto, and H. M. Hiroyuki Matsunami, *Japanese Journal of Applied Physics* **38**, 4013 (1999).
- <sup>545</sup>R. Nipoti, R. Scaburri, A. Hallén, and A. Parisini, *Journal of Materials Research* **28**, 17 (2013).
- <sup>546</sup>M. Obernhofer, M. Krieger, F. Schmid, H. B. Weber, G. Pensl, and A. Schöner, *Materials Science Forum* **556–557**, 343 (2007).
- <sup>547</sup>A. Parisini and R. Nipoti, *Journal of Applied Physics* **114**, 243703 (2013).
- <sup>548</sup>G. Pensl, F. Schmid, F. Ciobanu, M. Laube, S. A. Reshanov, N. Schulze, K. Semmelroth, A. Schöner, G. Wagner, and H. Nagasawa, *Materials Science Forum* **433–436**, 365 (2003).
- <sup>549</sup>M. Rambach, L. Frey, A. J. Bauer, and H. Ryssel, *Materials Science Forum* **527–529**, 827 (2006).
- <sup>550</sup>S. Rao, T. P. Chow, and I. Bhat, *Materials Science Forum* **527–529**, 597 (2006).
- <sup>551</sup>G. Rutsch, R. P. Devaty, W. J. Choyke, D. W. Langer, and L. B. Rowland, *Journal of Applied Physics* **84**, 2062 (1998).
- <sup>552</sup>N. S. Saks, A. K. Agarwal, S.-H. Ryu, and J. W. Palmour, *Journal of Applied Physics* **90**, 2796 (2001).
- <sup>553</sup>N. S. Saks, A. V. Suvorov, and D. C. Capell, *Applied Physics Letters* **84**, 5195 (2004).
- <sup>554</sup>F. Schmid, M. Laube, G. Pensl, G. Wagner, and M. Maier,

- Journal of Applied Physics **91**, 9182 (2002).
- <sup>555</sup>A. Schöner, S. Karlsson, T. Schmitt, N. Nordell, M. Linnarsson, and K. Rottner, Materials Science and Engineering: B **61–62**, 389 (1999).
- <sup>556</sup>Y. Tanaka, N. Kobayashi, H. Okumura, R. Suzuki, T. Ohdaira, M. Hasegawa, M. Ogura, S. Yoshida, and H. Tanoue, Materials Science Forum **338–342**, 909 (2000).
- <sup>557</sup>P. Terziyska, C. Blanc, J. Pernot, H. Peyre, S. Contreras, G. Bastide, J. L. Robert, J. Camassel, E. Morvan, C. Dua, and C. C. Brylinski, physica status solidi (a) **195**, 243 (2003).
- <sup>558</sup>G. Wagner, W. Leitenberger, K. Irmscher, F. Schmid, M. Laube, and G. Pensl, Materials Science Forum **389–393**, 207 (2002).
- <sup>559</sup>R. Wang, I. B. Bhat, and T. P. Chow, Journal of Applied Physics **92**, 7587 (2002).
- <sup>560</sup>S. Y. Ji, K. Kojima, Y. Ishida, H. Tsuchida, S. Yoshida, and H. Okumura, Materials Science Forum **740–742**, 181 (2013).
- <sup>561</sup>H. Matsuura, K. Aso, S. Kagamihara, H. Iwata, T. Ishida, and K. Nishikawa, Applied Physics Letters **83**, 4981 (2003).
- <sup>562</sup>S. Smith, A. Evvaraye, and W. Mitchel, MRS Proceedings **510**, 193 (1998).
- <sup>563</sup>K. Kawahara, H. Watanabe, N. Miura, S. Nakata, and S. Yamakawa, Materials Science Forum **821–823**, 403 (2015).
- <sup>564</sup>S. Beljakowa, S. A. Reshanov, B. Zippelius, M. Krieger, G. Pensl, K. Danno, T. Kimoto, S. Onoda, T. Ohshima, F. Yan, R. P. Devaty, and W. J. Choyke, Materials Science Forum **645–648**, 427 (2010).
- <sup>565</sup>C. Kisielowski, K. Maier, J. Schneider, and V. Oding, Materials Science Forum **83–87**, 1171 (1992).
- <sup>566</sup>J. Zhang, L. Storasta, J. P. Bergman, N. T. Son, and E. Janzén, Journal of Applied Physics **93**, 4708 (2003).
- <sup>567</sup>M. Kato, J. Di, Y. Ohkouchi, T. Mizuno, M. Ichimura, and K. Kojima, Materials Today Communications **31**, 103648 (2022).
- <sup>568</sup>A. Suzuki, H. Matsunami, and T. Tanaka, Japanese Journal of Applied Physics **12**, 1083 (1973).
- <sup>569</sup>N. T. Son, A. Henry, J. Isoya, M. Katagiri, T. Umeda, A. Gali, and E. Janzén, Physical Review B **73**, 075201 (2006).
- <sup>570</sup>A. Martinez, U. Lindefelt, M. Hjelm, and H.-E. Nilsson, Journal of Applied Physics **91**, 1359 (2002).
- <sup>571</sup>S. Greulich-Weber, physica status solidi (a) **162**, 95 (1997).

- <sup>572</sup>M. Bockstedte, A. Mattausch, and O. Pankratov, *Applied Physics Letters* **85**, 58 (2004).
- <sup>573</sup>M. L. Megherbi, F. Pezzimenti, L. Dehimi, M. A. Saadoune, and F. G. Della Corte, *IEEE Transactions on Electron Devices* **65**, 3371 (2018).
- <sup>574</sup>Y. Negoro, T. Kimoto, H. Matsunami, F. Schmid, and G. Pensl, *Journal of Applied Physics* **96**, 4916 (2004).
- <sup>575</sup>Y. Negoro, T. Kimoto, and H. Matsunami, *Electronics and Communications in Japan (Part II: Electronics)* **88**, 1 (2005).
- <sup>576</sup>K. Tian, J. Xia, K. Elgammal, A. Schöner, W. Kaplan, R. Karhu, J. Ul-Hassan, and A. Hallén, *Materials Science in Semiconductor Processing* **115**, 105097 (2020).
- <sup>577</sup>M. Usman, B. Buono, and A. Hallen, *IEEE Transactions on Electron Devices* **59**, 3371 (2012).
- <sup>578</sup>B. Buono, R. Ghandi, M. Domeij, B. G. Malm, C.-M. Zetterling, and M. Ostling, *IEEE Transactions on Electron Devices* **57**, 704 (2010).
- <sup>579</sup>A. K. Tiwari, M. Antoniou, N. Lophitis, S. Perkin, T. Trajkovic, and F. Udrea, *IEEE Transactions on Electron Devices* **66**, 3066 (2019).
- <sup>580</sup>A. K. Tiwari, F. Udrea, N. Lophitis, and M. Antoniou, in *2019 31st International Symposium on Power Semiconductor Devices and ICs (ISPSD)* (IEEE, Shanghai, China, 2019) pp. 175–178.
- <sup>581</sup>H. K. Henisch and R. Roy, *Silicon Carbide—1968: Proceedings of the International Conference on Silicon Carbide, University Park, Pennsylvania, October 20-23, 1968* (Elsevier, 2013).
- <sup>582</sup>J. Sullivan and J. Stanley, *IEEE Transactions on Plasma Science* **36**, 2528 (2008).
- <sup>583</sup>S. W. Huh, J. J. Sumakeris, A. Polyakov, M. Skowronski, P. B. Klein, B. Shanabrook, and M. J. O'Loughlin, *Materials Science Forum* **527–529**, 493 (2006).
- <sup>584</sup>G. Izzo, G. Litrico, L. Calcagno, G. Foti, and F. La Via, *Journal of Applied Physics* **104**, 093711 (2008).
- <sup>585</sup>F. Pezzimenti, L. F. Albanese, S. Bellone, and F. G. D. Corte, in *2009 IEEE Bipolar/BiCMOS Circuits and Technology Meeting* (IEEE, Capri, Italy, 2009) pp. 214–217.
- <sup>586</sup>G. Pensl, ed., *Silicon Carbide, III-nitrides and Related Materials: Proceedings of the 7th International Conference on Silicon Carbide, III-Nitrides and Related Materials, Stockholm, Sweden, September 1997*, Materials Science Forum No. 264/268 (1998).
- <sup>587</sup>K. Adachi, *Simulation and Modelling of Power Devices Based on 4H Silicon Carbide*, Ph.D. thesis, University of Newcastle (2003).
- <sup>588</sup>S. R. Smith, A. O. Evwaraye, W. C. Mitchel, and M. A. Capano,

Journal of Electronic Materials **28**, 190 (1999).

<sup>589</sup>A. Gali, P. Deák, R. P. Devaty, and W. J. Choyke, Physical Review B **60**, 10620 (1999).